

ANALYSIS OF GAIT AND COORDINATION FOR ARTHROPLASTY OUTCOME EVALUATION USING BODY-FIXED SENSORS

THÈSE N° 3594 (2006)

PRÉSENTÉE LE 14 AOÛT 2006

À LA FACULTÉ DES SCIENCES ET TECHNIQUES DE L'INGÉNIEUR
Laboratoire de mesure et d'analyse des mouvements
SECTION DE GÉNIE ÉLECTRIQUE ET ÉLECTRONIQUE

ÉCOLE POLYTECHNIQUE FÉDÉRALE DE LAUSANNE

POUR L'OBTENTION DU GRADE DE DOCTEUR ÈS SCIENCES

PAR

Hooman DEJNABADI

M. Sc. in Electronics, Sharif University of Technology, Tehran, Iran
de nationalité iranienne

acceptée sur proposition du jury:

Prof. J. R. Mosigg, président du jury
Dr K. Aminian, directeurs de thèse
Dr W. Zijlstra, rapporteur
Prof. F. Leyvraz, rapporteur
Prof. C. Frigo, rapporteur



ÉCOLE POLYTECHNIQUE
FÉDÉRALE DE LAUSANNE

Lausanne, EPFL

2006

Abstract

The importance of evaluation of an orthopedic operation such as hip or knee arthroplasty has long been recognized. Many definitions of outcome and scoring questionnaires have been used in the past to assess the outcome of joint replacement. However, these assessments are subjective and not accurate enough. In addition, orthopedic surgeons require now more subtle comparisons between potentially efficacious treatments (e.g. two types of prostheses). Therefore, the use of objective instruments that have a better sensitivity and specificity than traditional scoring systems is needed. Gait analysis is one of the most currently used instrumented techniques in this respect. However, a gait analysis system is accessible only in a few specialized laboratories, as it is complex, expensive, need a lot of room space and fixed devices, and not convenient for the patient.

In this thesis, we proposed an ambulatory system based on kinematic sensors attached on the lower limbs to overcome the limitations of the previously mentioned techniques. Technically the device is portable, easily mountable, non-invasive, and capable of continuously recording data in long term without hindrance to natural gait. The goal was to provide gait parameters as a new objective method to assess Total Knee Replacement (TKR). New solutions to fusing the data of accelerometers and gyroscopes were proposed to accurately measure lower limbs orientations and joint angles. The methods propose a minimal sensor configuration with one sensor module mounted on each segment. The models consider anatomical aspects and biomechanical constraints. In the proposed techniques, the angles are found without the need for integration, so absolute angles can be obtained which are free from any source of drift. These data were then used to develop a gait analysis system providing spatio-temporal parameters, kinematic curves, and a visualization tool to animate the motion data as synthetic skeletons performing the same actions as the subjects. Moreover, a new algorithm was proposed for assessing and quantification of inter-joint coordination during gait. The coordination model captures the whole dynamics of the lower limbs movements and shows the kinematic synergies at various walking speeds. The model imposes a relationship among lower limb joint angles (hips and knees) to parameterize the dynamics of locomotion for each individual. It provides a coordination score at various walking speeds which is ranged between 0 and 10. An integration of different analysis tools such as Harmonic Analysis, Principal Com-

ponent Analysis, and Artificial Neural Network helped overcome high-dimensionality, temporal dependence, and non-linear relationships of the gait patterns.

In order to show the effectiveness of the proposed methods in outcome evaluation, we have considered a clinical study where the outcomes of two types of knee prostheses were compared. We conducted a randomized controlled study, including 54 patients, to assess TKR outcome between patients with fixed bearing and mobile bearing tibial plates of implants. The patients were tested preoperatively and postoperatively at 6 weeks, 3 months, 6 months, and 1 year. Various statistical analyses were done to compare the outcomes of the two groups. Finally, we provided objective criteria, using ambulatory gait analysis, for assessing functional recovery following TKR procedure. We showed significant difference between the two groups where the standard clinical evaluation was unable to detect such a difference.

Keywords: Ambulatory system, Biomechanics, Coordination, Gait analysis, Kinematic sensors, Motion capture, Outcome evaluation, Total knee arthroplasty.

Résumé

L'importance de l'évaluation d'une opération orthopédique telle que l'arthroplastie de la hanche ou du genou a depuis longtemps été identifiée. De nombreux scores cliniques, ainsi que des questionnaires d'évaluation sont utilisés pour évaluer les résultats d'une arthroplastie. Cependant, ces évaluations sont subjectives et peu précises. De plus, le chirurgien a besoin de comparaisons plus subtiles entre les traitements potentiellement efficaces (par exemple deux types de prothèses). Par conséquent, l'utilisation d'instruments objectifs qui ont une meilleure sensibilité et spécificité que les systèmes d'évaluation traditionnels est nécessaire. L'analyse de la marche est l'une des techniques instrumentales les plus utilisées actuellement à cet égard. Pourtant, les systèmes d'analyse de la marche ne sont accessibles que dans quelques laboratoires spécialisés, car ils sont complexes et coûteux. Ces dispositifs nécessitent de grandes salles, ils sont fixes et non portables et ils ne sont pas toujours commodes pour le patient.

Dans cette thèse, nous avons proposé un système ambulatoire basé sur des capteurs cinématiques fixés sur les membres inférieurs afin de surmonter les limitations des techniques mentionnées précédemment. Le dispositif est techniquement portable, facilement utilisable, non invasif, et capable d'enregistrer des données de longue durée dans l'environnement naturel du patient. Le but consiste à évaluer une arthroplastie du genou (TKR) à partir des paramètres de marche fournis par une nouvelle méthode objective. De nouvelles solutions ont été proposées pour fusionner les données des accéléromètres et des gyroscopes afin de mesurer précisément les orientations des membres inférieurs et les angles des articulations. Ces méthodes utilisent une configuration minimale de capteur avec un seul module de capteur fixé sur chaque segment. Une modélisation considérant à la fois les aspects anatomiques et les contraintes biomécaniques est proposée. Dans les techniques proposées, les angles sont calculés sans intégration, ainsi on peut obtenir des angles absolus sans aucune dérive. Ces résultats ont été utilisés pour concevoir un système d'analyse de la marche fournissant des paramètres spatio-temporels, des courbes cinématiques et un outil de visualisation permettant d'animer un squelette virtuel effectuant les mêmes actions que le sujet. De plus, nous avons proposé un nouvel algorithme pour l'évaluation et la quantification de la coordination inter-segmentaire pendant la marche. Le modèle de coordination détermine la dynamique des mouvements des membres inférieurs et illustre les synergies cinématiques pour diverses

vitesses de marche. Le modèle impose une relation entre les angles des articulations des membres inférieurs (hanches et genoux) pour paramétrer la dynamique de la locomotion pour chaque individu. Il fournit des scores de coordination compris entre 0 et 10 pour diverses vitesses de marche. L'intégration de différents outils d'analyse tels que la décomposition harmonique, l'analyse par composants principaux et les réseaux de neurones artificiels a permis de simplifier la haute dimensionnalité, la dépendance temporelle et les relations non linéaires des patterns de la marche.

Afin de montrer l'efficacité des méthodes conçues dans l'évaluation des résultats, nous avons considéré une étude clinique où les résultats de deux types de prothèses de genou ont été comparés. Nous avons entrepris une étude randomisée comprenant 54 patients pour évaluer des résultats de TKR entre les patients portant des prothèses du genou à plateau mobile et articulé. Les patients ont été examinés avant l'opération, puis 6 semaines, 3 mois, 6 mois et 1 an après l'opération. Diverses analyses statistiques ont été réalisées pour comparer les résultats des deux groupes. En conclusion, nous avons fourni des critères objectifs, en utilisant l'analyse ambulatoire de la marche pour évaluer le rétablissement fonctionnel après une arthroplastie totale du genou. Nous avons montré également une différence significative entre les deux groupes, là où l'évaluation clinique standard ne pouvait pas détecter une telle différence.

Mots-clés: Système ambulatoire, biomécanique, coordination, analyse de la marche, capteurs cinématiques, capture de mouvement, évaluation des résultats, arthroplastie totale du genou.

Acknowledgements

Foremost, I would like to express my special thanks and appreciation to my thesis director, Dr. Kamiar Aminian, Head of the Laboratory of Movement Analysis and Measurement (LMAM), for providing me with the opportunity to work in the research area of Biomechanics and Human Movement Analysis, and for his encouragement, support, and supervision at all levels.

I would also like to express my gratitude to the members of my jury, Prof. Pierre-François Leyvraz, Dr. Wiebren Zijlstra, Prof. Carlo Frigo and Prof. Juan Mosig who took time to read and examine my thesis and provided me with valuable feedbacks.

I warmly thank Dr. Brigitte M. Jolles (Hôpital Orthopédique de la Suisse Romande), my clinical co-advisor, for her kind collaboration in preparing and supervising the clinical protocols, which enabled us to gather all the valuable clinical data. I deeply appreciate her enthusiasm, insightful comments, and helpful advices all along the way. Also, I would like to thank Caroline Voracek, Claude Pichonnaz and Angelina Poloni for their assistance in collecting the clinical data, and Estelle Martin for her statistical advices.

I would also like to thank Prof. Pascal Fua, Emilio Casanova, Raquel Urtasun, Mehdi Molkarai and Lorna Herda in CVLab for their valuable collaboration during these last few years.

I wish to thank Jean Gramiger (Fredo) and Pascal Morel for the design and implementation of the ambulatory system and the kinematic sensors used in this project.

My outmost gratitude goes to all my colleagues and friends in LMAM: Danielle Alvarez, Valérie Besson, Arash Salarian, Bijan Najafi, Brian Coley, Julien Favre, Anisoara Ionescu, Toma Knezovic, Hossein Rouhani, Hiroki Obata and Sébastien Halouze-Lamy.

I would also warmly thank the present and former colleagues at MET and NAM: Prof. Philippe Robert, Prof. Olivier Martin, Marianne Noè, Paulou Pierrette, Alexandre Fellay, Paolo Dainesi, Massimo Facchini, Stéphane Schilt, Dario Alasia, Jean-Philippe Besson, Luc Thévenaz, Fabien Briffod, Mario Mattiello, Miguel Gonzalez, Sebastien Le Floch, Juraj Poliak, Norik Janunts, Sang Hoon Chin, André Christ, Holger Fischer, Raquel

Gómez Medina, Gaëtan Lévêque, Mario Mattiello, Antonello Nesci for their daily contribution in creating excellent and friendly conditions at the laboratory.

I warmly thank my past colleagues and co-workers in Fara Sanat Shomal and Rad-Ravesh. I am especially indebted to Mr. Iraj Saravandi-Rad for his continuous encouragement.

I express my deepest gratitude to my parents who always supported and encouraged me. Finally, my warmest thanks belong to my wife, Shokufeh, for all your patience, love and support.

The work presented in this thesis was supported in part by the Swiss National Foundation under Grants FNRS 3200-064951 and 3200B0-105880. I thankfully acknowledge this support.

Table of Contents

ABSTRACT	I
RESUME	III
ACKNOWLEDGEMENTS	V
TABLE OF CONTENTS	VII
LIST OF FIGURES	IX
LIST OF TABLES	XIII
CHAPTER 1 INTRODUCTION	1
1.1 BACKGROUND	1
1.2 OBJECTIVES	3
1.3 OUTLINE OF DISSERTATION	4
CHAPTER 2 OUTCOME EVALUATION IN ARTHROPLASTY: A LITERATURE REVIEW ..	7
2.1 INTRODUCTION	7
2.2 KNEE ARTHROPLASTY OUTCOME EVALUATION	8
2.2.1 <i>Clinical scores</i>	8
2.2.2 <i>Psychometric considerations in outcome questionnaires</i>	8
2.2.3 <i>Review of common questionnaires</i>	9
2.2.4 <i>Instrumented techniques: Fluoroscopy</i>	12
2.2.5 <i>Instrumented techniques: Gait Analysis</i>	13
2.3 CONCLUSION	15
CHAPTER 3 ESTIMATION OF LOWER LIMBS JOINT ANGLES	17
3.1 INTRODUCTION	17
3.2 METHODS	18
3.2.1 <i>Model description</i>	18
3.2.2 <i>Sensor configuration</i>	22
3.2.3 <i>Test protocol</i>	23
3.2.4 <i>Data analysis</i>	26
3.3 RESULTS	26
3.4 DISCUSSION AND CONCLUSION	31
CHAPTER 4 ESTIMATION OF LOWER LIMBS ORIENTATIONS	35
4.1 INTRODUCTION	35
4.2 METHODS	38
4.2.1 <i>Estimation of Shank Orientation</i>	38
4.2.2 <i>Estimation of Thigh Orientation</i>	42
4.2.3 <i>Test Protocol</i>	42
4.2.4 <i>Data Analysis</i>	44
4.3 RESULTS	44
4.3.1 <i>Estimation of Shank and Thigh Orientations</i>	44
4.4 DISCUSSION AND CONCLUSION	50
CHAPTER 5 QUANTITATIVE GAIT ANALYSIS	53

5.1	INTRODUCTION.....	53
5.2	GAIT TERMINOLOGY	54
5.3	METHODS	55
5.3.1	<i>Estimation of Spatio-Temporal parameters</i>	55
5.3.2	<i>Kinematic diagrams</i>	57
5.3.3	<i>Visualization</i>	59
5.4	RESULTS.....	59
5.4.1	<i>Spatio-temporal Parameters</i>	60
5.4.2	<i>Kinematic Diagrams</i>	62
5.4.3	<i>Visualization</i>	64
5.5	DISCUSSION AND CONCLUSION.....	65
CHAPTER 6 ANALYSIS OF INTER-JOINT COORDINATION		67
6.1	INTRODUCTION.....	67
6.2	LITERATURE REVIEW.....	69
6.2.1	<i>Variable-Variable plots</i>	70
6.2.2	<i>Dynamic Systems (Relative Phase)</i>	71
6.2.3	<i>Frequency domain analysis</i>	73
6.2.4	<i>Principal Component Analysis</i>	73
6.3	METHODS	74
6.3.1	<i>Model Description</i>	74
6.3.2	<i>Test Protocol</i>	81
6.4	RESULTS.....	81
6.5	DISCUSSION AND CONCLUSION.....	89
CHAPTER 7 CLINICAL APPLICATION		93
7.1	INTRODUCTION.....	93
7.2	METHODS	95
7.2.1	<i>Subjects</i>	95
7.2.2	<i>Clinical Evaluation</i>	95
7.2.3	<i>Gait Analysis</i>	96
7.2.4	<i>Statistical Analysis</i>	96
7.3	RESULTS.....	96
7.3.1	<i>Clinical Evaluation</i>	96
7.3.2	<i>Gait Parameters</i>	103
7.4	DISCUSSION AND CONCLUSION	112
CHAPTER 8 CONCLUSIONS AND FUTURE RESEARCH.....		115
8.1	CONTRIBUTIONS OF DISSERTATION.....	115
8.2	PERSPECTIVES AND FUTURE RESEARCH.....	117
8.2.1	<i>Movement analysis and visualization</i>	118
8.2.2	<i>Gait analysis</i>	118
8.2.3	<i>Orthopedics and rehabilitation</i>	118
8.2.4	<i>Neuroscience</i>	119
REFERENCES.....		121
CURRICULUM VITAE.....		141

List of figures

FIGURE 2-1 FORCE PLATES MEASURE THE GROUND REACTION FORCES EXERTED BY A PERSON AS HE/SHE STEPS ON IT DURING GAIT. (PHOTO FROM KISTLER® FORCE PLATE, TYPE 9285).....	13
FIGURE 3-1 A PHYSICAL SENSOR MODULE AT POINT P, AND A VIRTUAL SENSOR MODULE ON POINT C ON A 2D RIGID BODY. EACH SENSOR MODULE CONSISTS OF 2D ACCELEROMETERS AND A GYROSCOPE.	19
FIGURE 3-2 POSITION OF SENSORS ON THIGH AND SHANK, AND THEIR CORRESPONDING VIRTUAL SENSORS ON THE KNEE JOINT CENTER OF ROTATION.	21
FIGURE 3-3 SENSOR CONFIGURATION USED THROUGHOUT THIS THESIS. FIVE MODULES OF SENSORS WERE PLACED ON THIGHS, SHANKS, AND SACRUM. THE KINEMATIC DATA WERE RECORDED BY THE PHYSILOG SYSTEM (DIMANTIONS 13 CM X 7 CM X 3 CM, WEIGHT: 300G).....	22
FIGURE 3-4 (A) ATTACHMENT OF THE KINEMATIC SENSORS ON BOTH THIGHS AND SHANKS USING STRAPS. THE PHYSILOG SYSTEM IS PLACED IN THE WAIST BAG. (B) SAGITTAL VIEW OF A SUBJECT WITH EXTENDED LEFT KNEE AND (C) WITH FLEXED LEFT KNEE, REPRESENTING THE SENSOR CONFIGURATIONS. THE WHITE CIRCLES INDICATE THE POSITION OF MARKERS (M_1 , C AND M_2), AND THE WHITE SQUARES INDICATE THE POSITION OF KINEMATIC SENSORS (P_1 AND P_2).	24
FIGURE 3-5 PHYSICAL ACCELEROMETERS AND GYROSCOPES (RAW DATA) READINGS DURING WALKING AT 3 KM/H. THE SITE ON THIGH CONSISTS OF TWO ACCELEROMETERS (S_{x1} AND S_{y1}) AND A GYROSCOPE (ω_1). SIMILARLY, THERE ARE TWO ACCELEROMETERS (S_{x2} AND S_{y2}) AND A GYROSCOPE (ω_2) ON SHANK MODULE.	27
FIGURE 3-6 VIRTUAL ACCELEROMETERS READINGS PLACED AT THE KNEE CENTER OF ROTATION ON THE ADJACENT SEGMENTS. $S_{x'1}$ AND $S_{y'1}$ ARE BIAxIAL VIRTUAL ACCELEROMETERS ON THIGH. CORRESPONDINGLY, $S_{x'2}$ AND $S_{y'2}$ ARE BIAxIAL VIRTUAL ACCELEROMETERS ON SHANK. THE SIGNALS ARE CALCULATED FROM THE RAW SIGNALS SHOWN IN FIGURE 3-5.	28
FIGURE 3-7 POLAR REPRESENTATION (MODULUS, ARGUMENT) OF THE VIRTUAL ACCELEROMETERS CALCULATED FROM THE SIGNALS SHOWN IN FIGURE 3-6. S'_1 AND S'_2 ARE COMPLEX VECTORS EQUAL TO $\begin{bmatrix} S_{x'_1} & S_{y'_1} \end{bmatrix}'$ AND $\begin{bmatrix} S_{x'_2} & S_{y'_2} \end{bmatrix}'$ RESPECTIVELY. THE TOP-RIGHT FIGURE SHOWS ALSO THE DIFFERENCE BETWEEN THE TWO MODULI SIGNALS ($modulus(S'_2) - modulus(S'_1)$) IN DASHED LINE.	28
FIGURE 3-8 (A) KNEE ANGLE CALCULATED FROM THE DIFFERENCE BETWEEN THE TWO ARGUMENT SIGNALS SHOWN IN FIGURE 3-7 ($argument(S'_2) - argument(S'_1)$). (B) CALCULATED FROM POSITION DATA AS MEASURED BY THE REFERENCE SYSTEM (SOLID LINE), AND DIFFERENCE ERROR BETWEEN THE TWO RESULTS (DASHED LINE).....	29
FIGURE 3-9 ABSOLUTE KNEE ANGLE DURING A FREELY ARBITRARY FLEXION AND EXTENSION OF KNEE. (A) CALCULATED FROM THE NEW ACCELEROMETERS AND GYROSCOPES SETTINGS. (B) CALCULATED FROM POSITION DATA AS MEASURED BY THE REFERENCE SYSTEM (SOLID LINE), AND DIFFERENCE ERROR BETWEEN THE TWO RESULTS (DASHED LINE).	30
FIGURE 4-1 POSITION OF SENSOR ON SHANK, AND ITS CORRESPONDING VIRTUAL SENSOR ON ANKLE.....	39
FIGURE 4-2 ATTACHMENT OF THE KINEMATIC SENSORS ON BOTH THIGHS AND SHANKS USING STRAPS. THE KINEMATIC DATA ARE RECORDED BY THE PHYSILOG® SYSTEM (DIMENSIONS: 13 CM X 7 CM X 3 CM,	

WEIGHT: 300 GR) PLACED IN A WAIST BAG. THE WHITE CIRCLES INDICATE THE POSITION OF MARKERS (P_1 , P_2 AND P_3), AND THE WHITE SQUARES INDICATE THE POSITION OF KINEMATIC SENSORS (Q_1 AND Q_2).....	43
FIGURE 4-3 PHYSICAL SENSOR READINGS ON SHANK DURING WALKING AT 3 KM/H. THE SENSOR MODULE CONSISTS OF TWO ACCELEROMETERS (S_x AND S_y) AND A GYROSCOPE (ϱ).	45
FIGURE 4-4 VIRTUAL ACCELEROMETER READINGS ON ANKLE DURING WALKING AT 3 KM/H. THE SIGNALS ARE CALCULATED FROM THE RAW SIGNALS SHOWN IN FIGURE 4-3.	46
FIGURE 4-5 POLAR REPRESENTATION (MODULUS: S' , ARGUMENT: φ_a) OF THE VIRTUAL ACCELEROMETER ON ANKLE CALCULATED FROM THE SIGNAL SHOWN IN FIGURE 4-4.	46
FIGURE 4-6 DETECTION OF THE PERIODS OF MOTION WITH LOW ACCELERATION BY EMPLOYING HYSTERESIS THRESHOLDING AND MORPHOLOGICAL FILTER. (A) MAGNITUDE OF TRANSLATIONAL ACCELERATION ON ANKLE $E(T)$ (SOLID GRAY LINE), AND TWO THRESHOLDS C_1 AND C_2 (DASHED LINES) SET FOR HYSTERESIS THRESHOLDING. (B) RESULT OF HYSTERESIS THRESHOLDING AS BINARY MASK M_1 . (C) RESULT OF MORPHOLOGICAL OPENING FILTER AS BINARY MASK M_2 . THE FILTER WAS APPLIED ON M_1 TO ELIMINATE NARROW PULSES SHORTER THAN $T_0=0.1$ S.	47
FIGURE 4-7 ESTIMATION OF DRIFT BY COMBINING THE TWO ANGLE INFORMATION OBTAINED BY GYROSCOPE AND VIRTUAL ACCELEROMETER. (A) ESTIMATED SHANK ANGLE USING GYROSCOPE (ϕ_g). (B) ESTIMATED SHANK ANGLE USING THE VIRTUAL ACCELEROMETERS (ϕ_a). THE ANGLE IS VALID ONLY DURING LOW ACCELERATION PERIODS INDICATED BY MASK M_2 . (C) ESTIMATED DRIFT BY COMBINING (A) AND (B). THE PROCEDURE CONSISTS OF SUBTRACTING THE TWO SIGNALS FOLLOWED BY APPLYING PIECEWISE CUBIC HERMITE INTERPOLATION. THE ESTIMATED DRIFT IS THEN USED TO CALCULATE THE CORRECT ORIENTATION OF SHANK (ϕ_{SHANK}).	48
FIGURE 4-8 COMPARISON BETWEEN THE MEASURED ANGLES USING THE PROPOSED METHOD AND THE REFERENCE ANGLES (A) SHANK ANGLE CALCULATED BY THE PROPOSED METHOD USING THE BODY-FIXED SENSORS. (B) CALCULATED FROM POSITION DATA AS MEASURED BY THE REFERENCE SYSTEM. (C) DIFFERENCE ERROR BETWEEN THE TWO RESULTS. NOTE THAT THE SCALE IS ZOOMED TO -5.0 TO 5.0 DEG FOR BETTER VIEWING.	49
FIGURE 4-9 COMPARISON BETWEEN THE MEASURED ANGLES USING THE PROPOSED METHOD AND THE REFERENCE ANGLES (A) THIGH ANGLE CALCULATED BY THE PROPOSED METHOD USING THE BODY-FIXED SENSORS. (B) CALCULATED FROM POSITION DATA AS MEASURED BY THE REFERENCE SYSTEM. (C) DIFFERENCE ERROR BETWEEN THE TWO RESULTS. NOTE THAT THE SCALE IS ZOOMED TO -5.0 TO 5.0 DEG FOR BETTER VIEWING.	49
FIGURE 5-1 SUBDIVISIONS STANCE (RIGHT), SWING (RIGHT), AND SINGLE AND DOUBLE SUPPORTS DURING GAIT CYCLE.	55
FIGURE 5-2 SHANK ANGULAR VELOCITY. MARKED AREA SHOW WHERE IMPORTANT GAIT EVENTS OCCUR.	56
FIGURE 5-3 ENSEMBLE AVERAGE GRAPHS FOR LOWER LIMB ANGLES OF A PATIENT (ID: MS-37) WITH KNEE ARTHRITIS PRE-OPERATIVELY DURING 30 COMPLETE. EACH GRAPH SHOWS THE MEAN VALUE (SOLID BLACK) WITH ITS VARIABILITY BAND (GRAY).	62
FIGURE 5-4 ENSEMBLE AVERAGE GRAPHS FOR LOWER LIMB ANGLES OF A PATIENT (ID: MS-37) 6 MONTHS AFTER KNEE ARTHROPLASTY.	63
FIGURE 5-5 ENSEMBLE KNEE-HIP ANGLE-ANGLE DIAGRAM OF A PATIENT (ID: MS-37) AT BASELINE.	64
FIGURE 5-6 ENSEMBLE KNEE-HIP ANGLE-ANGLE DIAGRAM OF A PATIENT 6 (ID: MS-37) MONTHS AFTER SURGERY.	64
FIGURE 5-7 INTERFACE OF OUR VISUALIZATION TOOL. THE ANIMATED SKELETON OF A PATIENT (ID: MS-37) DURING WALKING WITH KNEE ARTHROPLASTY IS SHOWN IN THE MIDDLE WINDOW. THE KNEE PROSTHESIS IS COLORED IN LIGHT GRAY. THE RIGHT WINDOW COMPARES THE GAIT OF THE SAME PATIENT JUST BEFORE OPERATION (BLACK) WITH 6 MONTHS LATER (GRAY).	65
FIGURE 6-1 HIP-KNEE PHASE PORTRAIT DURING GAIT: (A) NORMAL HEALTHY GAIT, (B) KNEE ARTHRITIS GAIT. ANGLES CORRESPOND TO THE HIP AND KNEE FLEXION-EXTENSION ANGLES DURING WALKING.	70
FIGURE 6-2 KNEE PHASE PLOTS DURING GAIT: (A) NORMAL HEALTHY GAIT, (B) KNEE ARTHRITIS GAIT.	71
FIGURE 6-3 RELATIVE PHASE BETWEEN SHANK AND THIGH DURING GAIT: (A) NORMAL HEALTHY GAIT, (B) KNEE ARTHRITIS GAIT. THE RP CURVES ARE TIME-NORMALIZED TO GAIT CYCLE TIME.	73

FIGURE 6-4 BLOCK DIAGRAM OF THE MODEL: (A) TRAINING, (B) TESTING.	76
FIGURE 6-5 TIME-NORMALIZATION OF LOWER LIMB JOINT ANGLES TO GAIT CYCLE TIME. THE CURVES REPRESENT 3 TYPICAL GAIT CYCLES OF A HEALTHY SUBJECT (NO. 1) AT SLOW (DASHED LINE), NORMAL (SOLID LINE), AND FAST SPEEDS (DOTTED LINE).	82
FIGURE 6-6 CHOOSING THE REQUIRED NUMBER OF HARMONICS (M) FOR 98% DEGREE OF DATA RECONSTRUCTION. THE DASHED LINE SHOWS THE THRESHOLD SET AT 0.98, AND THE NUMBER OF REQUIRED HARMONICS WHERE THE CRITERION (5.9) IS MET IS $M=9$	83
FIGURE 6-7 CHOOSING THE REQUIRED NUMBER OF PCAs BASED ON CUMULATIVE VARIANCE CRITERION (5.13). THE DASHED LINE SHOWS THE THRESHOLD SET AT 0.98, AND THE NUMBER OF REQUIRED COMPONENTS TO EXPLAIN 98% OF VARIANCE IS $P=8$	83
FIGURE 6-8 LOWER LIMBS TRAJECTORIES (ACTUAL AND PREDICTED) AND THE RESIDUAL ERROR (TOP PANEL: LEFT AND RIGHT HIPS, BOTTOM PANEL: LEFT AND RIGHT KNEES). THE TRAJECTORIES SHOWN IN THE TOP ROWS OF THE PANELS (X1 TO X4) REPRESENT ACTUAL MEASURED JOINT ANGLES OF PATIENT NO. 1 AT BASELINE WITH A VERY POOR COORDINATION. THE FIRST FEW CYCLES WERE CHOSEN FROM SLOW SPEED ($0<T<5s$), THE CYCLES IN THE MIDDLE PART ($5<T<10s$) WERE CHOSEN FROM NORMAL SPEED, AND THE LAST FEW CYCLES WERE CHOSEN FROM FAST SPEED TRIALS ($10<T<15s$). THE TRAJECTORIES SHOWN IN THE MIDDLE ROW OF THE PANELS (\hat{x}_1 TO \hat{x}_4) REPRESENT THE PREDICTED MOTIONS RECONSTRUCTED BY THE MODEL. THE RESIDUAL ERRORS BETWEEN THE ACTUAL AND PREDICTED TRAJECTORIES ($\hat{\epsilon}_1$ TO $\hat{\epsilon}_4$) ARE SHOWN IN THE BOTTOM ROW OF THE PANELS. NOTE THAT THE ERROR SCALES ARE ZOOMED TO -10.0 TO 10.0 DEG FOR BETTER VIEWING.	85
FIGURE 6-9 THE LOGARITHMIC MAPPING FUNCTION (5.16), USED IN THE SCORING BLOCK TO MAP NORMALIZED RMS ERROR ($E_{k,j}$) TO COORDINATION SCORE ($R_{k,j}$). THE OUTPUT SCORE ($R_{k,j}$) IS RANGED BETWEEN 0 AND 10. THE SCALING CONSTANTS WERE SET TO $R_{Max} = 10$, $E_{Min} = 0.01$, AND $E_{Max} = 0.15$	86
FIGURE 6-10 COORDINATION SCORE OF AFFECTED (LEFT) KNEE ($J=3$) OF PATIENT NO.1 AT 3 WALKING SPEEDS (SLOW, NORMAL AND FAST) AT BASELINE. THE DOTS INDICATE THE SCORE OF EACH GAIT CYCLE ($R_{k,3}$). A POLYNOMIAL CURVE WAS FITTED TO THE DATA (R_3) TO BETTER REPRESENT AND INTERPRET THE SCORES.	87
FIGURE 6-11 CONTRIBUTION OF EACH JOINT TO THE INTER-JOINT COORDINATION DURING GAIT (PATIENT NO.1, BASELINE). THE CURVES SHOW THE COORDINATION SCORE ASSIGNED TO EACH JOINT VERSUS WALKING VELOCITY. THE AFFECTED KNEE (LEFT KNEE) HAS THE LEAST SCORE (R_3).	87
FIGURE 6-12 OVERALL INTER-JOINT COORDINATION SCORE OF PATIENT NO.1 AT BASELINE AND 2 FOLLOW UP TESTS AT 6 WEEKS AND 6 MONTHS.	88

List of tables

TABLE 3-1 COMPARISON BETWEEN KNEE ANGLE MEASUREMENTS OBTAINED BY BODY-MOUNTED SENSORS AND ZEBRIS MARKERS FOR 8 SUBJECTS AT 3 SPEEDS. THE ERROR REPRESENTS THE RMS, MEAN AND SD OF THE DIFFERENCE SIGNAL BETWEEN ZEBRIS AND OUR MEASURING DEVICE. ‘R’ REPRESENTS THE CORRELATION COEFFICIENT BETWEEN THE TWO MEASURING SYSTEMS.....	31
TABLE 4-1 COMPARISON BETWEEN SHANK AND THIGH ANGLE MEASUREMENTS OBTAINED BY BODY-FIXED SENSORS AND ZEBRIS MARKERS FOR ALL SUBJECTS AT 3 SPEEDS. THE ERROR REPRESENTS THE MEAN AND SD OF RMS ERROR (THE DIFFERENCE SIGNAL BETWEEN ZEBRIS AND OUR MEASURING DEVICE), AS WELL AS THE MEAN AND SD OF THE CORRELATION COEFFICIENT BETWEEN THE TWO MEASURING SYSTEMS ..	50
TABLE 5-1 SPATIO-TEMPORAL PARAMETERS OF THE GAIT TRIALS OF A PATIENT (ID: MS-37) AT BASELINE AND 6 MONTHS AFTER SURGERY.	61
TABLE 6-1 COORDINATION SCORES OF 8 PATIENTS (P1 TO P8) AT 3 DIFFERENT FOLLOW UP TESTS, AND 8 HEALTHY SUBJECTS (H1 AND H8). THE SCORES OF EACH TRIAL AT SLOW, NORMAL, AND FAST SPEEDS, AS WELL AS THEIR MEAN AND STANDARD DEVIATION FOR EACH GROUP, ARE REPORTED SEPARATELY.....	89
TABLE 7-1 PATIENT DEMOGRAPHICS	95
TABLE 7-2 CLINICAL SCORES OF ALL PATIENTS AT BASELINE AND DIFFERENT FOLLOW UP TESTS AT 6-WEEK, 3-MONTH, 6-MONTH, AND 1-YEAR	97
TABLE 7-3 DIFFERENCES IN CLINICAL SCORES BETWEEN FOLLOW UP TESTS AND PRE-OP TEST. THE STATISTICALLY SIGNIFICANT DIFFERENCES (P<0.05) BETWEEN THE GROUPS ARE SHADED IN GRAY . THE P-VALUE IS PROVIDED ONLY FOR NON-SIGNIFICANT CHANGES	98
TABLE 7-4 GROUP COMPARISONS (FIXED- AND MOBILE-BEARING) USING THE CLINICAL SCORES. THE COMPARISON IS MADE BETWEEN THE CLINICAL SCORES AT 3 MONTHS (COLS. 1 AND 2), AND BETWEEN THE PATIENT IMPROVEMENTS (DIFFERENCE BETWEEN 3 MONTHS AND BASELINE, COLS. 3 AND 4). THE STATISTICALLY SIGNIFICANT DIFFERENCES (P<0.05) BETWEEN THE GROUPS ARE SHADED IN GRAY	100
TABLE 7-5 GROUP COMPARISONS (FIXED- AND MOBILE-BEARING) USING THE CLINICAL SCORES. THE COMPARISON IS MADE BETWEEN THE CLINICAL SCORES AT 6 MONTHS (COLS. 1 AND 2), AND BETWEEN THE PATIENT IMPROVEMENTS (DIFFERENCE BETWEEN 6 MONTHS AND BASELINE, COLS. 3 AND 4). THE STATISTICALLY SIGNIFICANT DIFFERENCES (P<0.05) BETWEEN THE GROUPS ARE SHADED IN GRAY	101
TABLE 7-6 GROUP COMPARISONS (FIXED- AND MOBILE-BEARING) USING THE CLINICAL SCORES. THE COMPARISON IS MADE BETWEEN THE CLINICAL SCORES AT 1 YEAR (COLS. 1 AND 2), AND BETWEEN THE PATIENT IMPROVEMENTS (DIFFERENCE BETWEEN YEAR AND BASELINE, COLS. 3 AND 4). THE STATISTICALLY SIGNIFICANT DIFFERENCES (P<0.05) BETWEEN THE GROUPS ARE SHADED IN GRAY	102
TABLE 7-7 GAIT PARAMETERS OF ALL PATIENTS AT BASELINE AND DIFFERENT FOLLOW UP TESTS AT 6 WEEKS, 3 MONTHS, 6 MONTHS AND 1 YEAR DURING WALKING AT NORMAL SPEED.....	104
TABLE 7-8 VARIABILITY (CV%) OF SPATIO-TEMPORAL GAIT PARAMETERS OF THE PATIENTS AT BASELINE AND DIFFERENT FOLLOW UP TESTS AT 6 WEEKS, 3 MONTHS, 6 MONTHS AND 1 YEAR DURING WALKING AT NORMAL SPEED	105
TABLE 7-9 DIFFERENCE IN GAIT PARAMETERS BETWEEN FOLLOW UP TESTS AND PRE-OP TEST. THE STATISTICALLY SIGNIFICANT DIFFERENCES (P<0.05) BETWEEN THE GROUPS ARE SHADED IN GRAY	106
TABLE 7-10 DIFFERENCE IN GAIT VARIABILITY BETWEEN FOLLOW UP TESTS AND PRE-OP TEST. THE STATISTICALLY SIGNIFICANT DIFFERENCES (P<0.05) BETWEEN THE GROUPS ARE SHADED IN GRAY	107
TABLE 7-11 COMPARISON BETWEEN FIXED BEARING AND MOBILE BEARING AT 3 MONTHS FOLLOW UP. THE COMPARISON IS MADE BETWEEN THE GAIT PARAMETERS AT 3 MONTHS (COLS. 1 AND 2), AND BETWEEN THE PATIENT IMPROVEMENTS (DIFFERENCE BETWEEN 3 MONTHS AND BASELINE, COLS. 3 AND 4). THE STATISTICALLY SIGNIFICANT DIFFERENCES (P<0.05) BETWEEN THE TWO GROUPS ARE SHADED IN GRAY.	109

TABLE 7-12 COMPARISON BETWEEN FIXED BEARING AND MOBILE BEARING AT 6 MONTHS FOLLOW UP. THE COMPARISON IS MADE BETWEEN THE GAIT PARAMETERS AT 6 MONTHS (COLS. 1 AND 2), AND BETWEEN THE PATIENT IMPROVEMENTS (DIFFERENCE BETWEEN 6 MONTHS AND BASELINE, COLS. 3 AND 4). THE STATISTICALLY SIGNIFICANT DIFFERENCES ($p < 0.05$) BETWEEN THE TWO GROUPS ARE SHADED IN GRAY.
..... 110

TABLE 7-13 COMPARISON BETWEEN FIXED BEARING AND MOBILE BEARING AT 1 YEAR FOLLOW UP. THE COMPARISON IS MADE BETWEEN THE GAIT PARAMETERS AT 1 YEAR (COLS. 1 AND 2), AND BETWEEN THE PATIENT IMPROVEMENTS (DIFFERENCE BETWEEN 1 YEAR AND BASELINE, COLS. 3 AND 4). THE STATISTICALLY SIGNIFICANT DIFFERENCES ($p < 0.05$) BETWEEN THE TWO GROUPS ARE SHADED IN GRAY.
..... 111

Chapter 1 Introduction

1.1 Background

Osteoarthritis (OA) is the most common type of arthritis or degenerative joint disease. It is a common chronic, progressive musculoskeletal disorder characterized by gradual loss of articular cartilage (Aigner et al. 2006). When knees or hips are affected, it becomes one of the most debilitating ones, considerably reducing the patients' physical and psychosocial functions. OA affects people of all ethnic groups in all geographic locations, it develops in both men and women, and it is the most common cause of long-term disability in most populations of people over 65. The World Health Organization (WHO) estimates that 10% of the world's people over the age of 60 years suffer from OA, and that 80% of people with OA have limitation of movement and 25% cannot perform major daily activities (Buckwalter and Martin 2006).

Arthroplasty is a surgery performed to relieve pain and restore range of motion by realigning or reconstructing a dysfunctional joint. In recent years, arthroplasty by joint replacement has become the operation of choice for most chronic knee and hip problems, particularly because of advances in the type and quality of prostheses (artificial joints). Elbow, shoulder, ankle, and finger joints are more likely to be treated with joint resection or interpositional reconstruction. Thanks to the continuing development of joint arthroplasties, physical therapy and psychosocial support, it is now possible to restore a near normal quality of life to patients. Joint replacement is usually reserved for older patients, because of the limited longevity of benefits. The younger the patient, the greater the reliance on medical treatment.

The importance of evaluation of arthroplasty outcome has long been recognized. The rapidly rising cost of healthcare with its financial impact on the individual and national economy, and deficiencies in clinical research methods such as patient oriented evaluation that is a functional and quality-of-life assessment, have stimulated the emergence of outcome research (Keller et al. 1993). A large variety of scores and evaluation systems have been used to assess the outcome of hip and knee arthroplasties. However, most of these assessments are subjective which is based on the observer's experience and individual bias. On the other hand, the large varieties of scores with different designs make it

difficult to compare the patient outcome, and none has been accepted as the universal standard (Konig et al. 1997).

The difficulty lies in attempting to quantify the surgical result. For example, should one be putting more emphasis on the patient's overall improvement or on the technical success of the surgery? Should one be putting more emphasis on a simple measure of the joint range of motion or the difficulties the patient has in changing positions or in coordinating his legs during walking? In fact, the increasing variety of outcome measures illustrates the need for an objective reference of assessing the results that is a gold standard outcome measure.

The effectiveness of an arthroplasty in relieving pain and improving function has been well documented over the past 20 years. The influence of surgical procedures on quality-of-life must be positive. However, health-related quality of life encompasses not only pain and physical functioning, but other domains such as social functioning and vitality. In addition, orthopedic surgeons require now more subtle comparisons between potentially efficacious treatments (e.g. two types of prostheses, two surgery procedures, and two rehabilitation programs). Therefore, the use of instruments that have a better sensitivity and specificity than traditional scoring systems is needed to evaluate the results of arthroplasty and enhance the surgeon's ability to assess the overall outcome (Lieberman et al. 1997; Lieberman et al. 1996).

Despite the fact that the most common human physical activity is walking, it still remains one of the least explored biological function (Banks et al. 1997b). This paradox is due to two facts. Walking is very easily accessible to a detailed clinical analysis. As a result, the diagnosis has been developed on a clinical basis. The indications for surgery have mostly been laid down several years ago and rely on analysis and experience. Although the approach is effective in practice, it allows neither for the quantification of the spatio-temporal parameters of walking, nor for the assessment of the physical activity of everyday life in a reliable way.

Quantitative gait analysis is one of the few measurement methods that offer objective evaluation of the effectiveness of arthroplasty. There is a growing acceptance of the clinical use of gait analysis system, and it has been shown to be of value in distinguishing between functional outcomes of different types of surgery and predicting the outcomes of surgery (Andriacchi et al. 1982; Andriacchi et al. 1997; Berman et al. 1987; Catani et al. 2003; Chao et al. 1980; Collopy et al. 1977; Deluzio et al. 1999; deQuervain et al. 1997; Kaufman et al. 2001; Kroll et al. 1989; Minns 2005; Otsuki et al. 1999; Simon et al. 1983; Smith et al. 2006; Solak et al. 2005; Steiner et al. 1989; Webster et al.

2003). However, all these measuring tools are accessible nowhere else than in a few specialized laboratories. They are often complex, expensive, need a lot of room space and fixed devices, and not convenient for the patient. In current practice, these techniques are not applicable for routine evaluation of patient outcomes. Moreover, instrumentation alone cannot make gait analysis clinically relevant. Clinical gait analysis is the correlation and interpretation of the data and should be able to relate objective findings to functional measures and outcomes. So the physicians lack a convenient and simple method to reliably assess their patients' activity and quality of life.

1.2 Objectives

In this thesis, we proposed an ambulatory system based on kinematic sensors attached on the lower limbs in order to overcome the limitations of the previously mentioned techniques. It involves development of improved methods for measurement and analysis of human gait.

The main features of the measurement device were to be portable, easily mountable, accurate, non-invasive, and capable of continuously recording data in long-term without hindrance to natural gait. Moreover, new algorithms were proposed to accurately measure joints and segments angles in the sagittal plane. These data were then used to develop a gait analysis system providing spatio-temporal parameters, kinematic curves, and skeleton visualization. In addition, a new algorithm was proposed for assessing and quantification of inter-joint coordination during gait. The method provided a coordination score for outcome evaluation.

In order to evaluate the efficacy of our method, we applied our gait analysis in a real orthopedic application: Total Knee Arthroplasty (TKA). We focused on comparing TKA using two prostheses types: posterior stabilized with fixed versus mobile tibial plateau bearings. Mobile bearing TKA system are emerging as the next wave of development in knee joint prosthetic reconstruction. Since 1977, mobile bearing knee prostheses have been designed and implanted in order to provide less constrained knee kinematics while minimizing polyethylene wear and reducing bone-cement prosthesis interface stress (Aglietti et al. 2002; Buechel and Pappas 1989; Catani et al. 2003; Lemaire 2002). Almost every manufacturer has introduced a mobile-bearing TKA system, or is developing one to introduce into the market. However, most studies on the outcomes of mobile-bearing TKA are open studies, and currently there is no objective evidence that mobile bearing prosthesis is more effective.

We designed a clinical protocol and conducted a randomized controlled study to provide gait parameters as a new objective method to assess TKA outcome. In this study, gait

analysis and knee scoring system results of 54 patients were evaluated. Preoperative results were compared with postoperative (6 weeks, 3 months, 6 months, and 1 year) results.

1.3 Outline of dissertation

Chapter 2 reviews different methodologies (both scoring questionnaires and instrumented techniques) used to assess TKA outcome. It discusses the requirements of a scoring questionnaire that must be valid, reliable and responsive; and explains the problems with the questionnaires that are subjective, restricted to a specific pathology, and their low sensitivity to change. Then, it reviews the instrumented techniques such as fluoroscopic analysis and gait analysis systems. Finally, after comparing the advantages and disadvantages of the different systems, an ambulatory gait analysis system using kinematic sensors is proposed, as a promising solution, for quantitative evaluation of TKA outcome.

Chapters 3 and 4 describe our new methods to estimate lower limbs orientations and joint angles using a combination of accelerometers and gyroscopes. The model of measuring joint angle, presented in chapter 3, is based on estimating the acceleration of the joint center of rotation by placing a pair of virtual sensors on the adjacent segments at the center of rotation. This way, joint angles are found without the need for integration of gyroscope signals, so absolute angles can be obtained free from any source of drift. Chapter 4 presents a new complementary method to estimate lower limbs (shank and thigh) orientation in sagittal plane during walking. The proposed techniques consider human locomotion and biomechanical constraints, and provide new solutions to fusing the data of gyroscopes and accelerometers.

The lower limbs motions data were then used in chapter 5 to design a gait analysis tool. Outputs from the software include spatio-temporal parameters of gait, kinematic diagrams, and animated graphic images simulating the patients' gait at various conditions. The spatio-temporal parameters as well as their variabilities provided a tool for objective outcome measures to quantify the expected gait improvement of patients after arthroplasty. The kinematic diagrams provide supplementary information for representing movement and its variability as a function of time or other movement parameter in continuous format. The graphs could help clinician qualitatively assess time evolution of lower limb movements, variability at different phases of gait, symmetry, and ranges of rotations. The visualization tool provide additional tool to see the time evolution of lower limb movements. The visualization tool gives the physician visually appealing and easy to interpret information about how the patient performs several activities such as walking at

different speeds or climbing ramps and stairs. In addition, it allows us to evaluate the progression of a patient at different follow up tests by superposing several skeletons.

Chapter 6 proposes a new method for quantitative analysis of inter-joint coordination during gait. A general model was designed to capture the whole dynamics of the lower limbs movement and show the kinematic synergies at various walking speeds. The proposed model imposed a relationship among lower limb joint angles (hips and knees) to parameterize the dynamics of locomotion for each individual. An integration of different analysis tools such as Harmonic analysis, Principal Component Analysis, and Artificial Neural Network helped overcome high-dimensionality, temporal dependence, and non-linear relationships of the gait patterns.

In chapter 7, the proposed gait and coordination analysis methods, proposed in previous chapters, were applied in a real clinical application. We conducted a randomized controlled study, and included 54 patients, to assess total knee arthroplasty outcome between patients with fixed bearing and mobile bearing tibial plates of implants. The chapter presents both clinical scores and gait analysis results of patients preoperatively and postoperatively at 6 weeks, 3 months, 6 months and 1 year. Various statistical analyses were done to compare the outcomes of the two groups at different follow up tests. We provided objective criteria, using ambulatory gait analysis, for assessing functional recovery following TKA procedure.

Finally, chapter 8 summarizes the contribution of this thesis and outlines some perspectives of the proposed methods.

Chapter 2 Outcome Evaluation in Arthroplasty: A Literature Review

2.1 Introduction

Many definitions of outcome and scoring questionnaires have been used in the past to assess the results after total joint replacement surgery. These differ in their approach to the measurement of outcome but all must be valid (they measure what they are designed to measure), reliable (they consistently produce the same score), and responsive (able to detect changes that may occur during a period). Responsiveness is crucial to distinguish those patients who benefit from a procedure from those who do not, and a more responsive test will theoretically be able to identify more subtle changes in patient status.

However, there are several problems with the questionnaires. The first is the subjectivity that governs most disability-oriented measurement tools, the second is the restriction to a specific pathology and the third is the low sensitivity to change. Therefore, the use of instruments that have a better sensitivity and specificity than traditional scoring systems is needed to evaluate the results of arthroplasty and enhance the surgeon's ability to assess the overall outcome (Lieberman et al. 1997; Lieberman et al. 1996).

Gait analysis is one of the most currently used instrumented techniques in this respect. There are several branches in studying gait analysis such as *Gait kinetics*, *Dynamic electromyography* (EMG), and *Gait kinematics*. A comprehensive gait analysis usually includes all branches (Vaughan et al. 1992) and this complex information can only be obtained in a dedicated laboratory. Kinematics, kinetics and electromyography are fundamental to characterize gait patterns and their underlying mechanisms (Frigo et al. 1996; Romanò et al. 1996). However, simplified kinematic analysis (e.g., spatio-temporal parameters) can also be clinically valuable, and an ambulatory device may be advantageous for these types of applications (Aminian et al. 2004b).

In this chapter, we review different methodologies used to assess total knee arthroplasty outcome.

2.2 Knee Arthroplasty Outcome Evaluation

2.2.1 Clinical scores

Judging the success of the intervention may relate more to subtler improvements in quality of life, including relief of pain and improvement in function. Furthermore, current prostheses have all benefited from technological learning curve in the design of the prostheses, and modern prostheses can be expected to survive in situ, barring infection, for at least a decade, or perhaps 2 decades, with relative certainty (Dunbar 2001). The net effect of the homogeneity of current prostheses (with respect to stable and lasting designs) has been for an emerging emphasis on somehow quantifying subtler outcomes after knee arthroplasty.

With the advent of prosthesis components that demonstrated predictably good results, it became evident that more formalized outcome metrics were necessary. The initial response was for surgeons to assess the results of their interventions. In 1976, Insall et al. introduced a surgeon derived outcome score for knee arthroplasty that incorporated various parameters including technical outcomes related to the procedure (e.g. alignment, range of motion, etc.) and subjective patient factors such as pain (Insall et al. 1976). This questionnaire has come to be known as the Hospital for Special Surgery Knee Score (HSS). In 1989, Insall et al. developed a second surgeon derived score, which incorporated similar parameters. This score has come to be known as the Knee Society's Clinical and Functional Scoring System (KSS) (Insall et al. 1989). The HSS and KSS have been used fairly extensively in outcome studies on knee arthroplasty (Amendola et al. 1989; Armstrong and Whiteside 1991; Barrack et al. 1998; Fehring and Valadie 1994; Hirsch et al. 1994; Joseph and Kaufman 1990; Knight et al. 1997; Nafei et al. 1993). Unfortunately, and despite their continued popularity, the HSS and KSS scores have never been validated using formal psychometric validation procedures (Dunbar 2001). Furthermore, these questionnaires have been found to be exceedingly unreliable, leading some authors to conclude that these scoring systems should not be used (Konig et al. 1997; Ryd et al. 1997).

2.2.2 Psychometric considerations in outcome questionnaires

Psychometrics can be defined as “the scientific measurement of mental capacities and processes and of personality” (Dalessandro 1994; Dunbar 2001). In other words, psychometrics is the process that allows researchers to apply scientific methodology to the measurement of subjective outcomes. In practical terms, the published psychometric properties of a questionnaire pertain mostly to the validation of the questionnaire, or, defining how well the questionnaire measures what is supposed to measure, in a global

sense. The validation process usually involves three specific aspects of questionnaire testing: validity, reliability, and responsiveness (Dunbar 2001; Finch et al. 2002).

Validity refers more specifically (as opposed to validation) to how well the questionnaire measures the question of interest. In order to comment on the validity of a questionnaire, the results of the questionnaire must be compared to something using criterion validity, construct validity, or content validity (Dunbar 2001).

Criterion validity refers to the comparison of the metric to a “gold standard”. Unfortunately there is no gold standard for knee arthroplasty (Kirshner and Guyatt 1985; Kreibich et al. 1996). Consequently, questionnaires for knee arthroplasty are usually validated against a postulated effect that should result from the intervention. *Construct validity* may be determined against another previously validated questionnaire or a consensus statement. However, construct validity in the absence of a gold standard is problematic. *Content validity* addresses whether a questionnaire has enough items and adequately covers the domain of interest (Dunbar 2001).

Reliability refers to the ability of an outcome metric to remain unchanged when applied on two separate occasions and no clinical changes has occurred. Essentially, in its most basic sense, reliability is the measure of the noise within a metric.

Responsiveness is a measure of a questionnaire’s ability to detect change when it is applied on separate occasions and a clinically significant change has occurred between applications.

2.2.3 Review of common questionnaires

In this section we review common scoring systems used to evaluate TKA outcome.

2.2.3.1 General Health Questionnaires

Nottingham Health Profile (NHP): The NHP is a self-report that poses 45 questions organized into 2 parts to which a response of yes or no is given. In Part 1, 38 questions are utilized to generate weighted scores for 6 domains: emotional reactions, physical mobility, pain, sleep, social isolation, and energy level. Scores in Part 1 range from 0–100 with 0 representing the best possible health state. Part 2 contains 7 questions regarding perceived health problems affecting activities of daily life and the effect of health problems on occupation, jobs around the house, personal relationships, social life and hobbies.

36-Item Short-Form Health Survey (SF-36): The SF-36 consists of 36 questions with Likertbox response keys that include 8 domains measuring Body Pain, Physical Func-

tioning, Vitality, General Health, Social Functioning, Role-Physical, Role-Emotion, and Mental Health. Response choices range from two-level to six-level scales. The scores on all subscales range from 0 to 100, with higher scores indicating better health states. A physical and mental health component can be derived from the items. These two sub-components have been standardized to have a mean of 50 and a standard deviation of 10.

12-Item Short-Form Health Survey (SF-12): The SF-12 consists of 12 questions which are a subset of those in the SF-36. One or two items from each of the 8 concepts represented in the SF-36 are included in the SF-12. Similarly, response choices range from two-level to six-level response scales, and physical and mental component summary scales are derived from the items.

Sickness Impact Profile (SIP): The SIP is a 136-item questionnaire that can be interviewed or self-administered. The questionnaire produces weighted results for 12 domains as well as 3 summary scores. The domains of the SIP include Body Care and Movement, Ambulation, Home Management, Mobility, Sleep and Rest, Alertness Behavior, Recreation and Pastimes, Social Interaction, Emotional Behavior, Communication, Work, and Eating. The summary scores include a Physical Dimension, a Psychosocial Dimension, and a Total Score. Scores range from 0–100 with 0 representing the best possible health state.

EuroQol (EQ-5D): The EuroQoL comprises two sections, the EQ-5D index and the EQ-5D visual analog scale (VAS). EQ-5D index has a 3-level, 5-dimensional format, which provides a simple descriptive profile and a single index value for health status. Domains of mobility, self-care, usual activities, pain/discomfort, and anxiety/depression are assessed using a 3-level response scale. The EQ-5D VAS is a 0 to 100 thermometer scale that assesses self-perceived health status. Anchors on the thermometer are 0 (worse possible health state) and 100 (best possible health state). EQ-5D is designed for self-completion by respondents and is ideally suited for use in postal surveys, in clinics and face-to-face interviews.

2.2.3.2 Disease Specific Questionnaires

Lequesne Index of Severity-Knee (Lequesne): The Lequesne consists of 11 questions with various scales utilized for different questions. Questions refer to Pain (5 questions), Walking (2 questions) and Activities of Daily Living (4 questions). Weights are applied in the scoring algorithm and a score range from 0 to 24 is produced. A score of 0 represents a perfect health state.

Western Ontario and McMaster Universities Osteoarthritis Index (WOMAC): The WOMAC consists of 24 Likertbox questions broken down into 3 domains: Pain (5 questions), Stiffness (2 questions) and Physical Function (17 questions). Scores range from 0-20 for Pain, 0-8 for Stiffness and 0-68 for Physical Function. A score of 0 represents the best possible health state. The Likert uses the adjectives none, mild, moderate, severe, and extreme. WOMAC scores can be transformed to a 0 to 100 percent scale to facilitate comparisons with other outcome measures.

Oxford-12 Item Knee Score (Oxford-12): 12 questions are posed relating specifically to the knee. Each question has a Likertbox response key from 1 to 5. A single score is produced ranging from 12 to 60, with 12 indicating the best possible health state.

Visual Analog Scale (VAS): The VAS is a subjective measurement of pain/stiffness intensity in clinical and experimental settings. It consists of a 10 cm (100 mm) straight line of either horizontal or vertical orientation. For instance, the line for pain assessment is anchored by two extremes: “no pain” and “pain as bad as it could be”.

Functional Assessment System of Lower-Extremity Dysfunction (FAS): The FAS is a performance and self-report-based measure developed for use by physiotherapists. It has been tested on patients with osteoarthritis in the hip or knee who are accepted for arthroplasty. It consists of 20 variables, representing major lower extremity dysfunction related to daily life activities. The variables are divided into 5 groups: hip impairment, knee impairment, physical disability, social variables, and pain.

In summary, there are two main categories of outcome questionnaires: general health and disease specific questionnaires. General health questionnaires inquire about various aspects of patients’ perception of their own health, including such diverse domains as ability to sleep, energy level, mood, and perception of body pain. General health questionnaires are not necessarily limited to any particular disease state. Disease specific questionnaires attempt to isolate the signal of interest by focusing questions around a particular disease state.

Although there are many questionnaires to apply to knee arthroplasty patients, there is no general agreement whatsoever regarding specifically which questionnaires to use. There are several problems, however, with the questionnaires. The first is the subjectivity that governs most disability-oriented questionnaires, the second is the restriction to a specific pathology and the third is the low sensitivity to change.

Biomechanical instrumentation, on the other hand, is precise and reliable enough. The main problem does not lie in obtaining the objective data, but in defining a clinical significance and reliable criteria from the data (Lafuente et al. 2000).

To assess the in-vivo functional performance of the different TKR designs, careful quantitative analyses during in-vivo tests must be carried out. Many different techniques for measuring knee kinematics have been reported. Techniques which rely on direct attachment of markers to bone, although potentially quite accurate (Murphy et al. 1985), cannot be considered with Total Knee Replacement (TKR) subjects for fear of infection (Banks and Hodge 1996).

The measurement techniques currently most used in this respect are Fluoroscopic Analysis and Gait Analysis.

2.2.4 Instrumented techniques: Fluoroscopy

Fluoroscopy based technique can measure single plane or 3D TKR kinematics during dynamic activities. The measurement approach is based on the concept that, given the imaging geometry of the fluoroscope and the surface geometry of the prosthetic components, a computer can create an image which matches any experimentally acquired image of the knee. Since the position and orientation (pose) of the prosthetic models are known for the synthesized images, these parameters can be used as estimates of the physical components' pose accurately by avoiding errors due to skin and muscle movements.

Fluoroscopic analysis provides sufficient accuracy to detect relative rotations even of a few degrees between the tibial and femoral components and relative translations even of a few millimeters (~1.5 mm) in the sagittal plane (Banks and Hodge 1996; Dennis et al. 1996; Hoff et al. 1998; Sati et al. 1996; Zihlmann et al.; Zuffi et al. 1999). Based on this method, several important observations on TKR kinematics have been reported. Mobile and Fixed bearing TKR designs have been analyzed during gait (Banks et al. 1997b; Callaghan et al. 2001; Stiehl et al. 1999), step-up (Banks et al. 1997a), and deep knee bend activity (Callaghan et al. 2001; Dennis et al. 1998; Dennis et al. 2001).

The Fluoroscopy based technique, however, has several drawbacks that include: (a) small field of view, which is usually in a fixed position with a field of view of 320 mm, making it impossible to obtain kinematic data from the knee during walking, and also confining the analysis to only a single joint; (b) patient exposure to radiation; and (c) the extensive analysis of the fluoroscopic images (Fantozzi et al. 2003).

2.2.5 Instrumented techniques: Gait Analysis

Gait analysis provides a non-invasive and convenient method for studying full body kinematics and kinetics over large fields of measurements. Gait analysis has been used to assess functional outcome after total knee arthroplasty in numerous studies (Andriacchi et al. 1982; Andriacchi et al. 1997; Berman et al. 1987; Catani et al. 2003; Chao et al. 1980; Collopy et al. 1977; Deluzio et al. 1999; deQuervain et al. 1997; Kaufman et al. 2001; Kroll et al. 1989; Minns 2005; Otsuki et al. 1999; Simon et al. 1983; Smith et al. 2006; Solak et al. 2005; Steiner et al. 1989; Webster et al. 2003).

In this section we review the common branches in studying gait analysis: *Gait kinetics*, *Dynamic electromyography* (EMG), and *Gait kinematics*.

2.2.5.1 Gait Kinetics

Gait kinetics is defined as the forces, moments, and powers that change over the gait cycle. These measurements are captured by the use of force plates embedded in a walkway (Figure 2-1). Gait analysis using pressure measuring system has shown that some temporal and kinetic parameters change significantly after knee arthroplasty (deQuervain et al. 1997; Macellari and Giacomozzi 1996; Weidenhielm et al. 1993). The kinetic pattern continues to improve, although walking pain is reduced sooner after surgery.



Figure 2-1 Force plates measure the ground reaction forces exerted by a person as he/she steps on it during gait. (Photo from Kistler® force plate, Type 9285)

2.2.5.2 Dynamic electromyography

Dynamic electromyography refers to the evaluation of muscle activity throughout the gait cycle. This is accomplished through the use of either surface or needle electrodes. Electromyography (EMG) techniques provide detection and monitoring of electrical muscle activity, however, it does not provide a direct measure of movement, and a substantial number of electrodes and huge amount of data processing are required for studying complex movements such as gait (Den Otter et al. 2006; Frigo et al. 2000; Kleissen et al.

1997; Sutherland 2005). While EMG measurements have provided information regarding the latency and sequencing of active muscle responses, the relationship between specific muscular activation and the resultant outcome cannot be determined from the EMG. In addition, the estimation of muscle force from EMG during dynamic contraction is difficult.

2.2.5.3 Gait kinematics

Gait kinematics refers to the branch of biomechanics that deals with joint angular changes over the gait cycle. Kinematic data can be captured by different motion capture systems such as camera system, electrogoniometer, inertial sensors, etc. Optical motion capture has in recent years become an increasingly helpful tool in the area of human movement science, typically providing valuable information for assessing orthopedic pathologies. In fact, most optical systems are manufactured for medical applications (Molet et al. 1999). The number of companies providing motion capture systems targeting the areas of biomechanics, sport performance, and gait analysis reflects their relevance in these domains. Complete systems are available from various providers, such as VICON™ system, Elite™ system, Ariel™ system, CODA™ system, Qualisys Proreflex system, Peak Performance's Motus system, and Motion Analysis HiRes system (Ehara et al. 1997; Richards 1999; Sutherland 2002). They allow the collection of information for illustrating and analyzing gait dynamics and studying the behavior of body limbs and joints during various motions, such as walking, running, limb raising, etc.

In addition, ultrasound based systems such as ZEBRIS system (ZEBRIS Medizintechnik GmbH, Germany), and magnetic tracking systems such as Liberty LATUS®, MotionStar® and (Inition Ltd., UK) allow a complete 3D kinematic analysis of human movements.

However, the level of detail that is available through motion capture is open to discussion (Cappozzo et al. 1997; Cappozzo et al. 1995; Cappozzo et al. 1996b). Because the markers/sensors are placed on the skin surface, and not directly on the bones and joints, some systematic error do occur. This results in significant measurement uncertainty for determining knee translation and out-of-sagittal plane rotations (Cappozzo et al. 1996b; Ramsey and Wretenberg 1999). Furthermore, high quality systems are very expensive, require a dedicated laboratory with a lot of room space, and not convenient for the patient. The most inconvenient aspect of these systems is that the subject must move inside a closed and restricted space, hence capturing the motion is limited to a short distance (e.g. only a few steps during walking) and it is assumed that this data corresponds to everyday and usual activity.

During the past decade, technical progress has made it possible to realize miniature kinematic sensors (e.g. accelerometers and gyroscopes) with integrated conditioning and capturing module (Dejnabadi et al. 2006). In addition, due to their very low consumption, these sensors can be battery powered and are promising tools for outdoor measurement and ambulatory monitoring. Unlike the standard technology which needs a dedicated controlled space, the body-fixed sensors can be used anywhere. They are highly transportable and do not need a stationary unit such as a transmitter, receiver, or camera. Therefore, signals can be continuously recorded without any trajectory loose due to obstacles or marker hiding. These sensors are much cheaper than ultrasonic, magnetic and optical motion captures. They are easy to set up and use, and do not require highly skilled operators. Furthermore, body-fixed sensors can also be used to determine kinetic parameters such as hip abduction moments (Zijlstra and Bisseling 2004).

Conversely, body-fixed sensors require a high number of sensors in order to be able to provide an accurate 3D kinematics. Cables between sensors and the recording units may in some cases limit the performance of the motion capture. So, the number of sensors and their sights of attachments must be reduced and optimized while keeping sufficient information to reconstruct and synthesize the movement. Additionally, unlike to camera-based systems, body-segment coordinates cannot be measured directly, and requires a complex kinematic modeling and data processing of raw sensory data.

Electro-goniometers (Myles et al. 2002b; Roduit et al. 1998; Shiratsu and Coury 2003a), foot pressure sensors (AbuFaraj et al. 1997; Zhu et al. 1991), accelerometers (Aminian et al. 1998; Aminian et al. 1999; Zijlstra 2004; Zijlstra and Hof 2003), gyroscopes (Dejnabadi et al. 2005a; Tong and Granat 1999b), and magnetic compass (Lee et al. 2003; Roetenberg et al. 2005) are the main body-fixed sensors used in ambulatory monitoring.

2.3 Conclusion

In this chapter we reviewed common evaluation systems (both scoring questionnaires and instrumented techniques) used to assess total knee arthroplasty outcome. A large variety of scoring questionnaires have been used to assess the outcome of TKR. There are, however, several issues with the questionnaires. The first is the subjectivity which is based on the observer's experience and individual bias, the second is the restriction to a specific pathology, and the third is the low sensitivity to change.

Therefore, the use of objective instruments that have a better sensitivity and specificity than traditional scoring systems is needed to evaluate the results of arthroplasty and enhance the surgeon's ability to assess the overall outcome. Among measuring tech-

niques used for TKR outcome evaluation, gait analysis is well standardized and currently most used. Gait analysis and questionnaires are complementary for arthroplasty outcome measure (Lindemann et al. 2006).

However, all these measuring tools are accessible only in a few specialized laboratories, as they are complex, expensive, need a lot of room space and fixed devices, and not convenient for the patient.

In this thesis, we proposed an ambulatory system based on kinematic sensors attached on the lower limbs in order to overcome the limitations of the previously mentioned techniques. The main features of the measurement device were to be portable, easy to use, accurate, unobtrusive, and capable of continuously recording data in long-term without hindrance to natural gait. Moreover, new algorithms were proposed to accurately measure joints and segments angles in the sagittal plane. These data were then used to develop a gait analysis system providing spatio-temporal parameters, multi-joint coordination analysis, kinematic curves, and skeleton visualization.

Chapter 3 Estimation of Lower Limbs Joint Angles

Abstract

In this chapter, a new method of measuring joint angle using a combination of accelerometers and gyroscopes is presented. The method proposes a minimal sensor configuration with one sensor module mounted on each segment. The model is based on estimating the acceleration of the joint center of rotation by placing a pair of virtual sensors on the adjacent segments at the center of rotation. In the proposed technique, joint angles are found without the need for integration, so absolute angles can be obtained which are free from any source of drift. The model considers anatomical aspects and is personalized for each subject prior to each measurement. The method was validated by measuring knee flexion-extension angles of eight subjects, walking at three different speeds, and comparing the results with a reference motion measurement system. The results are very close to those of the reference system presenting very small errors (RMS = 1.3, mean = 0.2, SD = 1.1 deg) and excellent correlation coefficients (0.997). The algorithm is able to provide joint angles in real-time, and ready for use in gait analysis. Technically, the system is portable, easily mountable, and can be used for long term monitoring without hindrance to natural activities.

3.1 Introduction

During the last decade, body-mounted sensors consisting of accelerometers and/or rate gyroscopes have been used to obtain kinematic values such as shank and thigh inclination angles, and knee joint angle (Aminian et al. 2002a; Mayagoitia et al. 2002). These data can be derived by integration of angular acceleration or angular velocity. However, data obtained from integration can be distorted by offsets or any drifts (Aminian and Najafi 2004; Willemsen et al. 1990). The two major sources of drift are: 1) Electronic bias error (Titterton and Weston 1997), and 2) Deviation and turning out from the sensing axis. In order to eliminate any drift during integration, Morris (Morris 1973) identified the beginning and the end of the walking cycles, and made the signal at the beginning and the end of the cycle equal. Tong et al. (Tong and Granat 1999a) applied a low-cut high-pass filter on the shank and thigh inclination angle signals. Time-frequency analysis (Wavelet Transform) was also applied to lower limb angular velocity in order to remove

the drift (Aminian et al. 2004a). However, all of these methods remove the dc and low frequency information of angles.

Willemsen et al. (Willemsen et al. 1990) developed a technique to measure human joint flexion-extension angle without the need for integration, which used four accelerometers on each segment. The system used two metal bars with eight accelerometers for measuring a single joint angle. Heyn et al. (Heyn et al. 1996) showed that shank and thigh inclination angles can be measured with eight accelerometers and two gyroscopes fixed on two rigid metal plates as well. They also found that using these metal plates was cumbersome.

In this chapter we present a new method to estimate flexion-extension angles based on a combination of accelerometers and gyroscopes. The number of sensor units has been optimized to one unit on each segment. The model is based on estimating acceleration of the joint center of rotation. Since it is not physically possible to place accelerometers at the joint center of rotation, virtual sensors are used by mathematically shifting the location of the physical sensors. In order to minimize the error, it is necessary to obtain accurate positions of the physical and virtual sensors. Therefore, the model was personalized by including anthropometric data and the position of the sensors obtained by photography.

3.2 Methods

3.2.1 Model description

Considering the two-dimensional model of a segment motion (Figure 3-1), a sensor module including a biaxial accelerometer and a gyroscope was placed at point P on the segment. The first step was to calculate the expected signals of a virtual sensor module placed at an arbitrary point C on the bone segment with an arbitrary orientation with respect to the physical sensor module. The vector \mathbf{r} indicates the PC distance, and the angles α and β represent the orientations of the physical and virtual sensors with respect to \mathbf{r} .

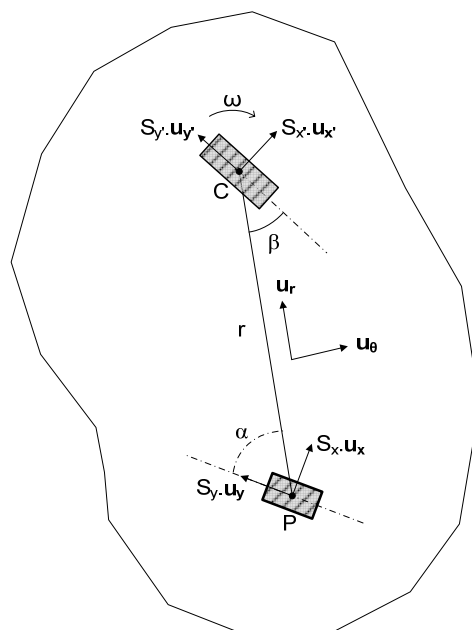


Figure 3-1 A physical sensor module at point P, and a virtual sensor module on point C on a 2D rigid body. Each sensor module consists of 2D accelerometers and a gyroscope.

In order to estimate the virtual signals, a description of the outputs of the sensors was required. A single axis accelerometer measures the difference of acceleration (\mathbf{a}) and gravity (\mathbf{g}) along its sensitive axis given by the unit vector (\mathbf{n}). The measured electrical signal (S) could thus be expressed as

$$S = (\mathbf{a} - \mathbf{g}) \cdot \mathbf{n}. \quad (3.1)$$

Similarly, by considering a 2D accelerometer with sensitive axes along \mathbf{u}_x and \mathbf{u}_y , the two measured signals were given by

$$\begin{aligned} S_x &= (\mathbf{a} - \mathbf{g}) \cdot \mathbf{u}_x \\ S_y &= (\mathbf{a} - \mathbf{g}) \cdot \mathbf{u}_y. \end{aligned} \quad (3.2)$$

The angular velocity of the segment was obtained by measuring the rate of change of the unit vector \mathbf{n}

$$\boldsymbol{\omega} = \mathbf{n} \times \frac{d\mathbf{n}}{dt}. \quad (3.3)$$

This parameter could directly be measured by a gyroscope with its sensitive axis perpendicular to the plane of motion.

For analytical convenience, human body segments were considered as rigid bodies. The main strategy in analyzing the motion of a rigid body was to split the motion into the linear motion of the non-inertial reference point P, and the angular motion of the segment about it. Thus the relationship between the physical and virtual sensors readings could be expressed as

$$R_{\beta} \cdot \begin{bmatrix} S_{x'} \\ S_{y'} \end{bmatrix} = R_{\alpha} \cdot \begin{bmatrix} S_x \\ S_y \end{bmatrix} + \frac{d^2 \mathbf{r}}{dt^2} \quad (3.4)$$

where S_x and S_y are physical 2D accelerometer readings; $S_{x'}$ and $S_{y'}$ are virtual accelerometer readings. R_{α} and R_{β} are axis rotation matrices of the physical and virtual sensors in relation to the direction of vector \mathbf{r} by angles α and β respectively. These rotations align both physical and virtual coordinate systems to the direction of PC line.

The first term in the right hand of (3.4) considers the effect of a linear motion, and the second term expresses the effect of a pure rotation about point P. The latter term can be expanded into components aligned with and normal to \mathbf{r} (unit vectors \mathbf{u}_r and \mathbf{u}_θ)

$$\frac{d^2 \mathbf{r}}{dt^2} = \frac{d}{dt} (\dot{\mathbf{r}} \cdot \mathbf{u}_r) = -r\dot{\theta}^2 \cdot \mathbf{u}_r + r\ddot{\theta} \cdot \mathbf{u}_\theta \quad (3.5)$$

where $\dot{\theta}$ and $\ddot{\theta}$ are the first and second derivatives of angle of \mathbf{r} with respect to a fixed inertial frame.

The two latter parameters can be measured by the gyroscope placed at point P. The virtual gyroscope reading at point C will also give the same signal (Tong and Granat 1999a). So considering $\dot{\theta}$ and $\ddot{\theta}$ equal to ω and $\dot{\omega}$ respectively, (3.4) can be rearranged to yield the virtual accelerometer readings with respect to known physical accelerometers and gyroscope readings

$$\begin{bmatrix} S_{x'} \\ S_{y'} \end{bmatrix} = R_{-\beta} \cdot \left(R_{\alpha} \cdot \begin{bmatrix} S_x \\ S_y \end{bmatrix} + \begin{bmatrix} -r \cdot \omega^2 \\ r \cdot \dot{\omega} \end{bmatrix} \right). \quad (3.6)$$

The next step was to calculate joint angle (φ) between two segments using two modules of sensors mounted on each segment Figure 3-2. Thus, the two physical sensor modules on each segment were shifted to the joint center, or more precisely the center of rotation point, such that each virtual sensor aligns with its corresponding segment orientation. Since one point should physically have a unique acceleration, the two virtual sensors

meeting at the center of rotation should give equal accelerations. However, the correction for coordinate frames rotation by angle φ should be considered

$$\begin{bmatrix} S_{x'_1} \\ S_{y'_1} \end{bmatrix} = R_\varphi \cdot \begin{bmatrix} S_{x'_2} \\ S_{y'_2} \end{bmatrix} \quad (3.7)$$

where $\mathbf{S}'_1 = [S_{x'_1} \ S_{y'_1}]'$ and $\mathbf{S}'_2 = [S_{x'_2} \ S_{y'_2}]'$ are virtual accelerometers readings at point C on segments 1 and 2 respectively. These vectors can be rewritten in polar representation

$$\begin{aligned} \mathbf{S}'_1 &= e^{i\theta_1} \cdot S'_1 \\ \mathbf{S}'_2 &= e^{i\theta_2} \cdot S'_2 \end{aligned} \quad (3.8)$$

where S'_i and θ_i represent for modulus and argument of \mathbf{S}'_i ; and thus equation (3.7) can be rewritten to yield joint angle φ

$$\begin{aligned} S'_1 &= S'_2 \\ \varphi &= \theta_2 - \theta_1. \end{aligned} \quad (3.9)$$

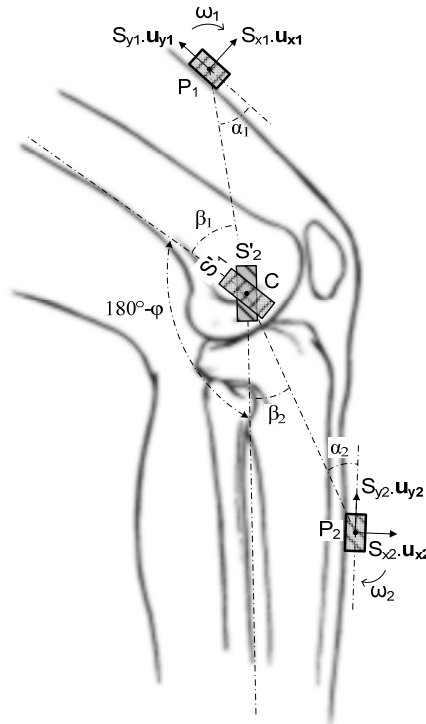


Figure 3-2 Position of sensors on thigh and shank, and their corresponding virtual sensors on the knee joint center of rotation.

3.2.2 Sensor configuration

Throughout this thesis, a unique sensor configuration was used. Lower limbs movements were captured by 5 modules of sensors attached on shanks, thighs, and sacrum. Each module consisted of a gyroscope and bi-axial accelerometers. Dual axis accelerometer chips ADXL202/210 and yaw rate gyro chips ADXRS150/300 were chosen. Temperature drift rates were less than 0.1 deg/s for the gyroscopes and few mg for the accelerometers.

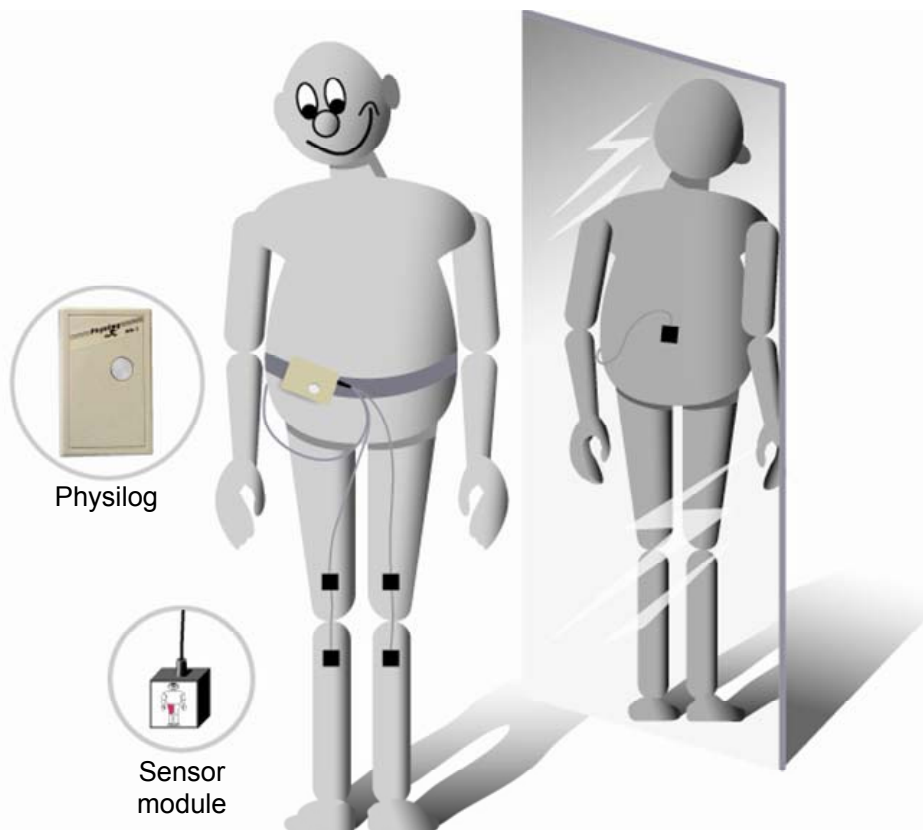


Figure 3-3 Sensor configuration used throughout this thesis. Five modules of sensors were placed on thighs, shanks, and sacrum. The kinematic data were recorded by the Physilog system (dimensions 13 cm x 7 cm x 3 cm, weight: 300g).

To calculate the knee angle (flexion-extension) using the proposed model, the sensor modules attached on thighs and shanks were used. The sensors (dimension: 20 mm x 20 mm x 10 mm) were mounted on the shank and thigh segments using a strap [Figure 3-4(a)]. The sensing axes were adjusted in the antero-posterior plane so that the flexion-extension angle could be measured. All signals were sampled at 200-Hz using the Physilog® [BioAGM, CH] ambulatory system carried on the waist (Aminian et al. 2002a).

3.2.3 Test protocol

Eight healthy subjects, who had given informed consent, participated in this experiment, 5 men and 3 women, aged between 44 and 70 yr (mean = 58.7 yr). The volunteers performed three 30 s flat treadmill walking trials at speeds 2, 3, and 4 km/h, wearing their basket shoes. One of the subjects was also requested to perform a freely arbitrary flexion and extension of knee, such as sitting, standing, and swinging.

Before the walking trials, three small markers were pasted over the left lateral malleolus (M_2), the lateral epicondyle (C), and the junction of the first and second proximal lateral third of the thigh (M_1) [Figure 3-4(b)]. Then each subject was asked to stand in two positions at extended [Figure 3-4(b)] and flexed [Figure 3-4(c)] left knee positions, while the shank was kept stationary. At each position the subject stayed for a few seconds (<5 s) at standstill, while the system was recording kinematic parameters, a lateral view photograph was taken as well. The camera's image plane was adjusted to be in parallel with sagittal plane to avoid perspective errors. The position and orientation of the camera was kept constant so that the two photos would have the same field of view. The known length of the metal frame (70 cm height) was used to calibrate the photos from pixels to metric units (cm). These images were used to estimate the coordinates of markers and kinematic sensors. Any arbitrary point in the images (e.g., top-left pixel) can be defined as the coordinate reference. The accelerometer's readings during standstill were used to estimate the sensor's orientation with respect to horizontal plane. These information were used to calculate the angles α_1 , α_2 , β_1 , β_2 , and the lengths of P_1C and P_2C .

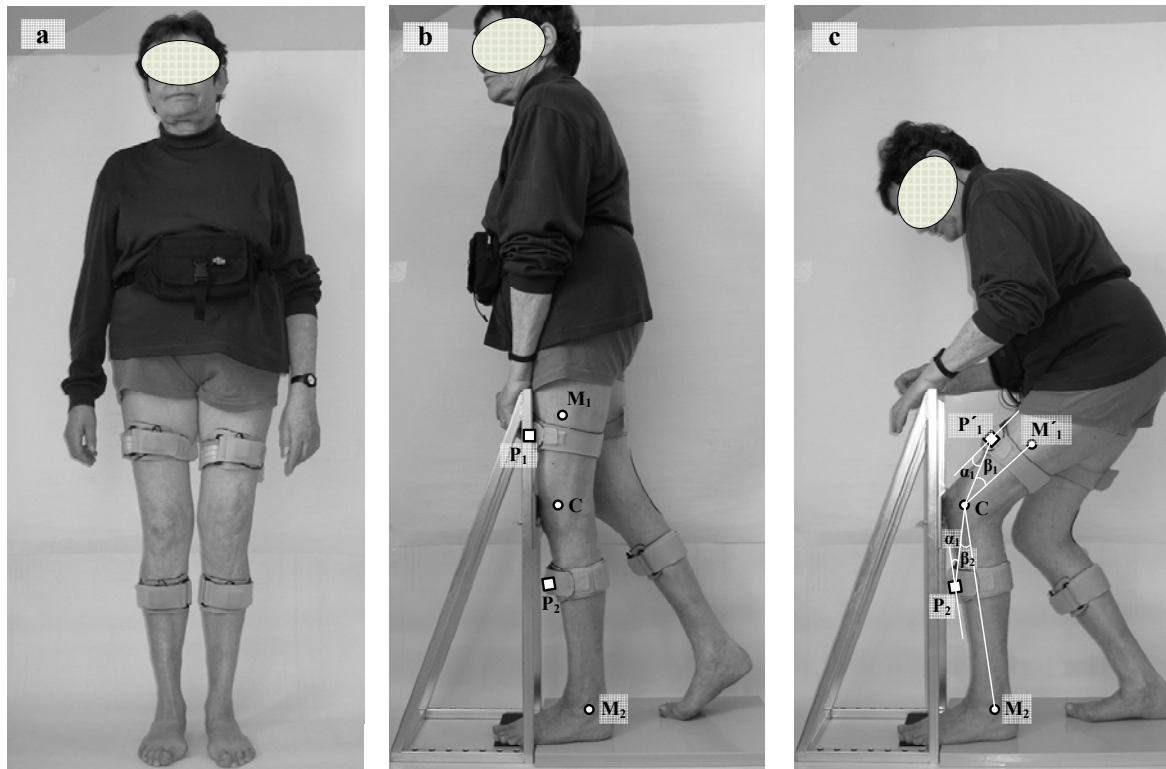


Figure 3-4 (a) Attachment of the kinematic sensors on both thighs and shanks using straps. The Physilog system is placed in the waist bag. (b) Sagittal view of a subject with extended left knee and (c) with flexed left knee, representing the sensor configurations. The white circles indicate the position of markers (M_1 , C and M_2), and the white squares indicate the position of kinematic sensors (P_1 and P_2).

It is important to accurately find the knee center of rotation. Many researchers have established methods based on minimizing an optimization function in which data from gait kinematics, anthropometric measurements and statistically derived morphological parameters are properly weighted (Frigo et al. 2000; Gamage and Lasenby 2002; Schwartz and Rozumalski 2005). In this study, we applied a simpler method to better adjust the position of the center of rotation (C). It is based on the geometric relationship between the positions of marker M_1 and sensor P_1 at the two different positions. Since the shank is stationary, any point on thigh always lies on the circle they form with the knee joint being the center. In this case the line connecting two different positions of the same point at the two different trials is always perpendicular to the line drawn from the joint to their mid point (Halvorsen et al. 1999)

$$\begin{aligned} \begin{bmatrix} x_{M_1} - x_{M'_1} & y_{M_1} - y_{M'_1} \end{bmatrix} \cdot \begin{bmatrix} \frac{x_{M_1} + x_{M'_1}}{2} - x_C \\ \frac{y_{M_1} + y_{M'_1}}{2} - y_C \end{bmatrix} &= 0 \\ \begin{bmatrix} x_{P_1} - x_{P'_1} & y_{P_1} - y_{P'_1} \end{bmatrix} \cdot \begin{bmatrix} \frac{x_{P_1} + x_{P'_1}}{2} - x_C \\ \frac{y_{P_1} + y_{P'_1}}{2} - y_C \end{bmatrix} &= 0 \end{aligned} \quad (3.10)$$

where the indices P_1 and M_1 indicate the sensor and marker on thigh in the first trial [Figure 3-4 (b)], and P'_1 and M'_1 in the second trial [Figure 3-4 (c)] respectively. Consequently, the modified coordinates of point C was obtained:

$$\begin{bmatrix} x_C \\ y_C \end{bmatrix} = \frac{1}{2} \cdot \begin{bmatrix} x_{P_1} - x_{P'_1} & y_{P_1} - y_{P'_1} \\ x_{M_1} - x_{M'_1} & y_{M_1} - y_{M'_1} \end{bmatrix}^{-1} \cdot \begin{bmatrix} (x_{P_1}^2 + y_{P_1}^2) - (x_{P'_1}^2 + y_{P'_1}^2) \\ (x_{M_1}^2 + y_{M_1}^2) - (x_{M'_1}^2 + y_{M'_1}^2) \end{bmatrix}. \quad (3.11)$$

The angle β_1 was obtained from the dot product formula:

$$\beta_1 = \cos^{-1} \left(\frac{\overline{\mathbf{P}_1\mathbf{C}} \cdot \overline{\mathbf{M}_1\mathbf{C}}}{|\overline{\mathbf{P}_1\mathbf{C}}| \cdot |\overline{\mathbf{M}_1\mathbf{C}}|} \right) \quad (3.12)$$

where $\overline{\mathbf{P}_1\mathbf{C}} = [x_{P_1} - x_C \quad y_{P_1} - y_C]'$, and $\overline{\mathbf{M}_1\mathbf{C}} = [x_{M_1} - x_C \quad y_{M_1} - y_C]'$.

The angle α_1 was obtained by calculating the difference between inclination angles of the kinematic sensor (S_1) and the vector $\overline{\mathbf{P}_1\mathbf{C}}$:

$$\alpha_1 = \tan^{-1} \left(\frac{\overline{S_{y1}}}{\overline{S_{x1}}} \right) - \tan^{-1} \left(\frac{y_{P_1} - y_C}{x_{P_1} - x_C} \right) \quad (3.13)$$

where $\overline{S_{x1}}$ and $\overline{S_{y1}}$ are averages of the 2D accelerometer readings during the standstill trial.

Similarly, the values of α_2 and β_2 were obtained by changing all indices '1' to '2' in equations (3.12) and (3.13).

For comparison, a Zebris CMS-HS (Zebris, D) ultrasound-based motion measurement system was used as the reference system (Kiss et al. 2004). This system consists of three fixed sonic emitters which send out a burst of ultrasound, and receivers placed on body

segments. The time taken for the burst to reach each receiver is recorded. Using this delay, the distances between the receiver and each emitter can be calculated from the sound velocity. Knowing the distance from three emitters, the coordinates of the receiver placed on body segment can be computed by triangulation with an absolute accuracy better than 1.0 mm (GmbH 1999; Overhoff et al. 2001) with a sampling rate of 100-Hz. In this study, three ultrasound receivers were attached over the same adhesive markers (M_1 , M_2 and C). Spatial marker positions (x , y , z) were recorded and used for calculation of knee flexion-extension angle. Synchronization between the reference and the Physilog systems was performed by electrical trigger. The angle data obtained by the body-fixed sensors were down sampled to 100-Hz for comparison purpose.

3.2.4 Data analysis

Matlab was used for all signal processing. A third order Savitzky-Golay filter (Savitzky and Golay 1964) was applied to smooth the accelerometers and gyroscopes signals. Anthropometry data obtained by photography were also fed to the model to estimate the expected virtual sensors readings shifted to the knee center of rotation.

For comparison with the reference system, the error signal was defined as the difference between the angle obtained by the proposed method and the reference system.

Statistical analyses comprised RMS, mean and standard deviation of difference error, as well as correlation coefficient calculations between the joint angles obtained by the proposed method and the reference system's data.

3.3 Results

Figure 3-5 to Figure 3-8 show the steps of calculating knee angle of subject no. 8 during a flat walking at 3 km/h. Figure 3-5 shows the physical accelerometers and gyroscopes (raw data) readings placed on thigh and shank. Figure 3-6 shows the virtual accelerometers readings placed at the knee center of rotation on the adjacent segments. Figure 3-7 shows the polar representation (modulus, argument) of the same virtual accelerometers, as well as the difference between the two moduli signals ($modulus(S'_2) - modulus(S'_1)$). Since both S'_1 and S'_2 express the accelerations of the same point C, the value of the difference is very small ($0.05 \pm 0.18 \text{ m/s}^2$). Figure 3-8(a) shows the final step yielding the knee angle calculated from the difference between the two argument signals ($argument(S'_2) - argument(S'_1)$). Figure 3-8(b) shows the knee angle calculated from

position data as measured by the reference system, and difference error between the two results.

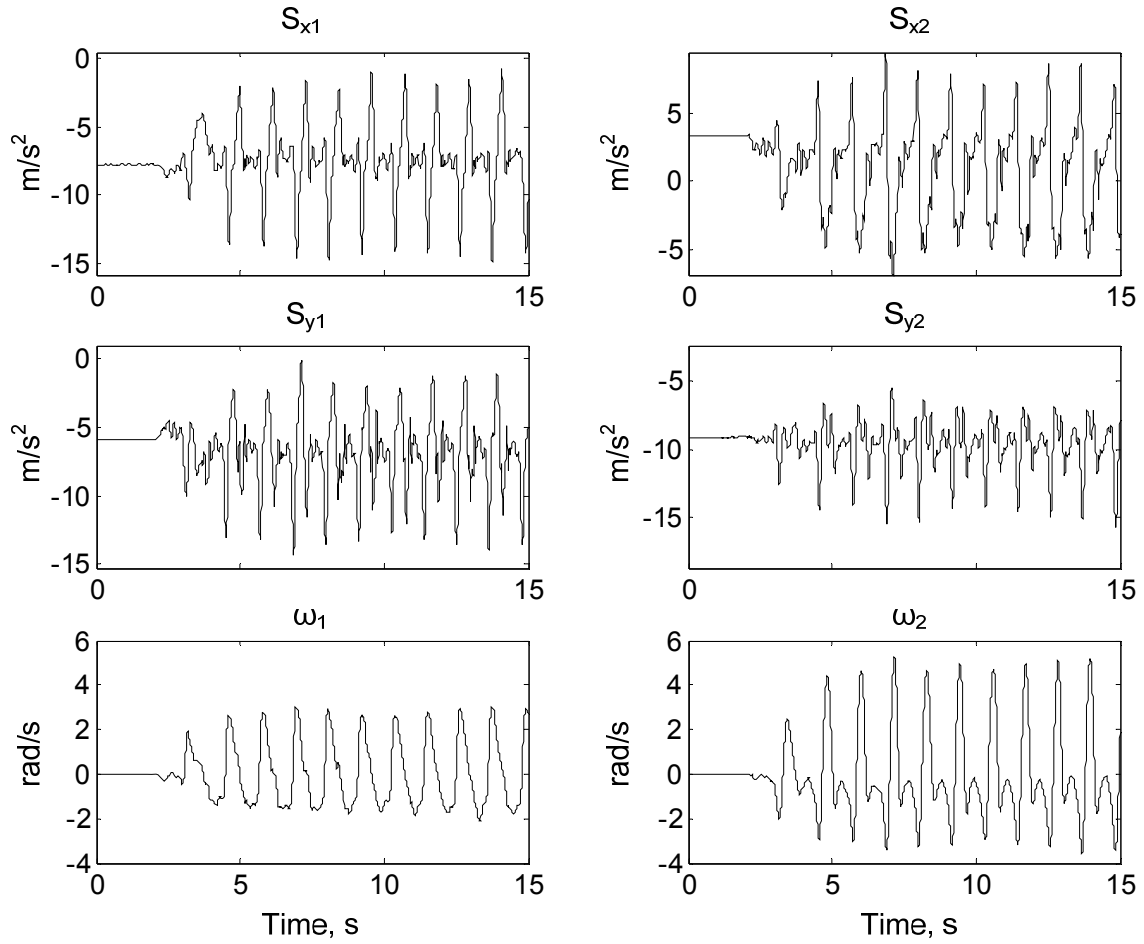


Figure 3-5 Physical accelerometers and gyroscopes (raw data) readings during walking at 3 km/h. The site on thigh consists of two accelerometers (S_{x1} and S_{y1}) and a gyroscope (ω_1). Similarly, there are two accelerometers (S_{x2} and S_{y2}) and a gyroscope (ω_2) on shank module.

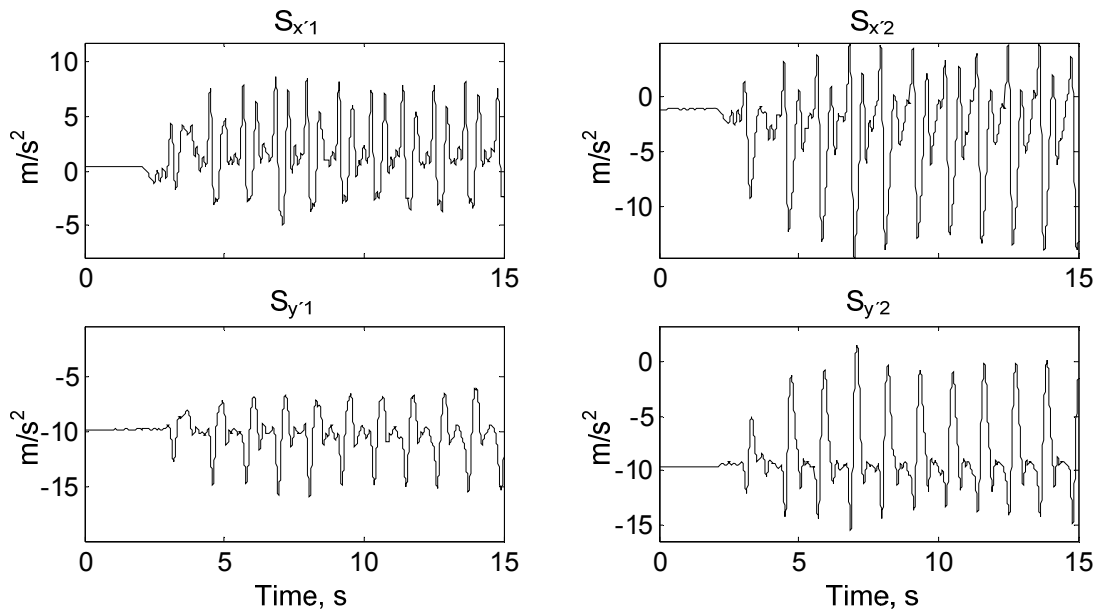


Figure 3-6 Virtual accelerometers readings placed at the knee center of rotation on the adjacent segments. $S_{x'1}$ and $S_{y'1}$ are biaxial virtual accelerometers on thigh. Correspondingly, $S_{x'2}$ and $S_{y'2}$ are biaxial virtual accelerometers on shank. The signals are calculated from the raw signals shown in Figure 3-5.

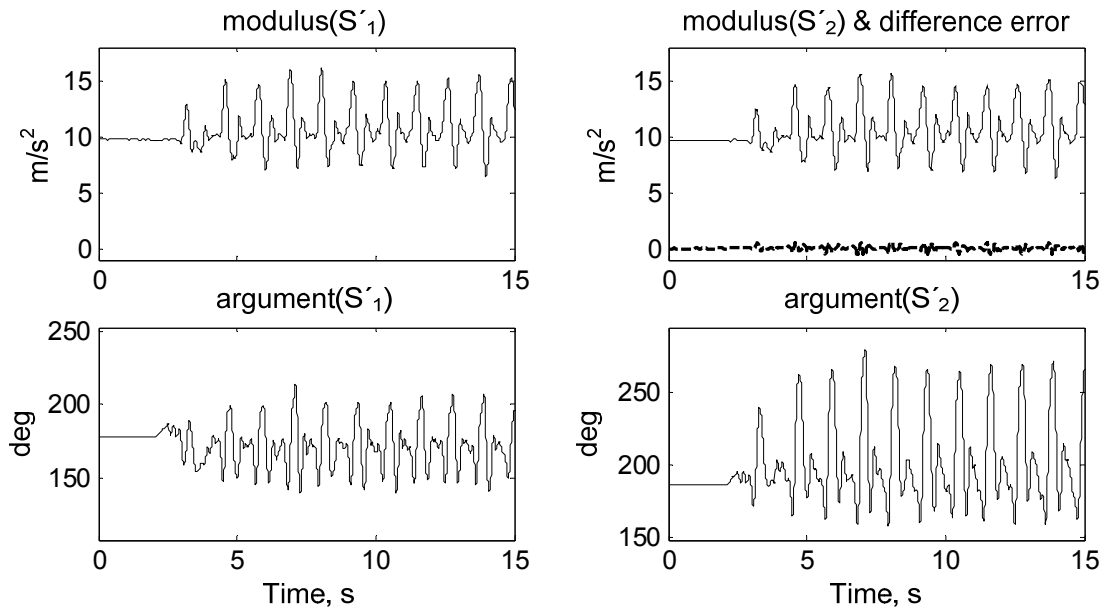


Figure 3-7 Polar representation (modulus, argument) of the virtual accelerometers calculated from the signals shown in Figure 3-6. S'_1 and S'_2 are complex vectors equal to $[S_{x'1} \ S_{y'1}]'$ and $[S_{x'2} \ S_{y'2}]'$ respectively. The top-right figure shows also the difference between the two moduli signals ($modulus(S'_2) - modulus(S'_1)$) in dashed line.

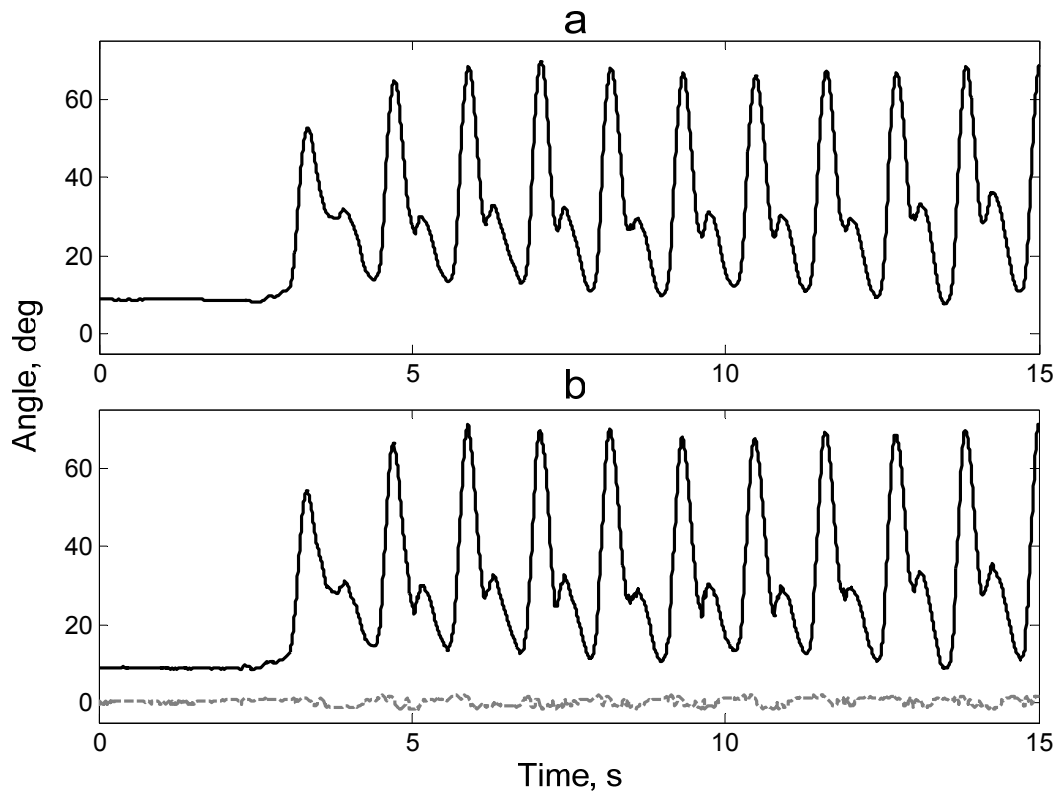


Figure 3-8 (a) Knee angle calculated from the difference between the two argument signals shown in Figure 3-7 ($\text{argument}(S'_2) - \text{argument}(S'_1)$). (b) Calculated from position data as measured by the reference system (solid line), and difference error between the two results (dashed line).

Figure 3-9 shows also the final step of calculating knee angle and its comparison with the reference system during a freely arbitrary flexion and extension of knee (correlation coefficient = 0.9995, error=0.30±1.1 deg).

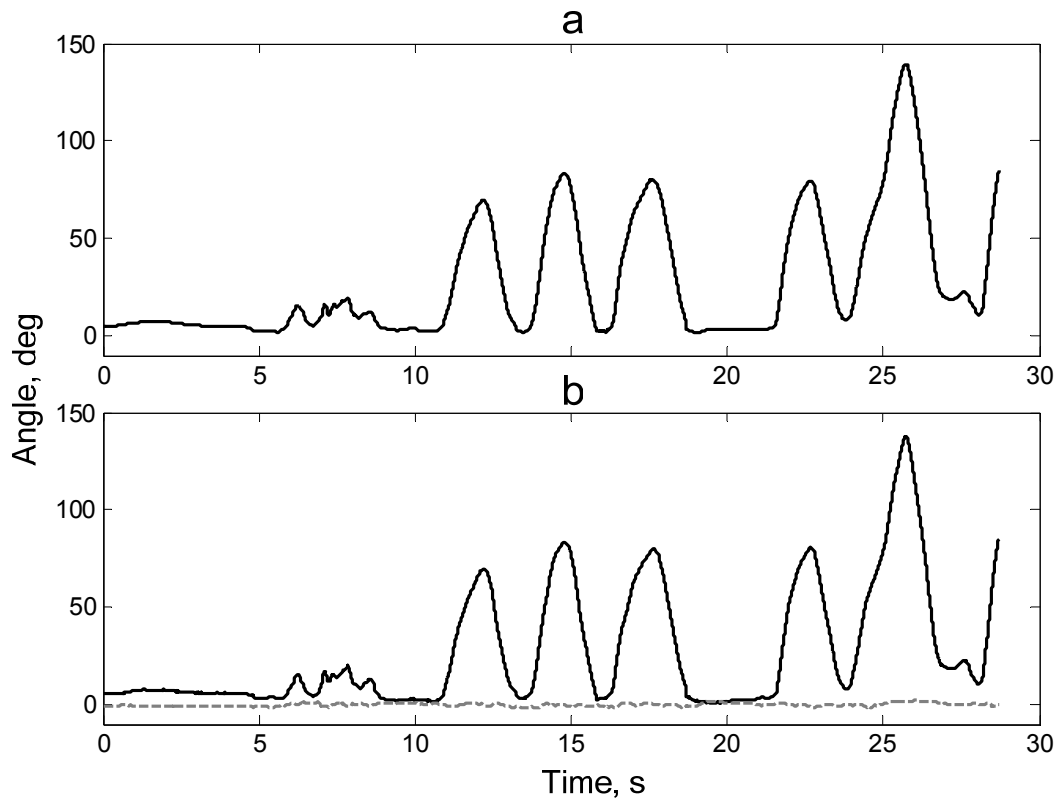


Figure 3-9 Absolute knee angle during a freely arbitrary flexion and extension of knee. (a) Calculated from the new accelerometers and gyroscopes settings. (b) Calculated from position data as measured by the reference system (solid line), and difference error between the two results (dashed line).

The whole results are summarized in Table 3-1, which outlines the mean and standard deviation of difference errors, together with the calculated correlation coefficients of eight subjects. The average RMS error is 1.30 degrees (mean = 0.20, SD = 1.1 deg) and the average correlation coefficient is 0.997.

Table 3-1 Comparison between knee angle measurements obtained by body-mounted sensors and Zebris markers for 8 subjects at 3 speeds. The error represents the RMS, mean and SD of the difference signal between Zebris and our measuring device. 'r' represents the Correlation Coefficient between the two measuring systems.

Subject	Slow (2km/h)		Intermediate (3km/h)		Fast (4km/h)	
	Error, deg RMS,(mean±SD)	Correlation Coefficient (r)	Error, deg RMS,(mean±SD)	Correlation Coefficient (r)	Error, deg RMS,(mean±SD)	Correlation Coefficient (r)
<i>Subject 1</i>	1.60, (0.70±1.04)	0.9975	1.75, (0.23±1.03)	0.9966	2.35, (-0.42± 1.07)	0.9941
<i>Subject 2</i>	1.11, (-0.16±1.09)	0.9984	1.10, (0.00±1.09)	0.9985	1.39, (-0.50±1.29)	0.9980
<i>Subject 3</i>	1.13, (-0.34±1.07)	0.9977	1.68, (-0.23±1.65)	0.9959	2.04, (0.009±2.04)	0.9956
<i>Subject 4</i>	1.00, (0.12±0.99)	0.9990	1.12, (-0.01±0.91)	0.9988	1.25, (-0.44±1.01)	0.9980
<i>Subject 5</i>	0.91, (-0.09±0.90)	0.9975	0.91, (-0.09±0.90)	0.9985	1.09, (-0.26±1.05)	0.9985
<i>Subject 6</i>	0.99, (0.39±0.90)	0.9978	1.07, (0.18±1.05)	0.9982	1.09, (0.11±1.07)	0.9984
<i>Subject 7</i>	0.98, (0.16±0.97)	0.9973	1.06, (0.10±1.05)	0.9982	1.38, (-0.02±1.38)	0.9962
<i>Subject 8</i>	1.30, (-0.32±1.26)	0.9975	1.36, (-0.48±1.27)	0.9975	1.77, (-0.08±1.16)	0.9953

3.4 Discussion and conclusion

The proposed method based on body-fixed sensors gave an accurate estimation of knee flexion-extension angles. Though the study has focused on the use of body-fixed sensors for measuring knee flexion-extension angle, the method can be applied to measure other joint angles like elbow (by attaching sensors on arm and forearm). Although multiaxial measurement is more powerful, in many cases a simple uniaxial measurement can be effective as well, giving a lot of information for pathologies related to knee.

The results of all tests (Table 3-1) were very close to those of the reference system presenting small errors in RMS (1.30 deg), mean (0.20 deg) and standard deviation (1.1 deg) of the difference signal, reflecting accurate and precise estimations respectively; and excellent correlation coefficient values (0.997) reflecting highly linear response.

In comparison with the previous methods using metal plates (Willemsen et al. 1990) which were cumbersome and needed 4 fixation sites of sensors, the proposed used a minimal sensor configuration with one fixation site on each segment. In addition, our method is more accurate and more precise, since the reported mean error in (Willemsen et al. 1990) is 2.9 deg, and standard deviation of error ranges from 2.3 deg to 5.1 deg.

Other authors reported joint angle measurement by integrating gyroscopes and accelerometers (Aminian et al. 2004a; Morris 1973; Tong and Granat 1999a). However, data obtained from integration can be distorted by offset or any drift, so additional filtering or assumptions based on cyclic nature of gait are required for drift canceling that will also remove the dc and low frequency information of angles. In contrast to other studies where the relative knee angle was estimated, in this study the absolute joint angle was found without the need of integration with the advantage to be free from any source of drift. In addition, no assumption based on cyclic nature of gait is made in the model, so the knee joint angle can be obtained for any freely arbitrary movements as it was shown in Figure 3-9.

Since the angle computation needs simple multiplications and derivative operations, this system is able to provide real-time knee angle for any type of activity. So the clinicians are able to view joint angle motion as the subject performs the prescribed activity, or generally it can be used in many other applications that require real-time feedback.

The proposed model considers anatomical aspects of each subject prior to each measurement that leads to higher accuracy in the results. In this way, a better orientation of bone segments (femur and tibia) can be estimated from the sensors placed on the skin as it was described in Figure 3-2 and (3.10)–(3.12).

However, there are some limitations in the model due to assuming the joint center of rotation as a fixed position point, and segments as rigid bodies. Although the joint center of rotation changes slightly depending on the knee angle (Moorehead et al. 2003), this effect induces very minimal changes in the knee joint angle. The model allows a uniaxial (flexion-extension) estimation of joint angle; however it does not constrain the joint motion to take place in sagittal plane: any flexion-extension even out of the sagittal plane can be estimated.

Skin motion artefact, a common source of error to all body mounted devices, affects the measurement accuracy. The thigh sensor is more susceptible to skin and soft tissue artifact where the majority of the femur is concealed by a substantial amount of soft tissue. The effect of skin artefact was minimized by using adequate elastic band to fix the sensors, and applying low-pass filtering on the raw signal.

From a practical standpoint, misalignment of the sensors or sensor deviation during movement reduces the system's accuracy. Fortunately, there is a redundant information in the system which can be used to check the overall effects of error sources, but the information is not enough to correct or compensate for the errors. This information is

obtained by checking the error difference between the moduli signals of the two virtual accelerometers (Figure 3-7).

Technically, the system is portable, easily mountable, and it can also be used for long term monitoring without hindrance to the natural gait (Aminian et al. 2002a). In comparison with video-based systems, this system can be an alternative solution for capturing kinematic information over a non-limited distance and outside a laboratory environment.

The proposed method was found very promising in providing actual knee flexion-extension angle during daily activities. Based on its MEMs technology, gyroscopes and accelerometers also offer a cheaper and more practical solution to the cumbersome electro-goniometer link over the knee as well (Myles et al. 2002a; Shiratsu and Coury 2003b). Moreover, unlike electro-goniometers, the proposed system provides also anterior-posterior rotations and linear accelerations of thigh and shank independently, which can further be used for a better estimation of lower limbs kinematics. However, with this method only relative motion of shank and thigh orientations is provided. In the next chapter, we will extend this method to estimate absolute thigh and shank orientations.

Chapter 4 Estimation of Lower Limbs Orientations

Abstract

A new method of estimating lower limbs orientations using a combination of accelerometers and gyroscopes is presented in this chapter. The model is based on estimating the accelerations of ankle and knee joints by placing virtual sensors at the centers of rotation. The proposed technique considers human locomotion and biomechanical constraints, and provides a solution to fusing the data of gyroscopes and accelerometers that yields stable and drift-free estimates of segment orientation. The method was validated by measuring lower limb motions of eight subjects, walking at three different speeds, and comparing the results with a reference motion measurement system. The results are very close to those of the reference system presenting very small errors (Shank: rms = 1.0, Thigh: rms = 1.6 deg) and excellent correlation coefficients (Shank: $r = 0.999$, Thigh: $r = 0.998$). Technically, the proposed ambulatory system is portable, easily mountable, and can be used for long term monitoring without hindrance to natural activities.

4.1 Introduction

Human motion capture is usually performed based on camera, magnetic and ultrasound systems (Dejnabadi et al. 2005b; Meyer et al. 1992). Although these standard technologies allow a complete 3D kinematics of body segment they require a dedicated laboratory where the subjects should walk in a pre-defined specific path, and assume that data measured from only a few seconds are representative of usual performance. This constraint beside the time needed for the analysis and also the cost of these technologies has limited the use of these standard technologies in clinical practice. Ambulatory monitoring of body movement takes a different approach: collecting data from body-fixed sensors in the natural environment of the subject. In this regard, movement analysis using body fixed inertial sensors as a complementary method has many potential in clinical field (Patla and Clous 1997; Saleh and Murdoch 1985).

While standard technologies provide directly body segment position and orientation relative to a fixed referential, the outputs of inertial sensors are rather relative angles, segment acceleration or velocity. Finding 3D segment orientation, absolute angles and complete kinematics are a major difficulty when using body fixed inertial sensors.

Orientation angle estimation using inertial sensors, consisting of accelerometers and/or rate gyroscopes has been studied by many authors. In fact, both an accelerometer and a gyroscope can measure orientation angle of a segment. However, an accelerometer is slow in response and sensitive to linear accelerations, and a gyroscope suffers from slow drift and unknown initial inclination (Foxlin 1996; Luinge and Veltink 2004; Rehbinder and Hu 2004). In order to eliminate drift of integration, Morris (Morris 1973) identified the beginning and the end of the walking cycles, and made the angle signal at the beginning and the end of the cycle equal. Tong et al. (Tong and Granat 1999a) applied a low cut-off high-pass filter on the shank and thigh angle signals obtained from integration of angular velocities. Time-frequency analysis (Wavelet Transform) was also applied to lower limb angular velocity in order to remove the drift (Aminian et al. 2004a). However, all of these methods remove the dc and low frequency information of angles. Heyn et al. (Heyn et al. 1996) showed that shank and thigh inclination could be measured with eight accelerometers and two gyroscopes fixed on two rigid metal plates. They found that using these metal plates was cumbersome.

Many authors designed Kalman filters to fuse gyroscope, accelerometer and/or magnetometer signals (Barshan and Durrant-Whyte 1995; Foxlin 1996; Luinge and Veltink 2004; Luinge and Veltink 2005; Marins et al. 2001; Rehbinder and Hu 2004; Zhu and Zhou 2004). Kalman filter is seeking for a fusion method to make the best use of all the data available from different types of sensors.

Foxlin (Foxlin 1996) described the design of a Kalman filter to integrate the data from gyroscopes and inclinometers (gravity accelerometer). He used a complementary Kalman filter which operates only on the errors. One advantage of this structure is that it guarantees that the rapid dynamic response of the inertial system will not be compromised by the Kalman filter.

By studying mobile robot attitude estimation, Vaganay et al. (Vaganay et al. 1993) provided a method in which gyroscope drift is compensated using two accelerometers. An extended Kalman filter was used to fuse the information from five inertial sensors: two accelerometers and three gyroscopes. The integration of angular rate is done outside of the Kalman filter, and is treated as part of a measurement system that provides gyroscopically determined measurements of pitch and roll.

Zhu and Zhou (Zhu and Zhou 2004) presented a real time motion-tracking system using tri-axis accelerometers, gyroscopes and earth magnetic sensors. Kalman-based fusion algorithm was applied to obtain dynamic orientations and further positions of segments of the subject's body. They showed that utilizing the Kalman filter to integrate the sen-

sors could incorporate excellent dynamics of gyroscope and stable drift-free performance of gravity acceleration and magnetic field. Haid and Breitenbach (Haid and Breitenbach 2004) presented a low cost inertial orientation tracking with Kalman filter using a gyroscope and a magnetic field sensor. They augmented the accuracy of an orientation detection system by estimating the drift of the gyroscope.

Rehbinder and Hu (Rehbinder and Hu 2004) proposed a state estimation algorithm that fuses the data from gyroscopes and accelerometers to give long-term drift free attitude estimation. They combined two linear Kalman filters between which a trigger based switching takes place. Thus the kinematics representation used made it possible to construct a linear algorithm that was shown to give convergent estimates for this nonlinear problem.

Luinge and Veltink (Luinge and Veltink 2004; Luinge and Veltink 2005) proposed a method for inclination measurement of human movement using a 3-D accelerometer. They designed a Kalman filter to estimate inclination from the signals of a triaxial accelerometer. The design was based on assumptions concerning the frequency content of the acceleration of the movement that was measured, the knowledge that the magnitude of gravity is 1g and taking into account a fluctuating sensor offset. They estimated inclination of trunk and pelvis and showed that their method was twice as accurate as an estimate obtained by low-pass filtering of the accelerometers.

Bachmann, Xiaoping et al. (Bachmann et al. 2003; Xiaoping et al. 2005; Xiaoping et al. 2004; Xiaoping et al. 2003) employed this configuration to track the movement of human limbs. The gyroscopes were used for fast movement periods and magnetometers and accelerometers during slow periods. A quaternion-based Kalman filter was used to fuse the data from the nine sensors. They designed a constant-gain complementary filter to estimate the attitude of a rigid body. It was based on minimizing the error by adjusting the derivative of an estimated orientation quaternion using Gauss-Newton iteration. As a result of this approach, the measurement equations of the Kalman filter become linear, making it possible to estimate orientation in real time.

However, the performance of the Kalman filter will considerably be reduced in measuring orientation angle of segments, like shank, with fast movements and large centripetal acceleration components (Luinge and Veltink 2004; Rehbinder and Hu 2004). Moreover, Kalman filter based methods do not consider biomechanical constraints and human locomotion aspects in their models.

In chapter 3, we proposed a method to estimate uniaxial joint angles based on two sensor modules, mounted on the shank and thigh, each containing two accelerometers and one

gyroscope. By considering the two-dimensional model of segments, we calculated the expected signals of virtual sensors placed at knee joint with respect to the physical sensors. The method of estimating joint angle, however, does not estimate orientations of shank and thigh segments with respect to a fixed frame.

This chapter presents a new complementary method to estimate shank segment orientation in sagittal plane during walking, and subsequently calculate thigh angle by adding the two values of shank and knee angles. We provide a solution to fusing data from a gyroscope and a biaxial accelerometer that provides stable estimates of the segment orientation. The fusing method considers human locomotion and biomechanical constraints, and incorporates excellent dynamic response of gyroscopes and stable drift-free performance of accelerometers. A geometric calibration is needed to give position of sensors to the model. These parameters are obtained by photography.

4.2 Methods

4.2.1 Estimation of Shank Orientation

To estimate orientation of shank segment, the kinematic data of the sensor module placed on shank at point Q_1 was processed (Figure 4-1). The sensor module consisted of a biaxial accelerometer and a gyroscope. Both the gyroscope and accelerometer signals contain information about the orientation of the sensor (Luinge and Veltink 2005). A gyroscope signal (S_g) is the sum of angular velocity (ω) and a slowly varying offset (b)

$$S_g = \omega + b \quad (4.1)$$

where the offset (b) is caused by electronic bias error and deviation from the sensing axis (see chapter 3).

The sensor orientation (φ_g) can be obtained by integration of the gyroscope signal

$$\varphi_g(t) = \int S_g dt = \int \omega dt + d(t) \quad (4.2)$$

where $d(t)$ including both offset and drift, distorts the sensor orientation.

On the other hand, a single axis accelerometer measures the difference of acceleration (\mathbf{a}) and gravity (\mathbf{g}) along its sensitive axis given by the unit vector (\mathbf{n}). The measured signal can thus be expressed as

$$S = (\mathbf{a} - \mathbf{g}) \cdot \mathbf{n} . \quad (4.3)$$

Similarly, by considering a biaxial accelerometer with sensitive axes along \mathbf{u}_x and \mathbf{u}_y , the two measured signals were given by

$$\begin{aligned} S_x &= (\mathbf{a} - \mathbf{g}) \cdot \mathbf{u}_x \\ S_y &= (\mathbf{a} - \mathbf{g}) \cdot \mathbf{u}_y \end{aligned} \quad (4.4)$$

The acceleration vector can be rewritten in polar form

$$\mathbf{S} = e^{i\varphi} \cdot S \quad (4.5)$$

where S and φ represent for modulus and argument of \mathbf{S} .

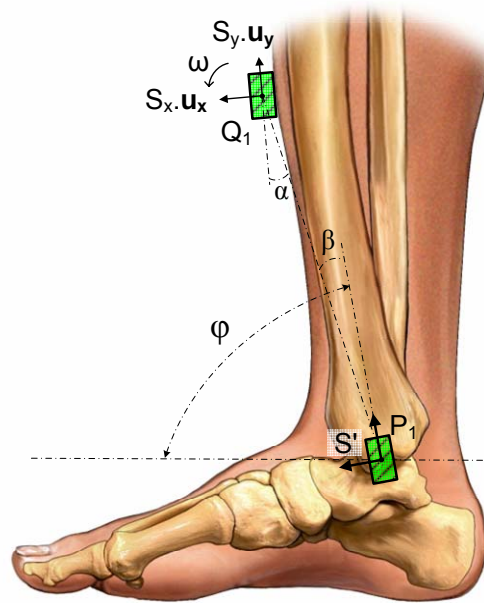


Figure 4-1 Position of sensor on shank, and its corresponding virtual sensor on ankle.

The gravitational component can be used to make an estimation of the inclination angle (Bouten et al. 1997; Kemp et al. 1998). The inclination is defined as the angle between the sensor axes and the horizontal plane. If the acceleration (\mathbf{a}) is small compared to the gravity (\mathbf{g}), the accelerometer can be used as an inclinometer, and the inclination angle is equal to the argument (φ). The problem is of course that when the segment is accelerated, the accelerometer is not an accurate inclination sensor (Foxlin 1996). When the acceleration is low, the amplitude of accelerometer (S) corresponds rather to the gravity constant (g), this is a necessary condition to detect low acceleration intervals. However, this condition alone is not enough. Since a body segment cannot sustain a constant linear acceleration very long with no rotation, therefore the rule for detecting low accel-

eration is to demand $S = g$ for a certain amount of time T_0 (Foxlin 1996; Foxlin and Harrington 2000; Rehbinder and Hu 2004).

In order to fuse the data from gyroscope and accelerometer, the constraints of having low accelerations on ankle during foot flat periods of gait and also during quiet standing were applied. In foot flat periods, the entire foot comes in contact with the floor and the shank segment performs a pure rotation around ankle joint, while the ankle joint does not move. In quiet standing periods, the shank segment has no rotation or translation.

Since the magnitude of acceleration on ankle is low during foot-flat and quiet standing periods, a virtual accelerometer placed on ankle and aligned with the shank segment orientation is a good estimator of inclination during those periods. Therefore, the first step was to calculate the expected signals of a virtual sensor placed on the ankle joint at point P_1 , and aligned with the shank segment orientation. The relationship between the virtual sensor and the physical sensor on shank could be derived as (see chapter 3)

$$\begin{bmatrix} S'_x \\ S'_y \end{bmatrix} = R_{-\beta} \cdot \left(R_\alpha \cdot \begin{bmatrix} S_x \\ S_y \end{bmatrix} + \begin{bmatrix} -r \cdot \omega^2 \\ r \cdot \dot{\omega} \end{bmatrix} \right) \quad (4.6)$$

where S_x and S_y are physical accelerometer readings; S'_x and S'_y are virtual accelerometer readings. R_α and R_β are axis rotation matrices of the physical and virtual sensors in relation to the direction of vector \mathbf{r} by angles α and β respectively (see also Figure 4-1). It is assumed that the two sensors are fixed on a rigid segment, so their distance (\mathbf{r}) is constant, and both sensors have identical angular velocities (ω). So the Coriolis term will not appear in (4.6).

Similarly, the virtual acceleration vector on ankle can be rewritten in polar form

$$\mathbf{S}' = e^{i\varphi_a} \cdot S' \quad (4.7)$$

where S' and φ_a represent for modulus and argument of \mathbf{S}' .

The second step was to detect the periods when the magnitude of translational acceleration on ankle is low. This magnitude could be expressed as

$$e(t) = |S' - g|. \quad (4.8)$$

Then the two necessary conditions for detecting low acceleration periods were applied on the magnitude signal $e(t)$. The first condition was to find the periods when $e(t)$ is small. So a binary mask was defined such that it has value '1' during low acceleration

periods, and '0' otherwise. The mask can be obtained by thresholding the magnitude signal $e(t)$. However, selection of an appropriate global threshold is difficult, and varies from subject to subject and for different walking speeds. So instead of using a single threshold value, a hysteresis thresholding method (Canny 1986) was applied on $e(t)$ to obtain the mask M_1

$$M_1(t) = \begin{cases} 1 & \text{if } e(t) < c_1 \\ 0 & \text{if } e(t) > c_2 \\ p & \text{otherwise} \end{cases} \quad (4.9)$$

where c_1 ('hard' threshold) and c_2 ('weak' threshold, $c_1 < c_2$) are small constant parameters chosen heuristically. All values in the magnitude signal $e(t)$ having a value less than c_1 are immediately accepted ('secure' values). Conversely, all values greater than c_2 are immediately rejected. 'Potential' samples (p) with values between both thresholds are accepted if they are connected to secure samples by a path of potential samples. Hysteresis thresholding is more immune to noise than simple 'hard' thresholding. It helps to ensure that a noisy interval (e.g.: foot flat) is not broken into multiple fragments and preserves the connectivity of the mask.

The second condition for detecting low acceleration intervals was to select only the high state (=1) periods in the mask (M_1) that persists for at least a certain amount of time T_0 . So narrow pulses shorter than T_0 in the mask were eliminated. This was performed by applying a morphological 'Opening' filter (Ronse and Heijmans 1991) on M_1 with window size T_0 to obtain the mask M_2

$$M_2 = OPEN(M_1, T_0). \quad (4.10)$$

The window size (T_0) was heuristically chosen as 0.1 s.

Based on the given conditions, the shank orientation angle, estimated by the virtual accelerometer on ankle (φ_a), was valid during the period where the resulting mask (M_2) had value equal to 1. These valid values of φ_a were used to correct the drift in the estimated shank angle using the gyroscope (φ_g)

$$d(t) = \begin{cases} \varphi_g - \varphi_a & \text{if } M_2 = 1 \\ \text{unknown} & \text{if } M_2 = 0 \end{cases} \quad (4.11)$$

where $d(t)$ represents for the drift signal expressed in (2).

In order to estimate the drift $d(t)$ at ‘unknown’ times, first the signal at known times were smoothed by applying a 2nd order Butterworth lowpass filter. This operation would not lose any information in the signal, because the drift was expected to have low variations in time. Then an interpolation technique based on Piecewise Cubic Hermite Interpolation was applied on the drift signal at known intervals (Fritsch and Carlson 1980). The resulting interpolant has no overshoots or oscillations during unknown times, and preserves monotonicity in the signal.

This drift is then subtracted from the angle estimated by gyroscope to yield absolute shank angle at all times

$$\varphi_{Shank}(t) = \varphi_g(t) - d(t). \quad (4.12)$$

4.2.2 Estimation of Thigh Orientation

We proposed in chapter 3 a method of measuring knee joint flexion-extension angle (φ_{Knee}) based on two modules of sensors placed on shank and thigh. We considered the two-dimensional model of segments, and calculated the expected signals of virtual sensor modules placed at knee joint with respect to the physical sensor modules. The method was validated by measuring knee flexion-extension angles during walking at different speeds. Joint motion is actually the relative motions between the articulating segments. So considering the thigh segment as an articulated rigid segment connected to the shank segment, the relative motion of thigh to shank could be expressed with knee joint motion (φ_{Knee}), and hence the orientation angle of thigh segment with respect to horizontal frame could be given by

$$\varphi_{Thigh} = \varphi_{Shank} + \varphi_{Knee}. \quad (4.13)$$

4.2.3 Test Protocol

Eight healthy subjects, who had given informed consent, participated in this experiment, 5 men and 3 women, aged between 44 and 70 yr (mean = 58.7 yr). The volunteers performed three 30 s flat treadmill walking trials at speeds 2, 3 and 4 km/h, wearing their basket shoes.

The sensor configuration is similar to the configuration in chapter 3. However, for validation with the reference system, only the data of left shank and thigh were used (Figure 4-2). The sensing axes were adjusted in the antero-posterior plane so that the motion in the sagittal plane could be measured. A geometric calibration was required to obtain position of sensors with respect to anatomical landmarks. This information was then

given to our proposed models to estimate the expected virtual sensor readings shifted to the ankle and the knee joints respectively. So before the walking trials, three small markers were pasted over the left lateral malleolus (P_1), the lateral epicondyle (P_2), and the junction of the first and second proximal lateral third of the thigh (P_3) (Figure 4-2). Then the subject stayed for a few seconds (<5 s) at standstill, while the system was recording kinematic parameters, a lateral view photograph was taken as well. The camera's image plane was adjusted to be in parallel with sagittal plane to avoid perspective errors. The known length of the metal frame (70 cm height) was used to calibrate the photo from pixels to metric units. This image was used to estimate the coordinates of markers and kinematic sensors. The accelerometer's readings during standstill were used to estimate the sensor's orientation with respect to horizontal plane. The calibration procedure is simple and can be completed within less than 60 seconds. It is not critical to find exact positions of markers (P_1 , P_2 , and P_3). For example, moving the markers 1cm in each direction causes very minimal changes in the segment angles (less than 2 deg).

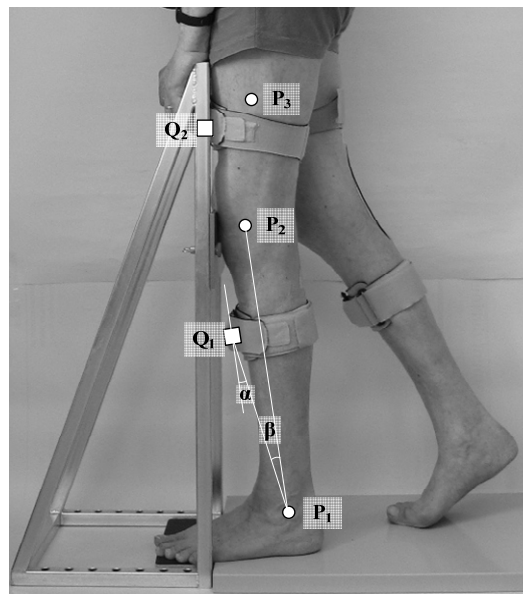


Figure 4-2 Attachment of the kinematic sensors on both thighs and shanks using straps. The kinematic data are recorded by the Physilog® system (dimensions: 13 cm x 7 cm x 3 cm, weight: 300 gr) placed in a waist bag. The white circles indicate the position of markers (P_1 , P_2 and P_3), and the white squares indicate the position of kinematic sensors (Q_1 and Q_2).

The angles α and β , and the length r were calculated afterwards to be used in (4.6). The angle α was obtained by calculating the difference between inclination angle of the sensor (S_1) and the vector $\overrightarrow{P_1Q_1}$

$$\alpha = \tan^{-1} \left(\frac{\overline{S_{y_1}}}{\overline{S_{x_1}}} \right) - \tan^{-1} \left(\frac{y_{P_1} - y_{Q_1}}{x_{P_1} - x_{Q_1}} \right) \quad (4.14)$$

where $\overline{S_{x_1}}$ and $\overline{S_{y_1}}$ are averages of the 2-D accelerometer readings during the standstill trial.

The angle β was obtained from the dot product formula

$$\beta = \cos^{-1} \left(\frac{\overline{\mathbf{P}_1 \mathbf{P}_2} \cdot \overline{\mathbf{P}_1 \mathbf{Q}_1}}{|\overline{P_1 P_2}| \cdot |\overline{P_1 Q_1}|} \right) \quad (4.15)$$

where $\overline{\mathbf{P}_1 \mathbf{P}_2} = [x_{P_1} - x_{P_2} \quad y_{P_1} - y_{P_2}]'$, $\overline{\mathbf{P}_1 \mathbf{Q}_1} = [x_{P_1} - x_{Q_1} \quad y_{P_1} - y_{Q_1}]'$, and finally $r = |\overline{P_1 Q_1}|$.

For comparison, a Zebris CMS-HS (Zebris, D) ultrasound-based motion measurement system was used as the reference system (see chapter 3). In this study, three ultrasound receivers were attached over the same adhesive markers (P_1 , P_2 and P_3). Spatial marker positions (x , y , z) were recorded and used for calculation of shank and thigh orientation angles. Synchronization between the reference and the Physilog systems was performed by electrical trigger. The angle data obtained by the body-fixed sensors were down sampled to 100-Hz for comparison purpose.

4.2.4 Data Analysis

Matlab was used for all signal processing. A third order Savitzky-Golay filter (Savitzky and Golay 1964) was applied to smooth the accelerometers and gyroscopes signals. For comparison with the reference system, the error signal $Er(t)$ was defined as the difference between the time series angle obtained by the proposed method and the reference system.

The accuracy of the results was calculated in terms of RMS, mean and standard deviation of the error signal ($Er(t)$), as well as correlation coefficient between the orientation angles obtained by the proposed method and the reference system's data.

4.3 Results

4.3.1 Estimation of Shank and Thigh Orientations

The main steps of calculating shank angle during typical walking trail at 3 km/h are shown in Figure 4-3 to Figure 4-8. Figure 4-3 to Figure 4-5 indicate how the magnitude

and phase of the virtual sensor on ankle are derived from the measured accelerometer and gyroscope signals. The measured accelerometer and gyroscope signals on shank (Figure 4-3) are transformed to the virtual accelerometer reading on ankle (Figure 4-1) using (4.5). The polar representation (modulus, argument) of the virtual accelerometer (Figure 4-5) is then obtained using (4.6).

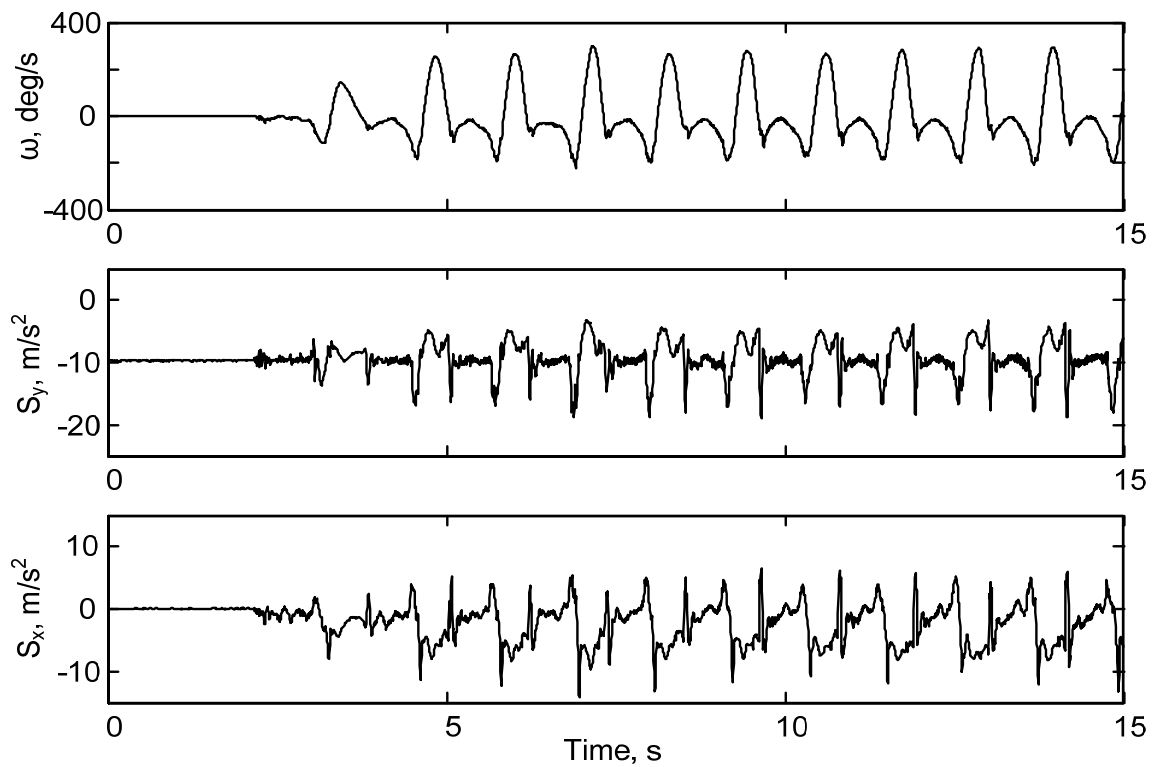


Figure 4-3 Physical sensor readings on shank during walking at 3 km/h. The sensor module consists of two accelerometers (S_x and S_y) and a gyroscope (ω).

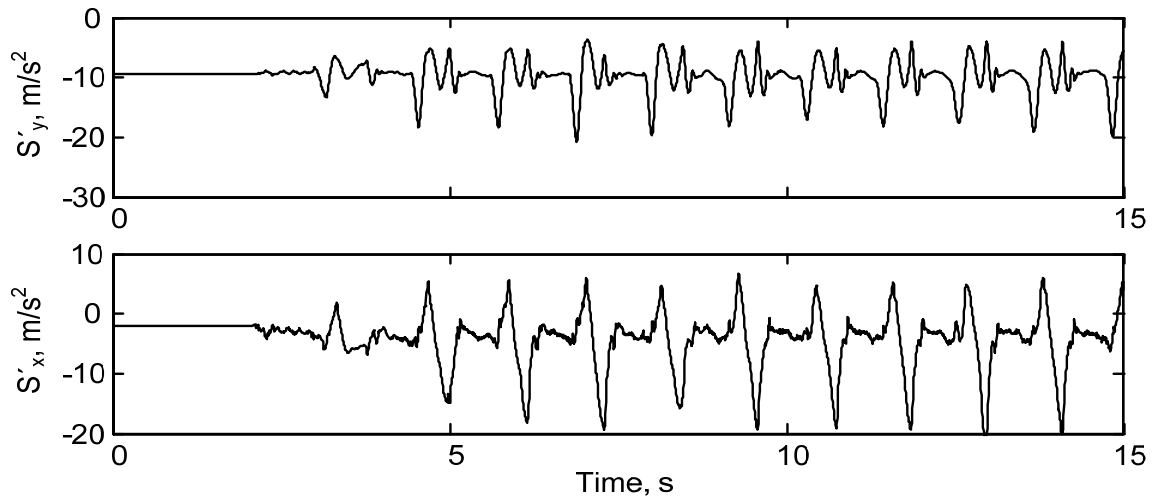


Figure 4-4 Virtual accelerometer readings on ankle during walking at 3 km/h. The signals are calculated from the raw signals shown in Figure 4-3.

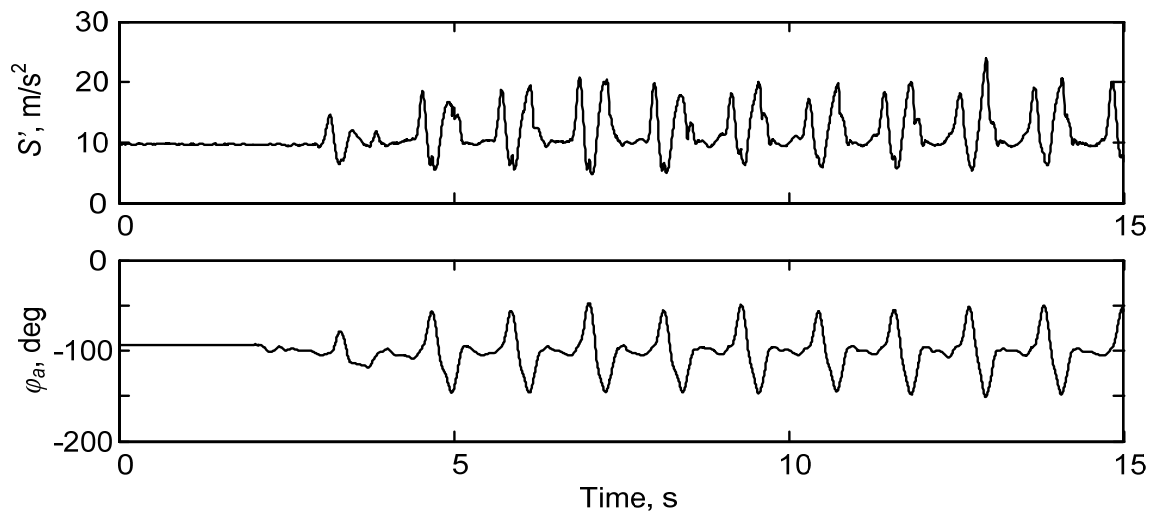


Figure 4-5 Polar representation (modulus: S' , argument: φ_a) of the virtual accelerometer on ankle calculated from the signal shown in Figure 4-4.

Figure 4-6 indicates how the periods of motion with low acceleration are detected by employing hysteresis thresholding and morphological filter. Figure 4-6(a) shows the magnitude of translational acceleration on ankle [$e(t)$ in solid line], and two thresholds ($c_1 = 0.4\text{m/s}^2$ and $c_2 = 0.8\text{m/s}^2$ in dashed lines) set for hysteresis thresholding. The result of hysteresis thresholding is the binary mask M_l [Figure 4-6(b)]. The second step applies

a morphological opening filter on M_1 to eliminate narrow pulses shorter than T_0 [Figure 4-6(c)].

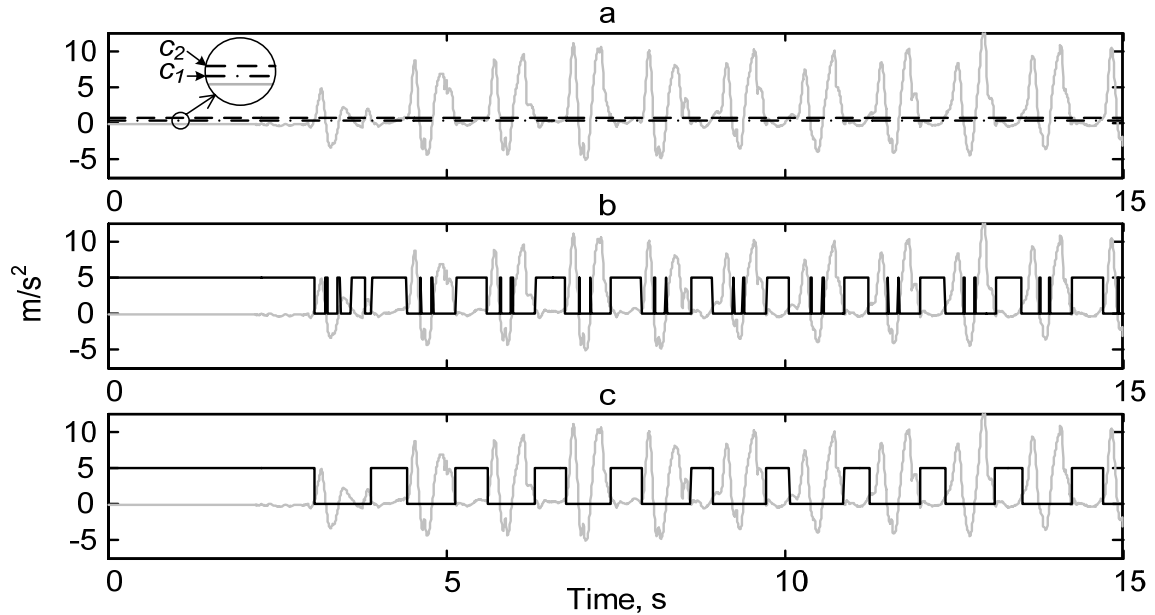


Figure 4-6 Detection of the periods of motion with low acceleration by employing hysteresis thresholding and morphological filter. (a) Magnitude of translational acceleration on ankle $e(t)$ (solid gray line), and two thresholds c_1 and c_2 (dashed lines) set for hysteresis thresholding. (b) Result of hysteresis thresholding as binary mask M_1 . (c) Result of morphological opening filter as binary mask M_2 . The filter was applied on M_1 to eliminate narrow pulses shorter than $T_0 = 0.1$ s.

Figure 4-7 shows how the two angle information obtained by gyroscope (φ_g) and virtual accelerometer (φ_a) are combined to estimate the offset and drift $d(t)$. The process consists of subtracting the two signals using (4.11) followed by applying the Piecewise Cubic Hermite Interpolation. The estimated drift $d(t)$ is then used to calculate the correct orientation of shank (φ_{Shank}) using (4.12).

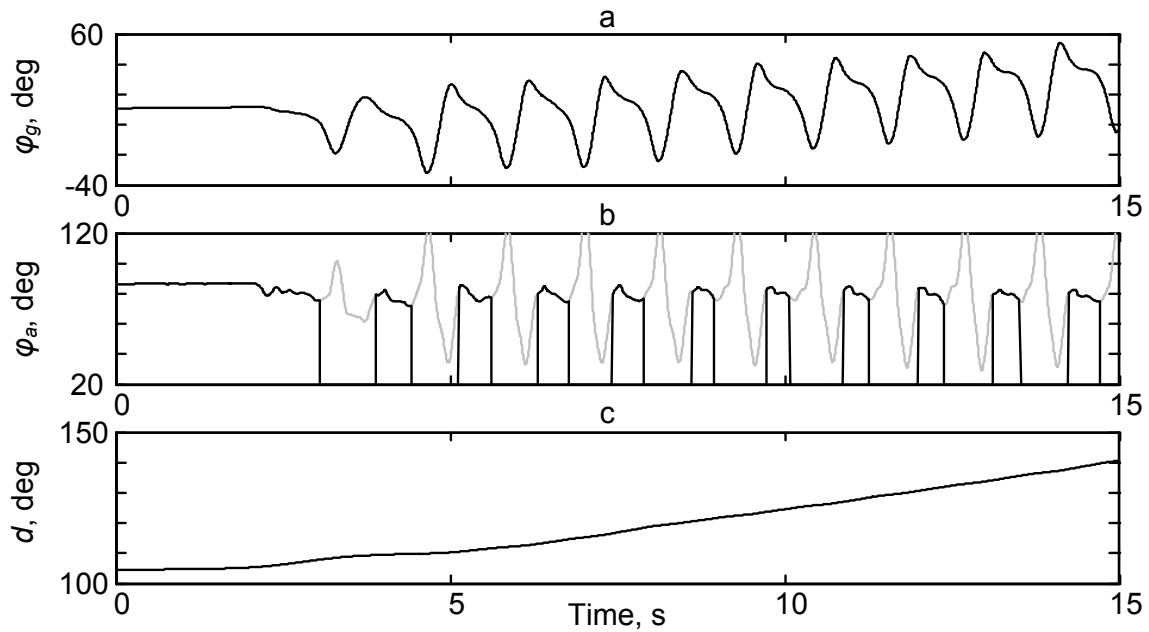


Figure 4-7 Estimation of drift by combining the two angle information obtained by gyroscope and virtual accelerometer. (a) Estimated shank angle using gyroscope (φ_g). (b) Estimated shank angle using the virtual accelerometers (φ_a). The angle is valid only during low acceleration periods indicated by mask M_2 . (c) Estimated drift by combining (a) and (b). The procedure consists of subtracting the two signals followed by applying Piecewise Cubic Hermite Interpolation. The estimated drift is then used to calculate the correct orientation of shank (φ_{Shank}).

The comparison between the reference angles and the measured angles using the proposed method for shank motion is shown in Figure 4-8. The error ($Er(t)$) is defined as the difference between the shank orientation angle (φ_{Shank}) estimated by the proposed method [Figure 4-8(a)], and calculated from position data as measured by the reference system [Figure 4-8(b)]. It can be seen that the value of the $Er(t)$ [Figure 4-8(c)] is very small (< 1.2 deg). Similarly, the thigh orientation angle (φ_{Thigh}), calculated using (4.13), is compared with its corresponding reference angle as shown in Figure 4-9.

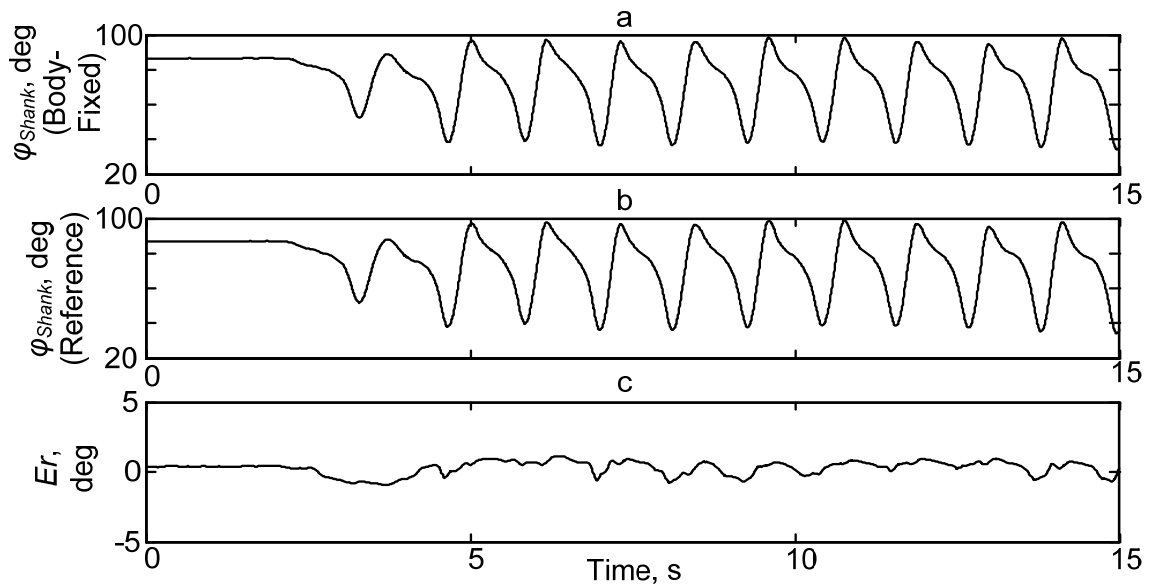


Figure 4-8 Comparison between the measured angles using the proposed method and the reference angles (a) Shank angle calculated by the proposed method using the body-fixed sensors. (b) Calculated from position data as measured by the reference system. (c) Difference error between the two results. Note that the scale is zoomed to -5.0 to 5.0 deg for better viewing.

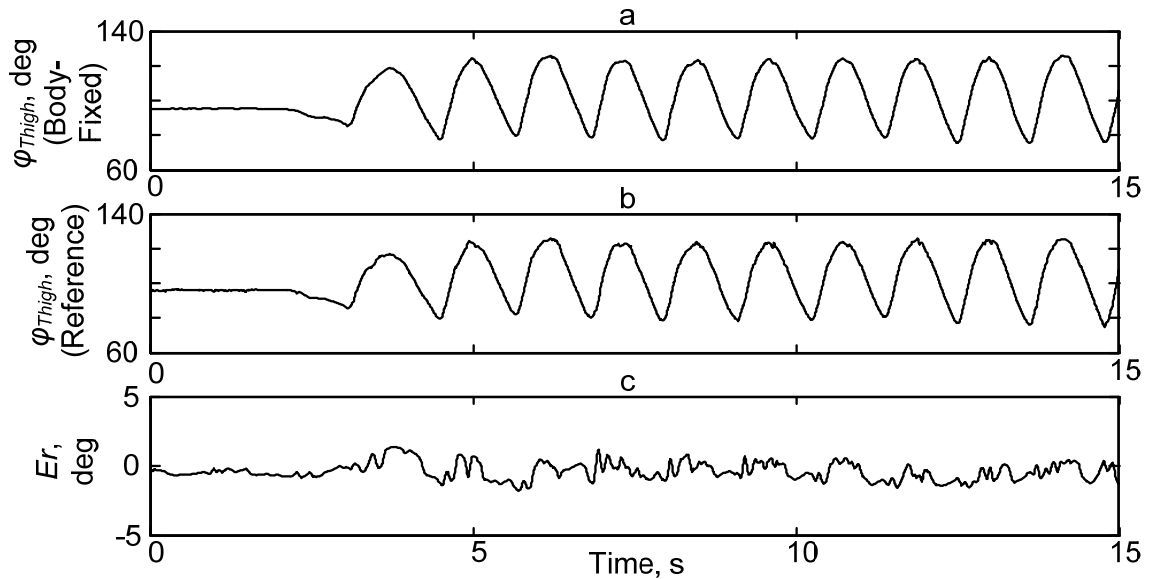


Figure 4-9 Comparison between the measured angles using the proposed method and the reference angles (a) Thigh angle calculated by the proposed method using the body-fixed sensors. (b) Calculated from position data as measured by the reference system. (c) Difference error between the two results. Note that the scale is zoomed to -5.0 to 5.0 deg for better viewing.

The whole results of the validating shank and thigh angles with reference system are summarized in Table 4-1, which outlines the mean and standard deviation of RMS errors and correlation coefficients of all subjects. The average RMS error for shank angles was

1.0 deg (mean = 0.5 deg, SD = 0.8 deg) and the average correlation coefficient was 0.999. In the same way, the average RMS error for thigh angles was 1.6 deg (mean = 0.1, SD = 1.4 deg) and the average correlation coefficient was 0.998.

Table 4-1 Comparison between shank and thigh angle measurements obtained by body-fixed sensors and Zebris markers for all subjects at 3 speeds. The error represents the mean and SD of RMS error (the difference signal between Zebris and our measuring device), as well as the mean and SD of the Correlation Coefficient between the two measuring systems

Segment	Slow (2km/h)		Intermediate (3km/h)		Fast (4km/h)	
	RMS Error	Correlation Coeff.	RMS Error	Correlation Coeff.	RMS Error	Correlation Coeff.
Shank	0.74± 0.18	0.9991±0.0008	0.73±0.14	0.9994±0.0004	0.78±0.17	0.9994±0.0003
Thigh	1.42±0.23	0.9985±0.0002	1.57±0.35	0.9986±0.0003	1.69±0.48	0.9986±0.0008

4.4 Discussion and Conclusion

The proposed method based on body-fixed sensors gave an accurate estimation of lower limbs orientations during gait. The results of all tests (Table 4-1) were very close to those of the reference system presenting small errors in RMS, mean and standard deviation of the difference signal, reflecting accurate and precise estimates respectively; and excellent correlation coefficients reflecting highly linear response.

Our method compares favorably with other methods used to estimate shank or body segment orientation. Mayagoitia et al. (Mayagoitia et al. 2002) showed that shank and thigh inclination angles can be measured with the need of signal integration with eight accelerometers as wells as two gyroscopes fixed on two rigid metal plate. They found that RMS error for shank ranges from 1.3 deg to 2.7 deg. Using single gyroscope on shank, Tong and Granat (Tong and Granat 1999a) estimated the RMS error of relative shank angle (not absolute) to around 4.95 deg while using two gyroscopes (shank and thigh), Aminian et al. (Aminian et al. 2004a) have found for arthritis patients standard errors of 3.3 deg and 4.2 deg respectively for relative shank and thigh orientation. In comparison with the methods using Kalman filtering, the proposed method has faster response, no phase delay, no convergence problem, and less computational load. Although the Kalman filter can have a higher accuracy in many applications, and can even be applied in real time, the performance of the filter will considerably be reduced in measuring orientation angle of segments, like shank, with fast movements and large centripetal acceleration components (Luinge and Veltink 2004; Rehbinder and Hu 2004). Many authors designed Kalman filters to fuse gyroscope, accelerometer and/or magnetometer signals (Barshan and Durrant-Whyte 1995; Foxlin 1996; Luinge and Veltink 2004; Luinge and Veltink 2005; Marins et al. 2001; Rehbinder and Hu 2004; Zhu and Zhou 2004). However, the performance of the filter was only validated on the motions of segments such as trunk or

head, which have relatively slower motions than shank and thigh. Nevertheless, the presented algorithm in this chapter is limited to post-processing of data, and the time lag to find low acceleration points is an inevitable consequence.

In contrast to the method presented in previous chapter for measuring joint angle, the proposed method in this chapter requires to find low acceleration points in order to measure orientation of a segment with respect to a fixed frame. Joint angle is the relative angle of two connecting segments with a known center of rotation at the joint point. So a pair of virtual sensors could be placed at the joint center of rotation to find joint angle. A similar concept was used in this chapter to find orientation of a segment by considering it as the joint angle between the segment and a fixed frame. However, a freely moving segment has not a constant center of rotation. So only at zero motion points the assumption is valid as the center of rotation is known.

From a practical standpoint, misalignment of the sensors or sensor deviation during movement reduces the system's accuracy, such that the sensor reading is multiplied by the cosine of the misalignment angle ε . However, this will not seriously disturb the signals, since $\cos \varepsilon \approx 1$ if ε is sufficiently small. The accuracy of the angles are still limited by the bias drift of the accelerometers, however it is much less severe than integrating gyro drift. In addition, skin motion artifact, a common source of error to all body mounted devices, affects the measurement accuracy. The thigh sensor is more susceptible to skin and soft tissue artifact where the majority of the femur is concealed by a substantial amount of soft tissue (Cappozzo et al. 1996a; Reinschmidt et al. 1997a; Reinschmidt et al. 1997b). The effect of skin artifact was minimized by using adequate elastic band to fix the sensors, and applying low-pass filtering on the raw signal.

The results show that using gait constraints imposed by ankle joint, and virtually placing an accelerometer on ankle, can improve the accuracy of the measurements. In addition, the information of the virtual sensor on ankle can further be used to detect foot-flat phases. Identifying the foot-flat phase (Loading Response) of the gait cycle is one of the most demanding tasks in the study of human locomotion (Coley et al. 2005; Hunt et al. 2001).

The current model is limited to 2-D sagittal measurement of lower limbs. However, in gait analysis, a 2-D sagittal approach seems to be satisfactory, because sagittal plane is the plane where majority of the movement takes place, and gives a lot of information for gait pathologies (Tong and Granat 1999a). Therefore many applications in gait analysis and orthopedics are concerned with the proposed method. For example, lower limbs absolute angles can be used to provide outcome evaluation after orthopedic surgery since there is

a correlation between functional improvement found by clinical Harris Hip Scores (HHS) (Harris 1969) and range of flexion of the thigh ($r = 0.69$, $p < 0.01$) in arthritis patients (Dejnabadi et al. 2003). Moreover main activity such as lying, sitting, standing, walking and stair climbing can be identified by a subtle combination of the shank, thigh and knee angle in sagittal plane (Coley et al. 2005; Morlock et al. 2001) and provide in this way useful outcome for mobility improvement after hip arthroplasty.

Chapter 5 Quantitative Gait Analysis

Abstract

In this chapter, a gait analysis tool using body-fixed sensors is presented. It provides both quantitative and qualitative evaluation of gait functionality. Outputs from the software include spatio-temporal parameters of gait, kinematic diagrams, and animated graphic images simulating the patients' gait at various conditions. The spatio-temporal parameters provide a tool for objective outcome measures to quantify the expected gait improvement of patients with knee or hip arthroplasty.

The kinematic diagrams including time series graphs and angle-angle graphs provide additional information for representing movement and its variability in continuous format. The graphs help clinician qualitatively assess time evolution of lower limb movements, variability at different phases of gait, symmetry, and ranges of rotations.

Finally, a visualization tool was designed to show the motion data as synthetic skeletons performing the same actions as the subjects. It provides auxiliary tool to see the time evolution of lower limb movements.

5.1 Introduction

Human gait is a very complicated, coordinated series of movements that involve both the upper and lower extremities. Winter states: "The sole purpose of walking or running is to transport the body safely and efficiently across the ground, on the level, uphill and downhill with a minimal expenditure of energy. The neuromuscular control system must also provide appropriate shock absorption, prevent collapse, and maintain balance of the upper extremity" (Valmassy 1996; Winter 2005). Human gait is one of the most difficult tasks that we learn but, once learned, it becomes almost subconscious. Only when walking is disturbed by injury, disease, degeneration or fatigue, we realize our limited understanding of this complex biomechanical process.

Observational gait analysis (OGA), or the visual evaluation of walking, is the clinician's primary tool for describing the quality of a patient's walking pattern. However, simple observation of a gait pattern cannot define and quantify its many potential and complex elements. Moreover, the identification and grading of gait deviations depends on the observer's experience and individual bias (Valmassy 1996). Attempts to systematize

observational gait analysis and to maximize its reliability have led quantitative (or instrumented) gait analysis. Quantitative gait analysis is a method by which modern technologies are used to incorporate information from a number of inputs to illustrate and analyze the dynamics of gait. It describes for the clinician (physician, surgeon, and therapist) in quantitative and dynamic terms the movement of the body and its limbs and the changing relationships of one extremity to other extremities during motion. Gait analysis has become particularly useful to the surgical team when decisions need to be made about the applicability of a surgical procedure for correction of a faulty gait. It is also valuable after surgery to learn whether the dysfunction has been corrected and how motion of the treated limb is now affecting the dynamics of walking.

As mentioned in chapter 2, there are several branches in studying gait analysis such as *Gait kinematics*, *Gait kinetics*, and *Dynamic electromyography* (EMG). A comprehensive gait analysis usually includes all branches (Vaughan et al. 1992) and this complex information can only be obtained in a dedicated laboratory. However, simplified kinematic analysis (e.g., spatio-temporal parameters) can also be clinically valuable, and an ambulatory device may be advantageous for these types of applications (Aminian et al. 2004b).

In this chapter, a gait analysis system based on body-fixed sensors is presented. The outputs of the system are spatio-temporal parameters of gait and kinematic diagrams. Spatial and temporal parameters of gait have clinical relevance in the assessment of motor pathologies, particularly in orthopedics (Aminian et al. 2004b). Additionally, a gait analysis tool was designed to visualize the motion data as synthetic skeletons performing the same actions as the subjects. The tool gives the physician an intuitive information about how the patient performs several activities such as stair climbing, or walking at different speeds.

5.2 Gait Terminology

Over the past several decades, the evolution of gait science has produced an array of terms and concepts relating to gait analysis. The terminology of human walking began with descriptive phrases obtained as a result of observational and kinematic analysis of normal subjects (Perry 1992; Saunders et al. 1953; Sutherland et al. 1994). This approach yielded terms such as “gait cycle”, “heel strike”, “toe off”, and so on. When we walk, we progress through a series of repetitive events. Our feet are picked up and swung forward, placed on the ground, walked over, and picked up and swung forward again. Each of these repetitive motions is termed a *gait cycle*. One gait cycle is measured from floor contact of the heel (*heel strike*) to the following heel contact of the same limb. So the

gait cycle time is the time between the two successive heel strikes. By contrast, the *gait stride* is the distance from heel strike of one foot to the following heel strike of the same foot (Ayyappa 1994; Najafi 2003).

Each gait cycle is divided into two periods, swing and stance. The *swing* phase is that period of time in which the foot does not touch the ground and is swung forward. The swing phase occupies approximately one third of a total gait cycle (38%-42%). The *stance* phase of the gait cycle is that period of time when the foot makes contact with the ground. The stance phase starts with heel strike, and ends with *toe off* (when the foot leaves the ground). The stance phase is approximately two thirds of the gait cycle (51%-62%). Both the start and end of the stance phase involve a period of bilateral foot contact with the floor, which is referred to as initial and terminal double supports respectively. In normal walking, each double support period occupies 8% to 12% of the gait cycle. Consequently, the period of time when only one foot is in contact with the ground is referred to as *single support*. Figure 5-1 shows subdivisions of stance, swing, and single and double support.

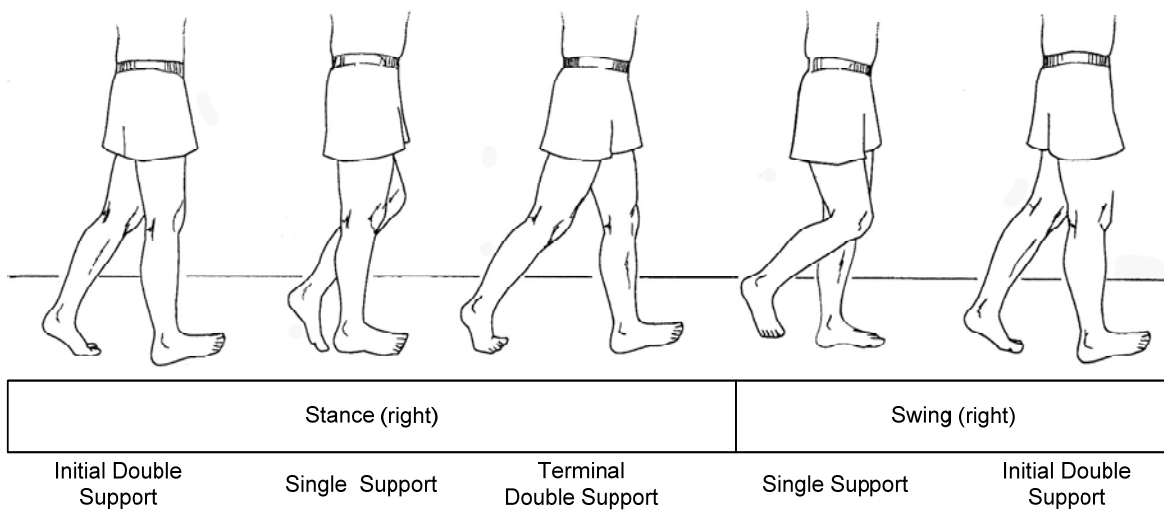


Figure 5-1 Subdivisions stance (right), swing (right), and single and double supports during gait cycle.

5.3 Methods

5.3.1 Estimation of Spatio-Temporal parameters

A method for computing spatio-temporal parameters of gait using gyroscopes was first proposed by Aminian et al. (Aminian et al. 2002b) and modified by Salarian et al. (Salarian et al. 2004). In this study, we used the sensor configuration explained in chapter 3, and applied the modified method proposed by Salarian et al. to determine the

precise moments of heel strikes and toe offs. The method utilizes shank sagittal angular velocities and searches the two minima on either sides of a peak in angular velocity (mid-swing area) (Figure 5-2). The first minimum was associated with toe off, and the second minimum with heel strike.

Based on these time events, the temporal parameters of gait were computed as a percentage of gait cycle time (*GCT*). These parameters were the durations of stance, swing, initial double support (*IDS*), terminal double support (*TDS*) and the sum of initial and terminal double supports (*DS*) (Aminian et al. 2002b).

Spatial parameters were estimated by first calculating the knee, shank, and thigh angles as explained in chapters 3 and 4. These angles were then used to find the range of rotations (difference between maximum and minimum) of thigh (left: $R_{\alpha L}$, right: $R_{\alpha R}$), shank (left: $R_{\beta L}$, right: $R_{\beta R}$), and knee (left: $R_{\gamma L}$, right: $R_{\gamma R}$) during each gait cycle. Afterwards, the stride length, stride velocity (Speed), and normalized speed (to subject's height) were calculated using the range of thigh and shank rotations and applying the double pendulum model for swing and inverse double pendulum model for stance (Aminian et al. 2002b). In addition, the maximum values of shank angular velocities (left: $PS_{\omega L}$, right: $PS_{\omega R}$) and knee angular velocities (left: $PK_{\omega L}$, right: $PK_{\omega R}$) were reported as spatial parameters.

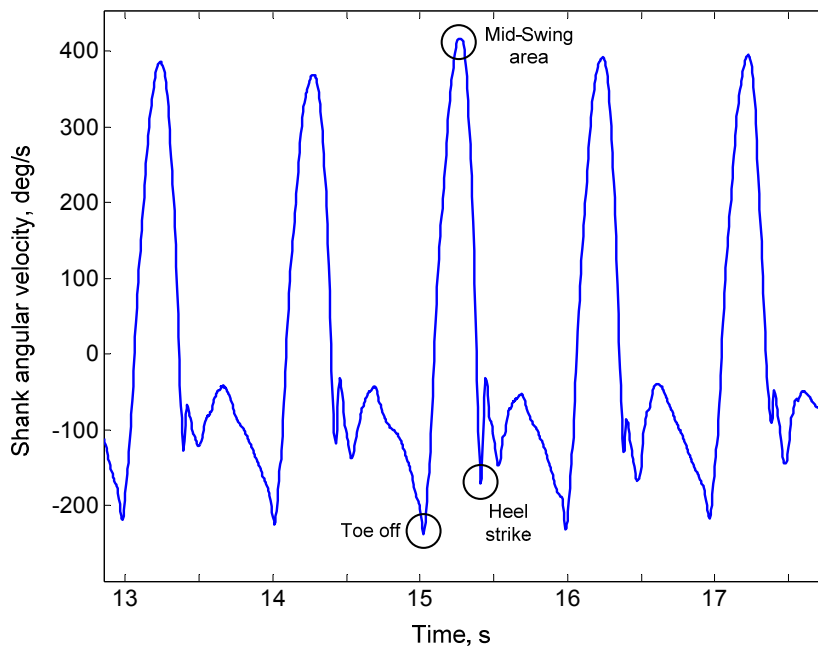


Figure 5-2 Shank angular velocity. Marked area show where important gait events occur.

The mean and variability of spatio-temporal parameters across gait cycles was assessed using 3 common descriptive statistics, including mean, variance, and coefficient of variation.

The first statistics measure used to describe a gait parameter was mean

$$M = \frac{\sum_{i=1}^n x_i}{n} \quad (5.1)$$

where M is the sample mean, x_i is the i th sample data value, and n is the number of gait cycles.

The second measure was standard deviation

$$SD = \left(\frac{\sum_{i=1}^n (x_i - M)^2}{n - 1} \right)^{1/2} \quad (5.2)$$

where SD represent the sample standard deviation.

The third quantity that represents a relative (normalized) variability measure is the coefficient of variation which is the standard deviation normalized to the percentage of the mean value

$$CV = (SD/M) \times 100 \quad (5.3)$$

where CV is the sample coefficient of variation.

5.3.2 Kinematic diagrams

Spatio-temporal parameters do not capture all of the information relevant for understanding the movement and movement variability of a motion pattern performed across the time (James 2004). Kinematic diagrams provide an alternative for representing movement and its variability as a function of time or other movement parameter and can also represent both spatial and temporal characteristics (Hamill et al. 2000). In this study, we utilized two common types of kinematic diagrams: time series graphs and angle-angle plots. The kinematic data, consisting of knee, shank and thigh angles, were obtained by the methods presented in chapters 3 and 4.

5.3.2.1 Time series graphs

Time series graphs (i.e., plot of a variable vs. time) are among the most commonly used methods for representing continuous biomechanical data. First, the kinematic signals were time normalized by first detecting the heel strike events of each leg, and then

rescaling each cycle time to have the same length (0% to 100%). Then, ensemble average curve was computed as the mean across multiple time-normalized gait cycles (James 2004)

$$M_i = \frac{\sum_{j=1}^n x_{ij}}{n} \quad (5.4)$$

where M_i is the mean for the i th sample, x_{ij} is the data value for the i th sample and j th gait cycle, and n is the number of gait cycles. The variability band was calculated using point-by-point method. Point-by-point method consists of calculating the standard deviation across all cycles for each data sample

$$SD_i = \left(\frac{\sum_{j=1}^n (x_{ij} - M_i)^2}{n-1} \right)^{1/2} \quad (5.5)$$

where SD_i is the standard deviation for the i th sample.

A graphical representation of these variability values can be obtained by plotting the ensemble average curve (M_i) plus and minus the standard deviation value for each data point (SD_i), that is, $M_i \pm SD_i$.

5.3.2.2 Angle-Angle graphs

Angle-angle graphs represent the angular movement of one body segment or joint against another segment or joint. Grieve (Grieve 1968b) is credited with devising the angle-angle diagram to evaluate walking patterns. In order to plot the ensemble angle-angle diagram, first ensemble average of each variable was calculated (Sidaway et al. 1995)

$$M_{xi} = \frac{\sum_{j=1}^n x_{ij}}{n} \quad (5.6)$$

$$M_{yi} = \frac{\sum_{j=1}^n y_{ij}}{n}$$

where x_{ij} and y_{ij} are the data values for the i th sample and j th gait cycle for the x- and y-axis variables, and M_{xi} and M_{yi} are corresponding x and y multiple-cycle mean values for the i th sample. Similarly, the variability band was calculated the standard deviation of each variable across all cycles for each data sample

$$\begin{aligned}
 SD_{xi} &= \left(\frac{\sum_{j=1}^n (x_{ij} - M_{xi})^2}{n-1} \right)^{1/2} \\
 SD_{yi} &= \left(\frac{\sum_{j=1}^n (y_{ij} - M_{yi})^2}{n-1} \right)^{1/2}
 \end{aligned} \tag{5.7}$$

where SD_{xi} and SD_{yi} are corresponding x and y multiple-cycle standard deviation values for the i th sample.

5.3.3 Visualization

In collaboration with Computer Vision Laboratory of EPFL (CVLab), we developed a data-driven visualization software for animating human gait. Motion data can be visualized as synthetic skeletons performing the same actions as the subjects. The tool gives the physician visually appealing and easy to interpret information about how the patient performs several activities such as walking at different speeds or climbing ramps and stairs. Because the animated skeleton is 3D it can be viewed from arbitrary angles, thereby further helping the physician to interpret the results.

The human body was modeled as a system of articulated rigid links, which represent the lower limb segments. The model employed forward kinematics that gets position and orientation of the end segment in a kinematic chain by defining angles for every joint. The kinematic structure contained 6 joints (for hips, knees and ankles), and the joint motions were generally 3D. In order to obtain the joint movement, quaternion representation (Shoemake 1985) of the rotations was used. The quaternion representation was chosen for its compactness and accuracy in representing rotations. The animation software takes data in the form of 2D sagittal orientation angles, then transform to quaternion representations, and computes the skeleton's configuration and position at each frame.

In addition, the visualization tool's interface provides clinicians with the ability to visualize the effect of treatment (e.g surgery, rehabilitation) by superimposing for instance the two gaits obtained before and after the treatment.

5.4 Results

Our system was tested on actual patients with knee arthroplasty at Hôpital Orthopédique de la Suisse Romande (HOSR). In this chapter we have selected a patient (ID: MS-37) and show the gait analysis results of the patient during walking at normal speeds at two

tests: baseline and 6 months after surgery. Each trial consisted of approximately 30 consecutive gait cycles.

5.4.1 Spatio-temporal Parameters

Table 5-1 illustrates the mean, standard deviation (SD), and coefficient of variation (CV) of spatio-temporal parameters of the gait trials of patient (ID: MS-37) at baseline and a follow up test (6 months).

Table 5-1 Spatio-temporal parameters of the gait trials of a patient (ID: MS-37) at baseline and 6 months after surgery.

Gait Parameter	Baseline			After 6 Months		
	Mean	SD	CV%	Mean	SD	CV%
Gait Cycle Time (GCT), s	1.12	0.04	3.9	1.07	0.03	2.4
Left Stance, %	60.29	2.19	3.6	62.76	1.16	1.8
Right Stance, %	64.94	2.16	3.3	60.20	0.74	1.2
Double Support, DS%	25.36	3.20	12.6	22.97	1.21	5.3
Limp, %	3.44	2.88	-	1.08	0.93	-
Left Stride, m	0.93	0.05	5.1	1.12	0.03	2.7
Right Stride, m	0.93	0.06	5.9	1.12	0.03	2.7
Speed, m/s	0.83	0.04	5.3	1.05	0.03	2.9
Normalized Speed, /s	0.50	0.03	5.3	0.64	0.02	2.9
Left Shank Peak Velocity, PS ω L, deg/s	225.5	24.7	11.0	343.7	17.3	5.0
Right Shank Peak Velocity, PS ω R, deg/s	292.6	22.5	7.7	303.6	13.6	4.5
Left Knee Peak Velocity, PK ω L, deg/s	238.5	24.8	10.4	376.1	28.1	7.5
Right Knee Peak Velocity, PK ω R, deg/s	291.2	35.9	12.3	366.4	20.2	5.5
Left Thigh Rotation, R α L, deg	30.7	2.1	6.7	35.7	1.1	3.1
Right Thigh Rotation, R α R, deg	32.0	2.4	7.5	37.6	1.1	2.9
Left Shank Rotation, R β L, deg	50.6	3.7	7.2	67.6	2.8	4.2
Right Shank Rotation, R β R, deg	54.0	3.1	5.8	65.4	2.2	3.4
Left Knee Rotation, R γ L, deg	31.0	3.8	12.2	56.1	2.8	4.9
Right Knee Rotation, R γ R, deg	40.5	2.8	6.8	48.2	1.51	3.1

5.4.2 Kinematic Diagrams

Figures 5-3 and 5-4 show ensemble average graphs for lower limb angles of the patient (ID: MS-37) with knee arthritis at baseline and 6 months after surgery respectively. Each graph shows the mean value (in solid black) with its variability band (in gray).

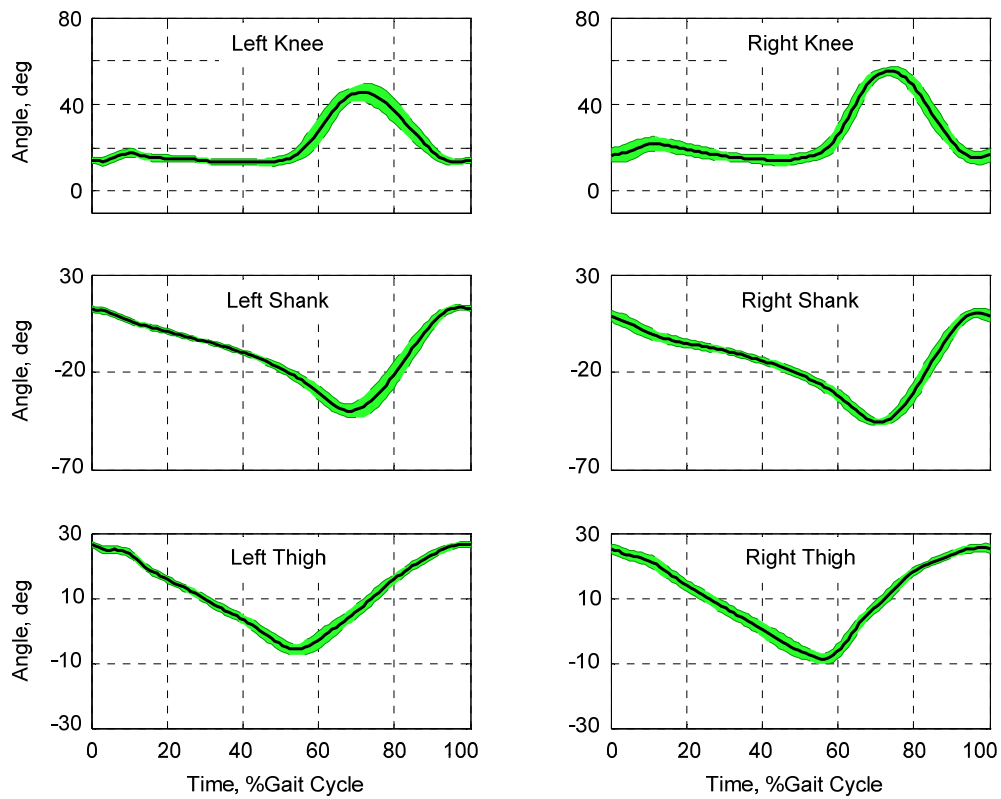


Figure 5-3 Ensemble average graphs for lower limb angles of a patient (ID: MS-37) with knee arthritis pre-operatively during 30 complete. Each graph shows the mean value (solid black) with its variability band (gray).

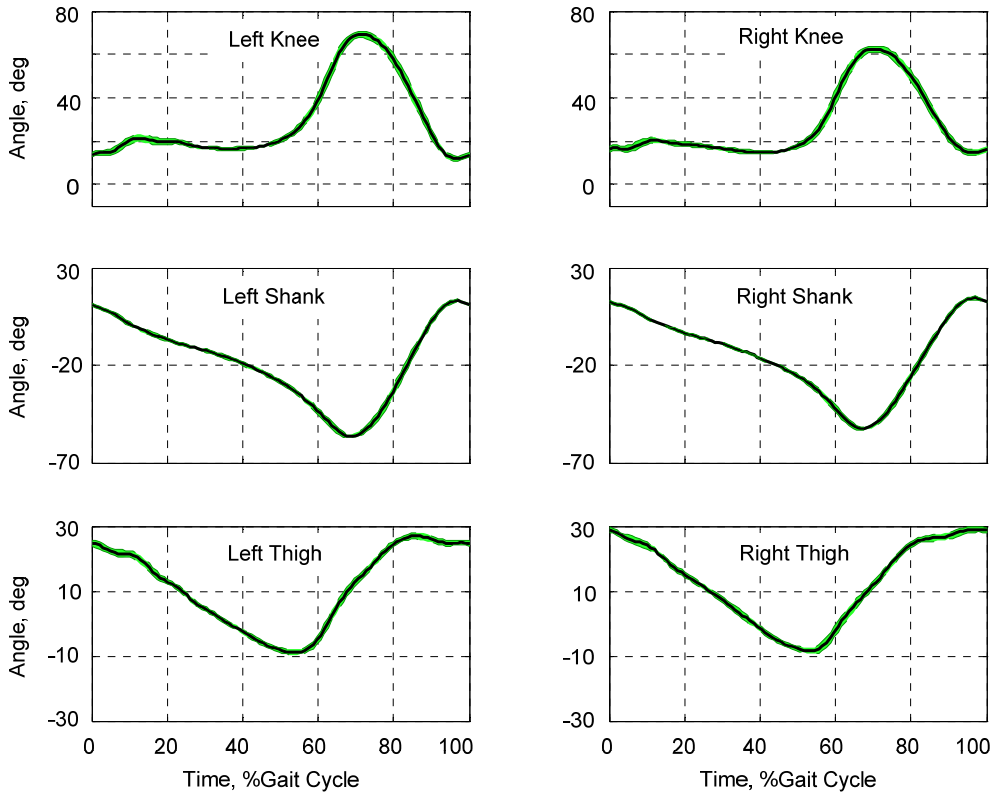


Figure 5-4 Ensemble average graphs for lower limb angles of a patient (ID: MS-37) 6 months after knee arthroplasty.

Figures 5-5 and 5-6 show ensemble knee-hip angle-angle diagrams of the patient (ID: MS-37) at baseline and 6 months after surgery respectively. The heel strike (HS) and toe off (TO) events are shown by circles on the graphs.

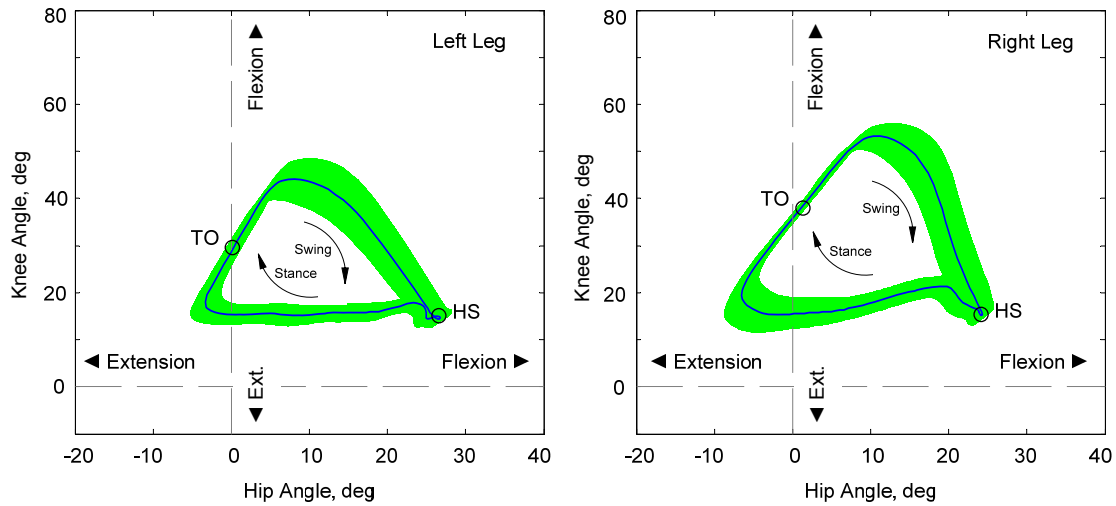


Figure 5-5 Ensemble knee-hip angle-angle diagram of a patient (ID: MS-37) at baseline.

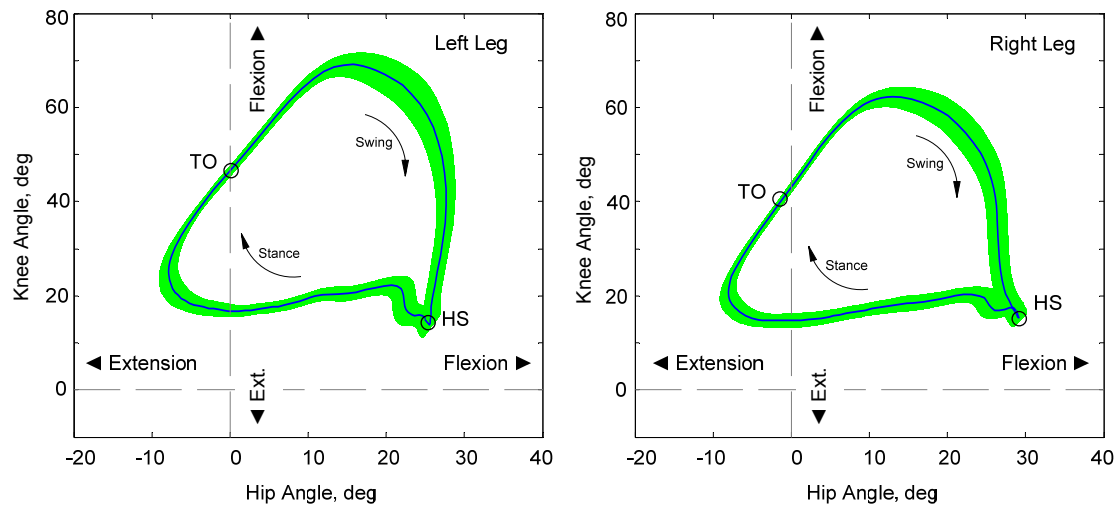


Figure 5-6 Ensemble knee-hip angle-angle diagram of a patient 6 (ID: MS-37) months after surgery.

5.4.3 Visualization

Figure 5-7 shows the visualization tool's interface. The middle window shows the animated skeleton of the patient (ID: MS-37) during walking at normal speed. The rightmost window of Figure 5-7 compares the gait of the same patient just before operation with 6 months later by superposing several skeletons.

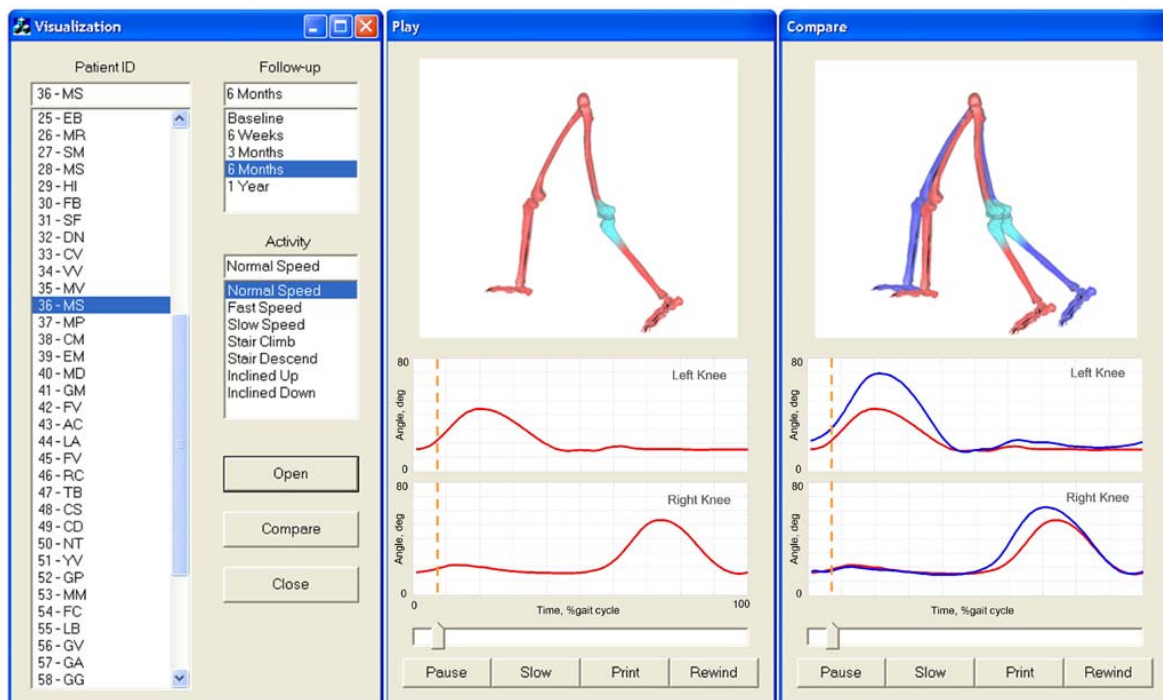


Figure 5-7 Interface of our visualization tool. The animated skeleton of a patient (ID: MS-37) during walking with knee arthroplasty is shown in the middle window. The knee prosthesis is colored in light gray. The right window compares the gait of the same patient just before operation (black) with 6 months later (gray).

5.5 Discussion and conclusion

We proposed a gait analysis tool based on body-fixed sensors (consisting of gyroscopes and accelerometers) with various types of reports: spatio-temporal gait parameters, kinematic diagrams, and visualization.

Spatio-temporal parameters of gait provide quantitative scores of gait analysis. It allows the clinician to compare the gait parameters of a patient at baseline and different follow up tests. For example, by looking at the Table 5-1 and comparing the gait parameters of the patient (ID: MS-37) between 6 months after surgery and baseline, we can see that the variability (CV%) of all parameters have decreased. This indicates that the patient could walk more consistently and regularly. Moreover, the parameters of speed, stride, ranges of rotations, maximum angular velocities have increased. This indicates that the patient could walk faster, and use more dynamic ranges of rotations. Finally, the 'Limp' parameter has decreased, which indicates that the patient could walk more symmetric after surgery.

The kinematic diagrams provide supplementary information for representing movement and its variability as a function of time or other movement parameter in continuous

format. The graphs help clinician qualitatively assess time evolution of lower limb movements, variability at different phases of gait, symmetry, and ranges of rotations.

Finally, the visualization tool provide additional tool to see the time evolution of lower limb movements. The visualization tool gives the physician visually appealing and easy to interpret information about how the patient performs several activities such as walking at different speeds or climbing ramps and stairs. In addition, it allows us to evaluate the progression of a patient at different follow up tests by superposing several skeletons.

The proposed system was tested on actual patients with knee arthroplasty at Hôpital Orthopédique de la Suisse Romande (HOSR), and appears a promising ambulatory gait analysis system for outcome evaluation or as a monitoring tool to assess progress through rehabilitation (see chapter 7).

Chapter 6

Analysis of Inter-Joint Coordination

Abstract

Control of movement is one of the most difficult issues in the area of human function. A range of different research approaches have been employed in an effort to understand human motor control, however knowledge of the mechanisms associated with limb movement are still limited. In this chapter, a new method of quantitative analysis of interjoint coordination during gait is presented. It provided a general model to capture the whole dynamics of the movement and showed the kinematic synergies at various walking speeds. The proposed model imposed a relationship among lower limb joint angles (hips and knees) to parameterize the dynamics of locomotion for each individual. An integration of different analysis tools such as Harmonic analysis, Principal Component Analysis, and Artificial Neural Network helped overcome high-dimensionality, temporal dependence, and non-linear relationships of the gait patterns. The trained model was fed with only 2 control parameters (cadence and stride length) at each gait cycle, and predicted the corresponding gait waveforms. Considering the differences between predicted and actual gait waveforms, a coordination score was defined at various walking speeds which ranged between 0 and 10. The scores determined the overall coordination as well as contribution of each joint to the total coordination. The model was applied on 8 patients with knee arthroplasty at different follow-ups as well as to 8 healthy subjects, walking at 3 different speeds. Although the study group was small, the results showed that knee replacement and rehabilitation programs improved the gait coordination. The technique, along with the ambulatory device using body-fixed sensors, provides an analytical tool that is easy to use in the clinical diagnosis of human gait abnormalities.

6.1 Introduction

Researchers and clinicians have been interested in understanding the kinematics and kinetics of human gait system for many years. Human gait is a complex cyclical activity that involves coordination of many oscillating segments. Given the number of segments involved in human locomotion, there are an infinite set of possible trajectories determined both by the path as well as by the time at which each point on the path is reached. Accessing or computing such trajectories would require significant motor

memory storage and computational power (Medendorp et al. 2000; Reisman et al. 2005; To et al. 2005). To produce a functional movement or synergy, the movement components have to be sequentially processed and temporally organized and their relative magnitudes need to be determined (Scholz 1990). This consideration leads to the question of whether the human motor system might use a simplified strategy that restricts the set of possible movement trajectories.

Coordination is a strategy chosen by the central nervous system (CNS) to control the movements and maintain stability during gait. Coordinated multi-joint movements demand a complex interaction between the motor outputs of the CNS, the biomechanical constraints, and the proprioception (Field-Fote and Tepavac 2002; Rosenbaum 1991; Skinner and Mulloney 1998). In a multi-joint movement, the motion at a particular joint depends not only on the muscular torques actively generated at that joint, but also on dynamic interactions with other joints. Thus, it presents the CNS with control problems distinct from those in single-joint coordination (Verschueren et al. 1999). The CNS appears to use proprioception to monitor and adjust for these interaction torques on-line, as a movement is launched, without consciously taking into account the complex limb dynamics. Proprioception can be described as afferent information arising from peripheral mechanoreceptors that contribute to postural control, joint stability and conscious sensation of movement. Patients with loss of proprioception encounter problems in the performance of multi-joint movements, at least in part, due to their inability to control for interaction torques (Abelew et al. 2000; Carson and Swinnen 2002; Cordo et al. 1994; Rosenbaum 1991; Sainburg et al. 1995; Sainburg et al. 1993; Verschueren et al. 2002; Wallace 1989).

Quantitatively understanding and modeling of gait coordination has been a challenging endeavor. The main challenges can be summarized as high-dimensionality, temporal dependence, and nonlinear relationships of the gait patterns (Chau 2001a; Kurz and Stergiou 2004; Winter 2005). Bernstein, who first identified the degree of freedom problem, defined coordination as a problem of mastering the very many degrees of freedom involved in a particular movement pattern, and to use a simplified strategy that restricts the set of possible movement trajectories, in other words, making it a controllable system (Bernstein 1967; Turvey 1990). He proposed that the motor apparatus was functionally organized into synergies or classes of movement patterns. Synergies are classes of movement patterns involving collections of joint variables that act as basic unit in the regulation and control of movement. Synergies are used by the nervous system to reduce the number of both controlled parameters and afferent signals needed to generate and guide an ongoing movement (Berthoz 2000). In this way, the CNS controls global variables, not

local variables (the multiplicity of the joint angles). Thus, a possible approach for studying gait coordination is to reduce the number of independent variables to be controlled, or summarize the relations between the various components by one or several essential variables. This approach to the degree of freedom problem supposes that there are dependencies between components of the motor system. Having such dependencies reduces the degree of freedom that must be independently controlled.

Many researchers have been carried out to determine the coordinative structure of human movements. A common limitation of the past studies is that they could not provide a general model to capture kinematic synergies at various walking speeds. In fact, the people alter their gait patterns and hence their kinematic synergies when they walk faster or slower than normal speed to maintain their stability and minimize the energy cost of locomotion (Frigo and Tesio 1986; Wallace 1989). Furthermore, a comprehensive quantitative description of the synergies under a multi-joint task paradigm has been lacking. This study was an attempt to fulfill these voids based on dynamical systems approach to quantitatively describe human gait coordination. Moreover, the model can synthesize classes of movement patterns at various walking speeds. To this end, different analysis techniques were integrated to parameterize the dynamics of locomotion of each individual.

6.2 Literature review

A full understanding of human movement and coordination can come about if we integrate behavioral work (which tends to focus on the outcome of performance) with kinesiology (which provides us with information about the kinematics of human movement) and neurophysiology (which tells us the nature of underlying neural mechanisms involved in controlling movement) (Kelso 1982). Classification of motor control theories in the past studies can be divided into two classes based on 1- neurophysiology, and 2- outcome of performance including kinematics and kinetics of human movement.

In this section, we focus on the motor control theories based on movement variables (kinematic and kinetics of movement). Schmidt (Schmidt 1988) has stated that the nervous system may control movement not muscles. This thought supports the perception that it is the goal or the movement pattern which seems to be what the performer is controlled of rather than the particular muscles or motor units involved.

The study of movement variables such as, movement time, displacement, velocity, or forces has provided information about a number of models or concepts which have aimed to elucidate the complexity of the control of movement. Many different models have been

proposed to explain movement coordination. In this section, we review some of the most common methods of analyzing movement coordination.

6.2.1 Variable-Variable plots

Variable-variable plots have been used extensively to analyze the motion of one joint relative to the motion of another joint (angle-angle plot) and the angle of one joint relative to the angular velocity of that joint (phase-plane plot) (Abelew et al. 2000; Bloomberg and Mulavara 2003; Davids and Renshaw 2005; Earhart and Bastian 2001; Grieve 1968a; Higgins and Higgins 1990; Ivanenko et al. 2002; Rushworth et al. 1998). Figure 6-1 shows examples of angle-angle plots of hip-knee segments in sagittal plane over several gait cycles for a healthy subject [Figure 6-1(a)] and a patient with knee arthritis [Figure 6-1(b)].

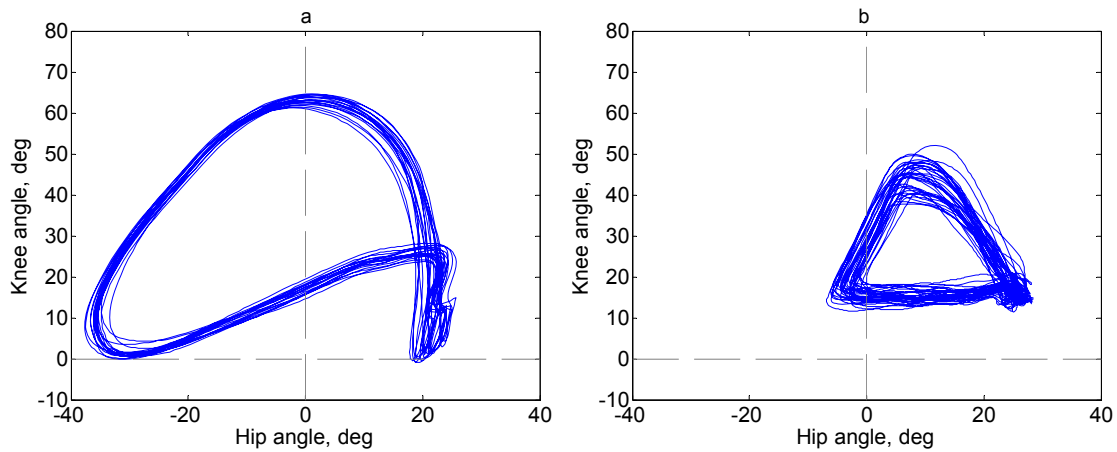


Figure 6-1 Hip-knee phase portrait during gait: (a) normal healthy gait, (b) knee arthritis gait. Angles correspond to the hip and knee flexion-extension angles during walking.

Figure 6-2 presents the corresponding phase plots for the knee joint for a healthy subject [Figure 6-2 (a)] and a patient with knee arthritis [Figure 6-2 (b)] during gait. The phase plots consist of the joint angle on the x-axis and the joint's angular velocity on the y-axis.

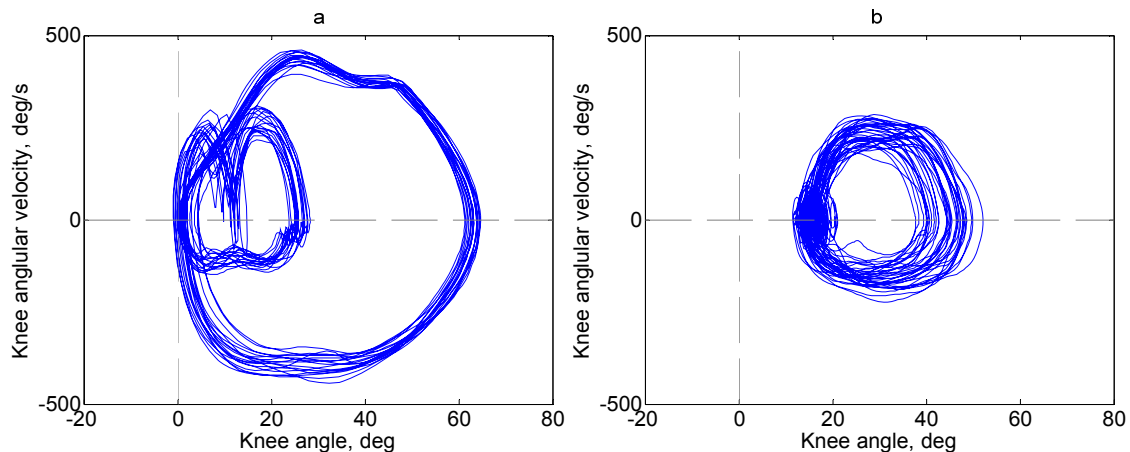


Figure 6-2 Knee phase plots during gait: (a) normal healthy gait, (b) knee arthritis gait.

Inspection of Figures 6-1 and 6-2 indicates that the behavior of the lower extremity joints during the gait cycle conforms to the shape of a limit cycle system that has a closed periodic orbit. Additionally, it is evident that there are slight variations in the path of the trajectory for each gait cycle. The plots help understand the behavior of the dynamic system, although the differential equation for the system is typically unknown. The disadvantages of phase plane plots and angle-angle plots are that time is omitted from an explicit representation. Moreover, quantitatively understanding the inter-joint coordination and control mechanisms cannot be achieved with this methodology alone.

6.2.2 Dynamic Systems (Relative Phase)

Another possible approach to uncover the coordinative structure of gait is to model it as a dynamical system and to study its stability and performance in terms of input-output characteristics. A dynamical system is any well-specified set of functions (rules, equations) that specifies how variables change over time. A key feature of the dynamical system approach is that systems comprised of many elements (i.e., having high dimensionality) can be described in low dimensional terms (e.g., one variable). A common dynamical systems technique to the study of interjoint coordination has been based upon the relative phase (RP) analysis (Beek et al. 2002; Burgess-Limerick et al. 1993; Calvitti and Beer 2000; Hamill et al. 2000; Kelso 1995; Kurz and Stergiou 2002; Lamothe et al. 2004; Marghitu and Hobatho 2001; Reisman et al. 2005; Ridderikhoff et al. 2005; Stergiou et al. 2001; Swinnen and Carson 2002). RP represents the phasing relationships (the spatial and temporal coupling) of a pair of interacting joints during a movement.

The first step to calculate RP is to obtain phase angles of each of the two interacting segments (proximal and distal)

$$\Phi = \tan^{-1} \left(\frac{\text{Segment Angular Velocity}}{\text{Segment Angle}} \right) \quad (6.1)$$

Then the relative phase is calculated by subtracting the phase angles of the proximal segment from that of the distal segment for each i -th data point of the time-normalized gait cycle (Peters et al. 2003)

$$\theta_{\text{relative phase}} = \Phi_{\text{distal segment}} - \Phi_{\text{proximal segment}} \quad (6.2)$$

where $\theta_{\text{relative phase}}$ is the relative phase angle between the distal and proximal segments, $\Phi_{\text{distal segment}}$ is the phase angle of the distal segment, and $\Phi_{\text{proximal segment}}$ is the phase angle of the proximal segment. The uniqueness of the relative phase measure is that it compresses 4 variables (i.e., proximal and distal segments' angles and angular velocities) into one measure.

Relative phase values close to 0° indicate that the two segments are moving in a similar fashion or in-phase, while values close to 180° indicate that the two segments are moving in opposite directions or out-of-phase. Positive relative phase values indicate that the distal segment is ahead of the proximal segment in phase space, and negative relative phase values indicate that the proximal segment is ahead in phase space. The slope of the relative phase configuration indicates which segment is moving faster during periods of the gait cycle. A positive slope indicates that the distal segment is moving faster in phase space, while a negative slope indicates that the proximal segment is moving faster in phase space. The local minimum and maximum of the relative phase curve provide insight into changes in coordination between the two segments, since they represent reversals in the coordination dynamics. Changes in the timing of the reversals and the number of reversals help advance understanding of normal and pathological gait patterns.

Figure 6-3 shows the time-normalized relative phase angles between shank and thigh segments during gait for a healthy subject [Figure 6-3 (a)] and a patient with knee arthritis [Figure 6-3 (b)].

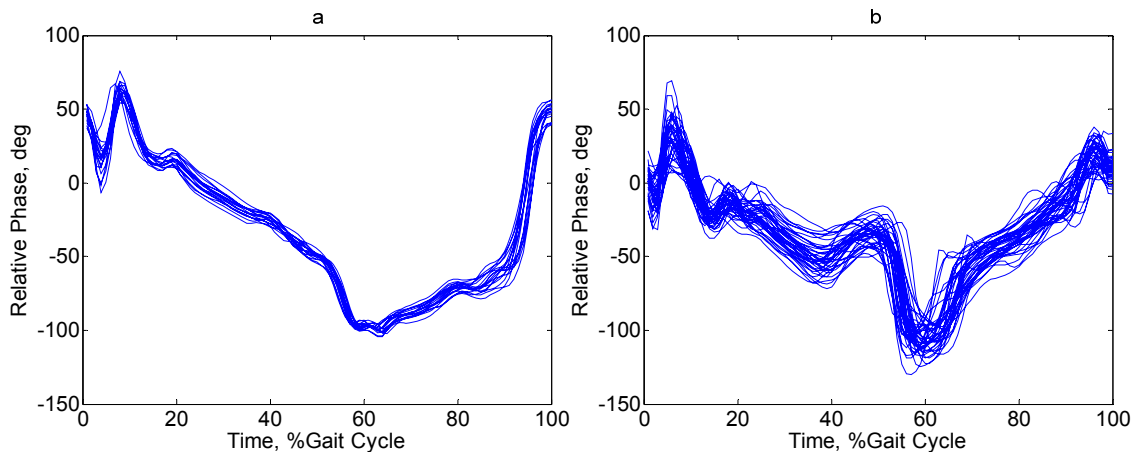


Figure 6-3 Relative phase between shank and thigh during gait: (a) normal healthy gait, (b) knee arthritis gait. The RP curves are time-normalized to gait cycle time.

Additionally, variability in the relative phase provides objective information about the stability of the selected gait pattern. Some researchers utilized the variability of RP on the basis of inter-cycle standard deviation of ensemble relative phase curves as an index of coordinative stability (Barela et al. 2000; Donker and Beek 2002; Lamoth et al. 2002; Yang et al. 2002). Functionally, a low variability indicated a more stable relationship between the two joints' movements. Although relative phase provides a quantitative variable for the assessment of interjoint coordination, interpretation of this collective variable is difficult.

6.2.3 Frequency domain analysis

Many authors employed frequency-domain analysis (cross correlation and spectral analysis) to evaluate the degree of coupling between pair of joint angles (Amblard et al. 1994; Bianchi et al. 1998; Cheron et al. 1998; Crosbie and Vachalathiti 1997; Li and Caldwell 1998; Wu and Meijer 2002). Frequency-domain techniques are based on the assumption that linear relationships exist between two sets of kinematic time series data and identify the best fit linear transfer function between pairs of angles (Davids and Renshaw 2005). So they are not particularly useful in determining the degree of linkage between body segments that have a nonlinear relationship. On the other hand, the latter studies have focused on pair of joint movements, whereas coordination of multi-joint movements has remained largely unexplored (Verschueren et al. 1999).

6.2.4 Principal Component Analysis

Many authors applied principal components analysis (PCA) to examine temporal covariation between joint angles (Alexandrov et al. 1998; Braidó and Zhang 2004; Chau 2001a; Courtine and Schieppati 2004; Daffertshofer et al. 2004; Deluzio et al. 1999; Deluzio et

al. 1997; Grasso et al. 1998; Gueguen et al. 2005; Jerde et al. 2003; Ko et al. 2003; Martin et al. 2002; Mouchnino et al.; Reisman and Scholz 2003; Sanger 2000; Yang et al. 2002). They could show that the multi-joint movements could be described as a linear combination of a small number of principal components or eigencurves. The results indicated that a strong coupling existed between joint movements. There are however limitations to the use of PCA, as it does not model nonlinear relationships among variables, and interpretation of components is heavily subjective as well.

6.3 Methods

6.3.1 Model Description

As defined earlier, coordination is the imposing or constraining of a relationship among multiple variables (Kugler et al. 1980). This relationship can be lawfully described as a function that somehow captures all the relevant information of the process. In coordination dynamics this process can be generally expressed as an equation of motion of the form (Mitra et al. 1998; Scott Kelso and Clark 1982)

$$\dot{\mathbf{x}}(t) = F(\mathbf{x}, \mathbf{c}; \varepsilon) \quad (6.3)$$

where $\mathbf{x} = \mathbf{x}(t)$ is the system state vector, \mathbf{c} is control parameter, and F is the dynamical law governing the process. The remaining term ε refers to random influences or chance events, arising from the multiple degrees of freedom, not absorbed by, or organized through, the state vector \mathbf{x} . There are, therefore, two aspects of (5.2): A deterministic aspect in which the time-evolution of the process is specified uniquely by the values of \mathbf{x} , \mathbf{c} , and F , and a stochastic aspect ε that perturbs the systematically changing process. Roughly speaking, the process of learning a new coordination characterized by (5.2) entails discovering the deterministic part and reducing the stochastic part.

In this study, we considered a five segment model in the sagittal plane with two legs and a trunk. Each leg had a knee with a degree of freedom, and a hip with another degree of freedom. Thus, we defined \mathbf{x} as the spatio-temporal patterning of lower limb angles and their consecutive derivatives during a gait cycle

$$\mathbf{x} = [x_1, x_2, x_3, x_4] \quad (6.4)$$

where $x_j = x_j(t)$ ($1 \leq j \leq 4$) represents the time series of the left hip, right hip, left knee and right knee angles respectively. These flexion-extension angles were obtained using the methods presented in chapters 3 and 4. The control parameters, \mathbf{c} , were considered the parameters that are controllable in human gait to adjust the walking velocity

(Magdalena and Monasterio 1993). Walking velocity is the product of cadence and stride length, implying that a certain walking velocity can be achieved by different combinations of these two parameters

$$\mathbf{c} = [\text{Cadence}, \text{StrideLength}]. \quad (6.5)$$

The control parameters are constant during the execution of a gait cycle, so they carry no information about the patterns that emerge.

The dynamical system expressed by (5.2) can be identified by observing a sequence of gait cycles at different walking speeds and fitting a parametric model to the dataset. Consequently, by feeding the model with control parameters, we can obtain a simulated trajectory of the joint angles. The definition of coordination by (5.2) implies that the system is able to reproduce consistent movement patterns of knee and hip angles over multiple cycles knowing the control parameters for each cycle. So the difference error between the actual and predicted trajectories at a given control parameter yields an estimation of the stochastic part ε

$$\hat{\varepsilon}_j(t, \mathbf{c}) = x_j(t) - \hat{x}_j(t, \mathbf{c}) \quad (6.6)$$

where $x_j(t)$ is the actual trajectory of joint j , and $\hat{x}_j(t, \mathbf{c})$ is the predicted trajectory with the given control parameter \mathbf{c} . This residual error was used to define a score for coordination, since a low value of the residual error implies that the system is in possession of a lawful way of producing a wide variety of systematically related, functionally specific patterns over different control parameters.

Figure 6-4 shows a block diagram of the proposed method. The model consisted of two main parts: Training and Testing. In this model, the focus was to use the least number of parameters to describe the synergies and dynamics of lower limbs in a more manageable and understandable format. Sections 6.3.1.1 through 6.3.1.7 discuss each of these blocks in detail.

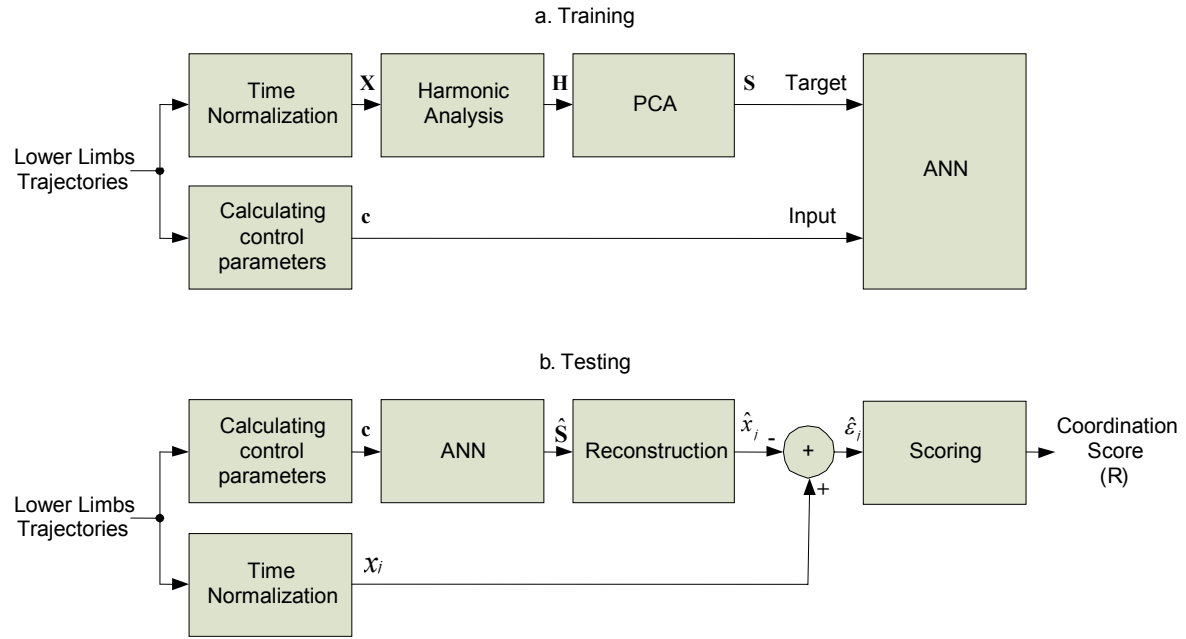


Figure 6-4 Block diagram of the model: (a) Training, (b) Testing.

6.3.1.1 Calculating Control Parameters

The control parameters were calculated by first detecting the heel strike instances of the right leg, and subsequently calculating the cadence and stride length at each gait cycle using the algorithm proposed in (Aminian et al. 2002b). So, for a sequence containing K gait cycles, the control parameter matrix could be expressed as

$$\mathbf{C}^{K \times 2} = [\mathbf{c}_k] \quad (6.7)$$

where k ($1 \leq k \leq K$) is gait cycle number.

6.3.1.2 Time Normalization

In order to account for the temporal differences between strides, kinematic signals were time normalized for adjusting the gait cycles to have the same length (Beek et al. 2002; Crosbie and Vachalathiti 1997; Li et al. 2005; Sadeghi et al. 2003; Schollhorn 2004). Moreover, the invariance in the spatial trajectories can be more clearly found in the normalized curves (Yang et al. 2002). Time normalization of gait cycles was performed by rescaling each cycle time, based on right heel strikes, to a fundamental period length of 1. The normalized waveforms were re-sampled using a cubic spline interpolation to $N = 100$ samples per cycle (Lamoth et al. 2004). Therefore, the whole dataset containing K gait cycles could be expressed as

$$\mathbf{X}^{K \times 4 \times N} = [x_{k,j}(t_N)] \quad (6.8)$$

where j ($1 \leq j \leq 4$) is joint number and t_N ($0 \leq t_N < 1$) is normalized time.

6.3.1.3 Harmonics Analysis

Harmonic Analysis is a common method for reducing a long periodic time series to a small number of Fourier coefficients (Unuma et al. 1995). In general, a discretised signal with N sample points during a cycle can be expressed with a finite number of terms in the series

$$f(t) = A_0 + \sum_{n=1}^{N/2} ((A_n \cos(2\pi nt) + B_n \sin(2\pi nt))) \quad (6.9)$$

where $f(t)$ is a periodic function with the fundamental frequency of 1, n is the harmonic number, and t is time.

From the mathematical point of view, (5.8) is a parametric curve fitting which can be used to study the entire temporal gait waveforms, and also reflects the periodic behavior of the waveforms. Fourier transforms, on the other hand, is an effective smoothing technique (Dujardin et al. 1997) that eliminates the high-frequency noise such as skin artifact.

The magnitude spectrum of the hip and knee rotations drop to near-zero at around 5Hz (Cunado et al. 2003). Accordingly, only the low order components of Fourier series are required to reconstruct the signal (Grasso et al. 2000). The essential number of harmonics, m , required for 98% degree of data reconstruction was defined as the number of harmonics satisfying the condition that the sum of the relative amplitudes of each harmonic over total amplitude was less than or equal to 0.98 (White et al. 2005)

$$\eta_m = \frac{\sum_{n=1}^m \sqrt{A_n^2 + B_n^2}}{\sum_{n=1}^{N/2} \sqrt{A_n^2 + B_n^2}} \leq 0.98. \quad (6.10)$$

The required number of harmonics, m , was calculated for each gait cycle in the database (all subjects, all trials, and all joints), and for consistency the maximum value was considered as the required number of harmonics, m , for all analyses.

However, truncating the Fourier series or rectangular windowing (by m harmonics) causes oscillations in the neighborhood of discontinuities or sharp changes in $f(t)$. This oscillation or ringing is known as Gibb's phenomenon. The Gibb's oscillations could be greatly

damped using other windows with better frequency behavior (Jerri 1998). We used Hamming window (Acton 1990) and evaluated the function as:

$$f(t) = A_0 + \sum_{n=1}^m \left[\frac{\sin(n\pi/2m)}{n\pi/2m} \right] \cdot ((A_n \cos(2\pi nt) + B_n \sin(2\pi nt))) \quad (6.11)$$

where m is the last term in the finite series that we are using. So considering A'_n and B'_n as the modified Fourier coefficients by the Hamming window, the function $f(t)$ could be mapped to a new vector of harmonic components

$$\mathbf{h} = [A_0, A'_1, B'_1, \dots, A'_m, B'_m] \quad (6.12)$$

where \mathbf{h} has $2m+1$ elements. Similarly, the Fourier coefficients of the dataset \mathbf{X} could be expressed by concatenating the harmonic components of $x_{k,j}$ of the 4 joints

$$\mathbf{H}^{K \times Q} = [\mathbf{h}_{k,1}, \mathbf{h}_{k,2}, \mathbf{h}_{k,3}, \mathbf{h}_{k,4}] \quad (6.13)$$

where $Q = 4 \times (2m+1)$.

6.3.1.4 Principal Components Analysis (PCA)

PCA is a statistical technique used to reduce the dimensionality of data and examine the relationship between a set of correlated variables (Jackson 2003). The history of PCA technique in gait data analysis does back more than a decade (Chan-Su and Elgammal 2004; Chau 2001a). We applied PCA to represent most of the variation of the harmonic components (\mathbf{H}) using only a few ‘‘Principal Components’’. This step is a further reduction of the dimensions of the gait waveforms.

The principal components (PCs) are linear combinations of the original data, and a weighted sum of the PCs can exactly reconstruct the original data. The PCs are ordered by the amount of variance they account for in the data, so that the majority of variation is captured by the first few PCs.

We examined the cumulative variance threshold criterion to choose the required number of PCs to keep. The cumulative variance accounted for by the first P principal components is given by

$$\eta_P = \frac{\sum_{i=1}^P \lambda_i}{\sum_{i=1}^Q \lambda_i} \quad (6.14)$$

where λ_i is i -th eigenvalue which is equal to the variance of the i -th PC. Assuming a cumulative variance threshold $\eta = 0.98$, P is the smallest value for which $\eta_p \geq \eta$. Hence, the harmonic components matrix (**H**) was transformed to the reduced space

$$\mathbf{S}^{K \times P} = \begin{bmatrix} s_{k,p} \end{bmatrix} \quad (6.15)$$

where $s_{k,p}$ is the p -th PC of the k -th gait cycle.

Since the PCA solution is sensitive to the units of input data, the input data (**H**) were standardized (data centered and scaled) (Orloci 1967) before applying PCA. This implies that they were normalized to have zero-mean and unit variance. Moreover, this standardization avoids saturation of the processing units and facilitates training of the artificial neural network (Schollhorn 2004).

6.3.1.5 Artificial Neural Network (ANN)

ANNs can model the nonlinear relationship between inputs and desired outputs. This nonlinear property can facilitate the study of complicated behavior of locomotor system which has traditionally been difficult to model with conventional linear tools (Barton and Lees 1997; Ohno-Machado and Rowland 1999; Schollhorn 2004; Secco and Magenes 2002; Stergiou et al. 2004). Furthermore, ANNs has the ability to generalize, meaning to be able to make reliable predictions for new inputs that are not in the training set. It enables the system to provide smooth interpolations for the untrained data space.

We implemented a multilayer perceptron (MLP) architecture because of its good predicting power in supervised training mode for mathematical functional relationships. During the training [Figure 6-4(a)], the inputs consisted of the control parameters (**C**), and the output layer (target) should produce the principal components of the gait waveforms (**S**). The total number of layers in the MLP and the number of nodes in each layer were empirically determined, since they depend on the degree of nonlinearity of the model. However, a two-layer network is known to be theoretically sufficient for learning most functional relationships (Chau 2001b). So, a two-layer network with $3 \times P$ neurons in the first (hidden) layer and P neurons in the output layer was configured. Then the neural network was trained by employing the Levenberg-Marquardt algorithm (Hagan and Menhaj 1994). During the testing phase [Figure 6-4(b)], based on estimated coefficients of training phase, the ANN outputs provided an estimate of the principal components of the gait waveforms ($\hat{\mathbf{S}}$).

6.3.1.6 Reconstruction

In order to reconstruct the predicted trajectories in time domain, first inverse PCA transform followed by inverse standardization (centering and scaling) were applied on the ANN outputs ($\hat{\mathbf{S}}$) to go back to the harmonics domain. Knowing the harmonics, the joint angles in time domain (\hat{x}_j) were obtained through an inverse Fourier transformation.

6.3.1.7 Scoring

As shown before, the residual error expressed by (5.5) was used to define a score for coordination. First, the normalized Root Mean Squared (RMS) error of each joint, j , during each gait cycle, k , was computed as

$$E_{k,j} = \frac{\left[\frac{1}{N} \sum_{t=1}^N \varepsilon_{k,j}^2(t) \right]^{1/2}}{\left[\frac{1}{N} \sum_{t=1}^N x_{k,j}^2(t) \right]^{1/2}}. \quad (6.16)$$

Since the error value grows with the amplitude of the joint rotation, the RMS error was normalized to the RMS of the actual joint rotation to obtain a dimensionless relative error.

Then a logarithmic mapping function was applied to give a coordination score between 0 and 10

$$r_{k,j} = r_{Max} \frac{\log\left(\frac{E_{k,j}}{E_{Max}}\right)}{\log\left(\frac{E_{Min}}{E_{Max}}\right)} \quad (6.17)$$

where $r_{Max} = 10$ is scaling constant to adjust the maximum score output, and E_{Min} and E_{Max} are constants chosen experimentally to adjust the range of the normalized RMS error values. E_{Min} corresponds to the highest coordination score (minimum normalized RMS error) in healthy population, and E_{Max} corresponds to the lowest coordination score (maximum normalized RMS error) in patients population. Logarithmic mapping nonlinearly compresses the high dynamic range of E , such that small values of error are used for scoring in more detail (Stockham 1972). This score allows us to determine the contribution of each joint to the total inter-joint coordination.

Consequently, the overall coordination score during each cycle was defined as the average of coordination scores of each joint

$$R_k = \frac{1}{4} \sum_{j=1}^4 r_{k,j}. \quad (6.18)$$

In order to evaluate the coordination scores at various speeds, the values of $r_{k,j}$ and R_k were calculated for each gait cycle, k , and then plotted versus the speed. Then a 3rd order polynomial (cubic) curve was fitted to the data (r_j and R respectively) to better represent and interpret the results. Additionally, the coordination scores (R_k) of each trial at slow, normal, and fast speeds were averaged over their gait cycles, k , to give an average score, R , for each gait trial.

6.3.2 Test Protocol

In this framework, we applied our model on 8 patients with knee arthroplasty at different follow-ups as well as 8 healthy subjects. The subjects, 9 men and 7 women, had given informed consent. The patients were tested pre-operatively (baseline) and post-operatively at 6 weeks and 6 months. Each subject was asked to perform 6 walking trails of 30m long at 3 different self-selected speeds: normal (trials 1 and 2), slow (trials 3 and 4), and fast (trials 5 and 6). Only steady-state parts of walking trials were used for analysis, and the transient (initial and terminal) cycles were eliminated. Trials 1, 3, and 5 were used for training the model (ANN), and trials 2, 4, and 6 were used for testing coordination.

To capture lower limbs motions, 5 sensor modules, each consisting two accelerometers and one gyroscope, were used. The sensors (dimension: 20mm x 20mm x 10mm) were mounted on sacrum, and both thighs and shanks. The sensing axes were adjusted in the antero-posterior plane so that the motion in the sagittal plane could be measured. All signals were sampled at 200-Hz using the Physilog® [BioAGM, CH] ambulatory system carried on the waist.

Statistical comparison of the results were made using paired Wilcoxon sign rank tests for comparison within patient groups, and independent Wilcoxon rank sum tests for comparison of patient group with the normal subjects. A value of $p < 0.05$ was considered significant.

6.4 Results

Figures 5-2 to 5-6 show the intermediate steps of calculating the main parameters and outputs of the blocks indicated in Figure 6-4. The result of time-normalization of joint angles to gait cycle time is shown in Figure 6-5. The curves represent joint angles at 3 typical gait cycles of a healthy subject (no. 1): slow (dashed line), normal (solid line), and fast speeds (dotted line). Figure 6-6 shows the result of applying the criterion (5-8) to

choose the essential number of harmonics, m , required for 98% degree of data reconstruction (a typical case where m was maximum: patient no.3, gait cycle no.1, left knee). The dashed line shows the threshold set at 0.98, and the number of required harmonics where the criterion was met was $m = 9$, or $2m + 1 = 19$ numbers including the DC component, to reconstruct the joint motion during the gait cycle. So the total numbers required to reconstruct the 4 joints motions during a cycle was $4 \times 19 = 76$.

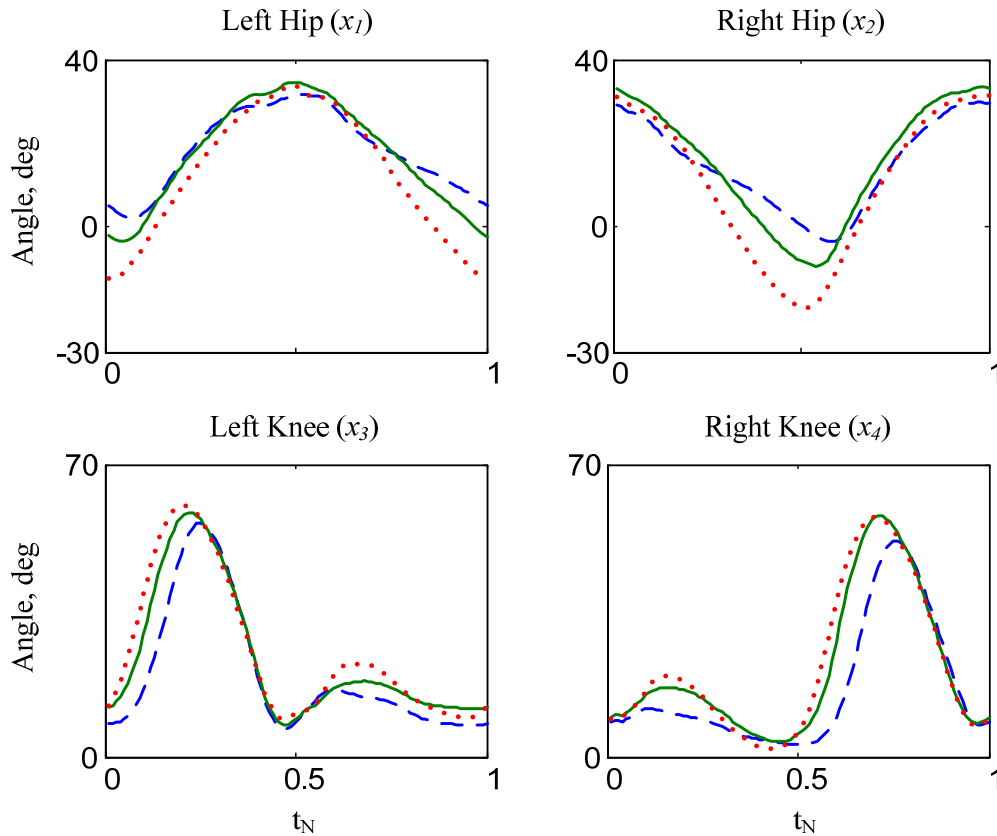


Figure 6-5 Time-normalization of lower limb joint angles to gait cycle time. The curves represent 3 typical gait cycles of a healthy subject (no. 1) at slow (dashed line), normal (solid line), and fast speeds (dotted line).

The cumulative variance of principal components vs. component numbers is reported in Figure 6-7. Based on the criterion (5.13), the number of required principal components to explain 98% of variance of the harmonic components (**H**) was $P = 8$.

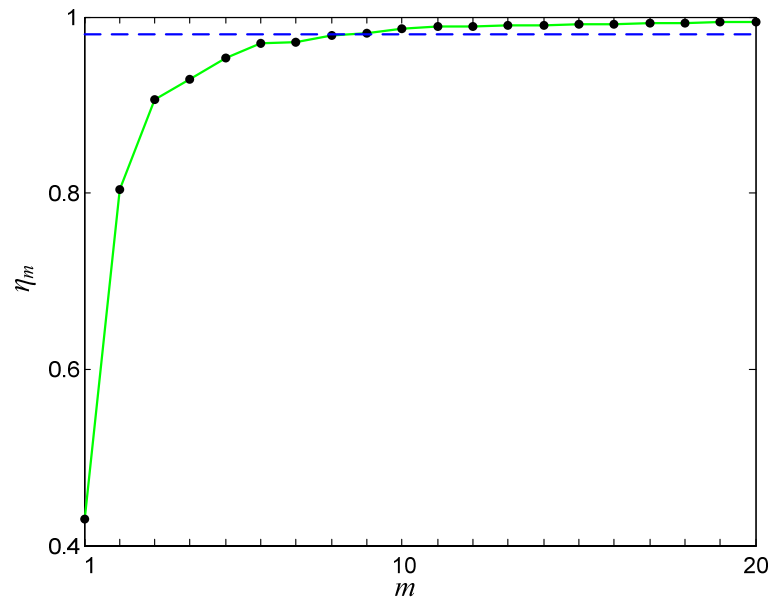


Figure 6-6 Choosing the required number of harmonics (m) for 98% degree of data reconstruction. The dashed line shows the threshold set at 0.98, and the number of required harmonics where the criterion (5.9) is met is $m=9$.

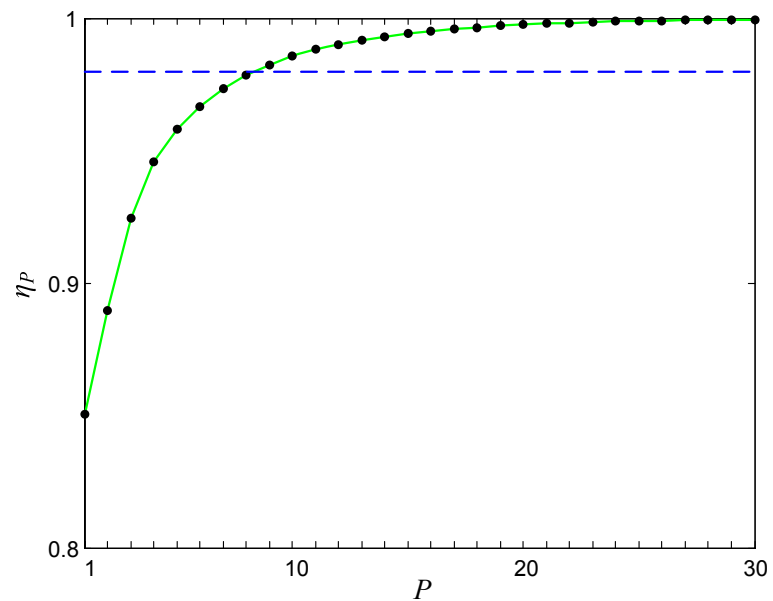


Figure 6-7 Choosing the required number of PCAs based on cumulative variance criterion (5.13). The dashed line shows the threshold set at 0.98, and the number of required components to explain 98% of variance is $P=8$.

The results of predicting lower limbs trajectories and the residual error is shown in Figure 6-8. The trajectories shown in the top row (x_l to x_4) represent actual measured joint angles of patient no. 1 at baseline with a very poor coordination. The first few cycles were chosen from slow speed, and the last few cycles were chosen from normal and fast speed trials respectively. The trajectories shown in the middle row (\hat{x}_1 to \hat{x}_4) represent the predicted patterns reconstructed by the model. The residual errors between the actual and predicted trajectories ($\hat{\varepsilon}_1$ to $\hat{\varepsilon}_4$) are shown in the bottom row.

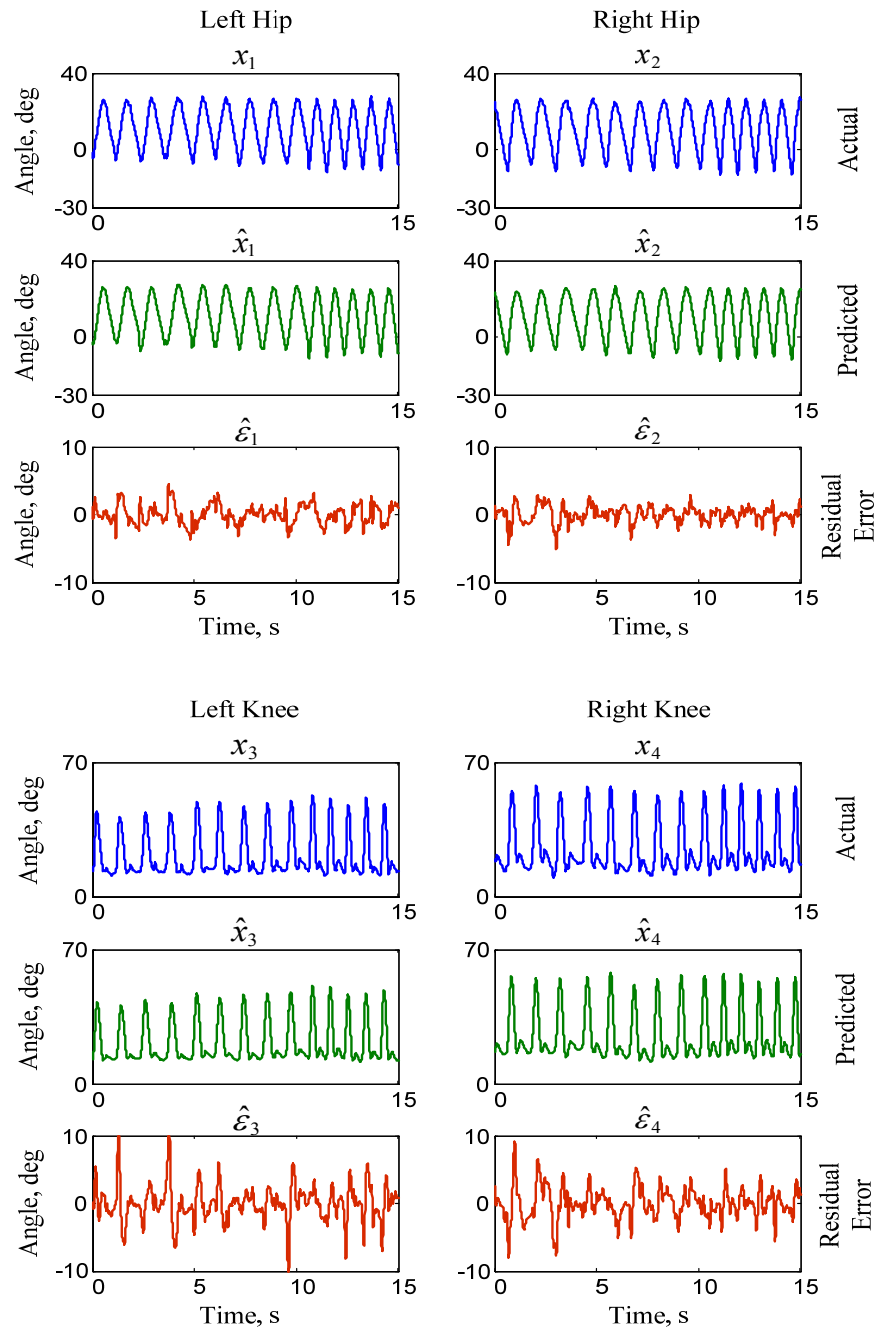


Figure 6-8 Lower limbs trajectories (actual and predicted) and the residual error (Top panel: Left and Right Hips, Bottom panel: Left and Right Knees). The trajectories shown in the top rows of the panels (x1 to x4) represent actual measured joint angles of patient no. 1 at baseline with a very poor coordination. The first few cycles were chosen from slow speed ($0 < t < 5$ s), the cycles in the middle part ($5 < t < 10$ s) were chosen from normal speed, and the last few cycles were chosen from fast speed trials ($10 < t < 15$ s). The trajectories shown in the middle row of the panels (\hat{x}_1 to \hat{x}_4) represent the predicted motions reconstructed by the model. The residual errors between the actual and predicted trajectories ($\hat{\epsilon}_1$ to $\hat{\epsilon}_4$) are shown in the bottom row of the panels. Note that the error scales are zoomed to -10.0 to 10.0 deg for better viewing.

The logarithmic mapping function, used in the scoring block to map normalized RMS error ($E_{k,j}$) to coordination score ($r_{k,j}$), is plotted in Figure 6-9. The output score ($r_{k,j}$) is ranged between 0 and 10, and the mapping function is identical for all subjects. The scaling constants in (5.16) were set to $r_{Max} = 10$, $E_{Min} = 0.01$, and $E_{Max} = 0.15$. E_{Min} corresponds to the minimum normalized RMS error or the highest coordination score of a gait cycle in the dataset (a healthy subject), and E_{Max} corresponds to the maximum normalized RMS error or lowest coordination score (a patient with poorest coordination).

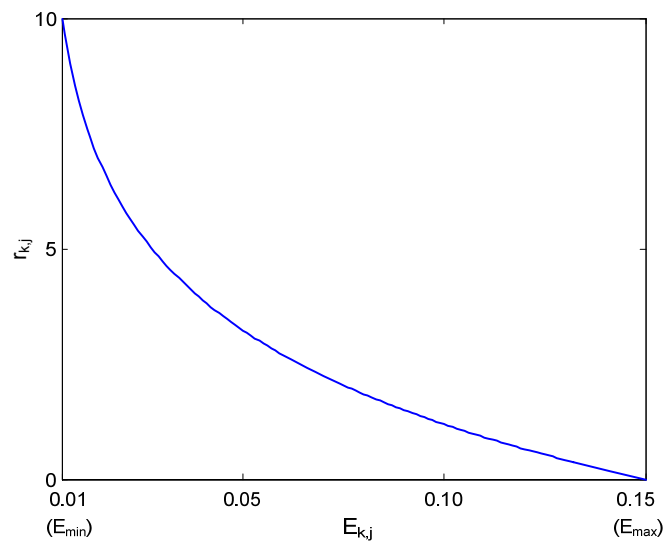


Figure 6-9 The logarithmic mapping function (5.16), used in the scoring block to map normalized RMS error ($E_{k,j}$) to coordination score ($r_{k,j}$). The output score ($r_{k,j}$) is ranged between 0 and 10. The scaling constants were set to $R_{Max} = 10$, $E_{Min} = 0.01$, and $E_{Max} = 0.15$.

Figure 6-10 to 5-9 show the results of coordination scores of patient no. 1. Figure 6-10 shows the coordination score of affected (left) knee during the 3 walking speeds (slow, normal and fast) at baseline. The dots indicate the scores calculated for each gait cycle using (5.16). A polynomial curve was fitted to the data to better represent and interpret the scores. Figure 6-11 shows the coordination score of each joint versus walking velocity. The curves, obtained by polynomial curve fitting, allow us to determine the contribution of each joint in gait coordination. The affected knee (left knee) indicates the least score. Figure 6-12 shows the overall coordination scores of patient no. 1, at baseline and 2 follow up tests at 6 weeks and 6 months, using (5.17).

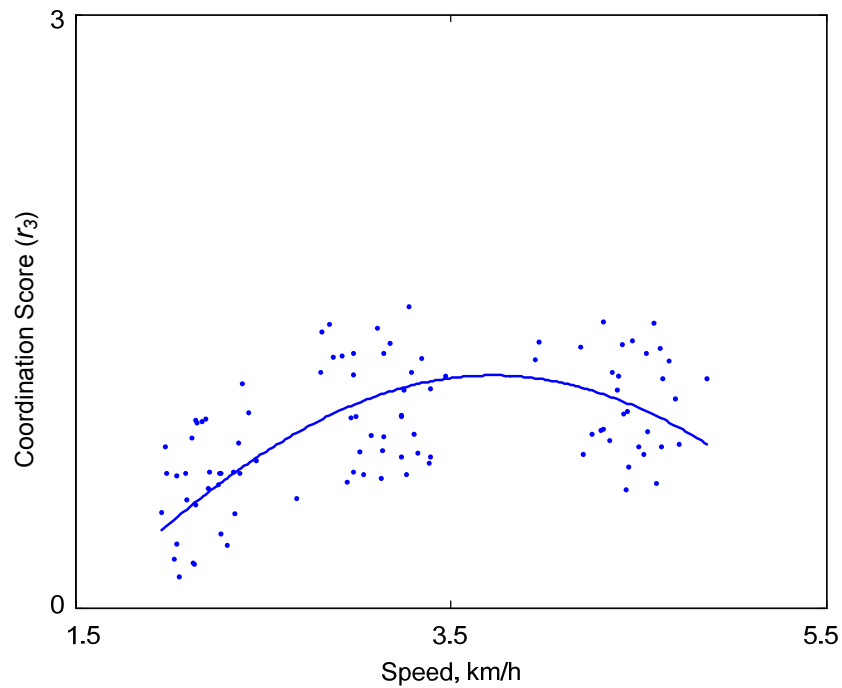


Figure 6-10 Coordination score of affected (left) knee ($j=3$) of patient no.1 at 3 walking speeds (slow, normal and fast) at baseline. The dots indicate the score of each gait cycle ($r_{k,3}$). A polynomial curve was fitted to the data (r_3) to better represent and interpret the scores.

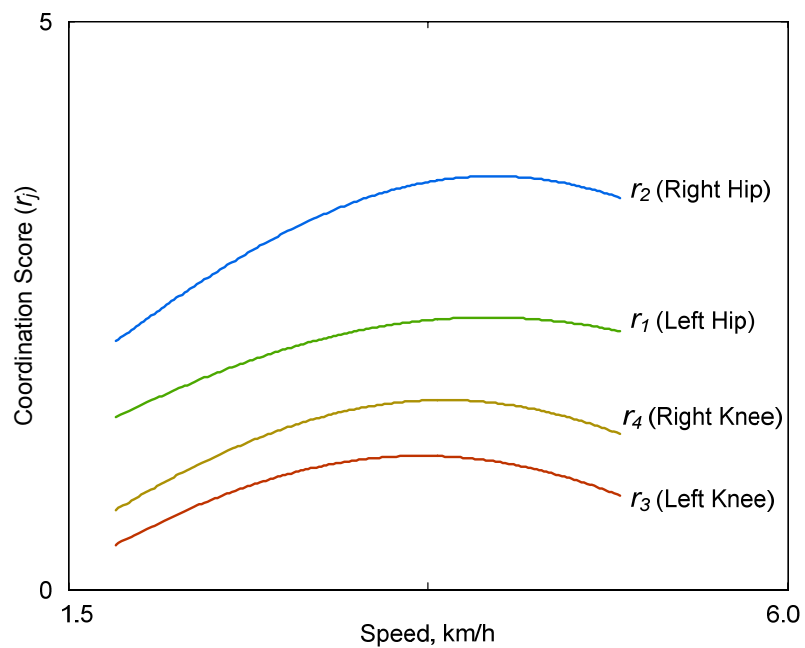


Figure 6-11 Contribution of each joint to the inter-joint coordination during gait (patient no.1, baseline). The curves show the coordination score assigned to each joint versus walking velocity. The affected knee (left knee) has the least score (r_3).

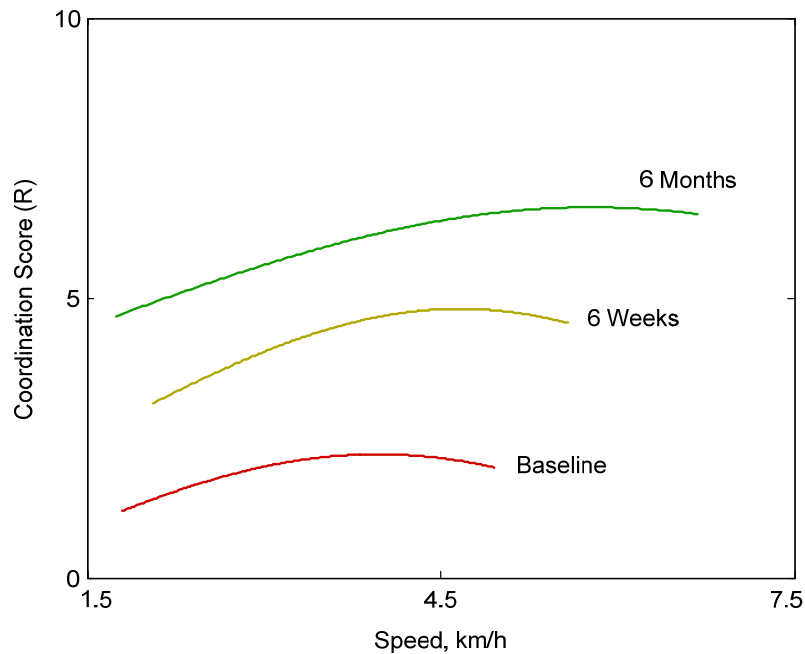


Figure 6-12 Overall inter-joint coordination score of patient no.1 at baseline and 2 follow up tests at 6 weeks and 6 months.

The whole results of obtaining coordination scores of all subjects are summarized in Table 6-1, which outlines the scores of 8 patients (*P1* to *P8*) at 3 different follow up tests, and 8 healthy subjects (*H1* and *H8*), as well as their mean and standard deviation. The scores of each trial at slow, normal, and fast speeds are reported separately. By comparing the scores of patients during follow up tests with baseline at each corresponding speed, all of the scores significantly increased. For instance, considering the patients' scores at normal speeds, the mean value of scores at baseline was 4.4, which significantly increased to 5.7 ($p = 0.008$) and 6.6 ($p = 0.008$) at 6 weeks and 6 months follow up tests respectively. However, the score of the healthy subjects was significantly higher than the score of patients at all tests ($p < 0.05$).

Table 6-1 Coordination scores of 8 patients (*P1* to *P8*) at 3 different follow up tests, and 8 healthy subjects (*H1* and *H8*). The scores of each trial at slow, normal, and fast speeds, as well as their mean and standard deviation for each group, are reported separately.

Subject	Baseline			+ 6 Weeks			+ 6 Months		
	Slow	Normal	Fast	Slow	Normal	Fast	Slow	Normal	Fast
<i>P1</i>	1.4	2.3	2.1	3.7	4.8	4.6	5.2	6.5	6.5
<i>P2</i>	2.0	2.8	2.8	3.3	4.3	3.0	5.1	5.7	5.8
<i>P3</i>	3.5	4.0	4.1	5.6	5.8	6.1	5.6	6.7	6.9
<i>P4</i>	4.1	6.7	5.0	5.9	6.8	6.7	6.0	6.8	6.8
<i>P5</i>	4.4	6.0	5.5	5.4	6.2	6.0	5.8	6.4	6.6
<i>P6</i>	3.9	4.4	4.2	5.8	6.7	6.7	6.7	7.1	7.1
<i>P7</i>	2.7	4.5	3.7	5.2	5.6	5.9	6.0	6.7	6.9
<i>P8</i>	3.9	4.4	4.1	4.8	5.7	5.5	6.1	6.6	6.2
mean±SD	3.2±1.1	4.4±1.5	4.0±1.1	5.0±1.0	5.7±0.9	5.6±1.2	5.8±0.5	6.6±0.4	6.6±0.4
<i>H1</i>	6.1	8.1	7.6	-	-	-	-	-	-
<i>H2</i>	6.7	7.4	7.1	-	-	-	-	-	-
<i>H3</i>	5.0	6.6	5.1	-	-	-	-	-	-
<i>H4</i>	6.2	7.5	7.6	-	-	-	-	-	-
<i>H5</i>	7.3	7.4	8.4	-	-	-	-	-	-
<i>H6</i>	6.5	7.2	7.0	-	-	-	-	-	-
<i>H7</i>	6.1	7.8	6.6	-	-	-	-	-	-
<i>H8</i>	6.4	7.4	6.5	-	-	-	-	-	-
mean±SD	6.3±0.7	7.4±0.4	7.0±1.0	-	-	-	-	-	-

All subjects' scores during normal and fast speeds were higher than their corresponding scores at slow speed. For example, the mean scores of patients at baseline during normal and fast speeds were 4.4 and 4.0 respectively, that were higher than the mean score at slow speed (3.2) ($p < 0.05$). This result is in accordance with (Li et al. 2005; Stergiou et al. 2001), as in general, if one tries to walk at extremely slow pace, the movement is highly dis-coordinated, unstable and of poor efficiency.

6.5 Discussion and conclusion

We proposed a method that quantitatively analyzed multi-joint gait coordination at various walking speeds. In this study, the focus was to use the least number of parameters to capture the whole dynamics and describe the classes of movement patterns, as trajectories with small number of components are properties of coordinated movements.

We indicated how an integration of different analysis tools such as Harmonic analysis, Principal Component Analysis, and Artificial Neural Network helped overcome high-dimensionality, temporal dependence, and nonlinear relationships of the gait patterns.

The Harmonic analysis adopted in this study is an optimum curve fitting that reflects also the periodic behavior of the gait waveforms. Higher order polynomials or other complex techniques might be used to parameterize the curves, but the number of the fitting parameters would increase. We showed that with $m = 9$ harmonics, or the total number of $4 \times (2m + 1) = 76$ parameters, the motions of the 4 joints during a gait cycle could be reconstructed with 98% accuracy. Then, the principal component analysis examined the relationship between the harmonic components of the various joints, and could reduce the redundancy and dimensionality of the data to $P = 8$ components. Since PCA only detects linear relationships in the data, the artificial neural network was used to model the nonlinear gait variable relationships, which has traditionally been difficult to model analytically. The ANN could model the data with only 2 inputs as control parameters (cadence, stride length). Although the ANN would not offer biomechanical insight into the locomotion system and the basis has a lack in correspondence to the biomechanical system, the advantage of the technique was that the necessity to build a model of the human body was eliminated.

The model could parameterize the locomotion, and hence it has the ability to generalize. It enables the system to make reliable predictions for new inputs that are not in the training set. Generalization allows us to generate new motion patterns by smooth interpolations for the untrained data set.

We applied our proposed model on patients with knee osteoarthritis to delineate how pathology affects walking coordination. Knee osteoarthritis is marked by the progressive erosion of articular cartilage, subchondral sclerosis, and osteophytes growth at the joint margins. Individuals with knee osteoarthritis experience debilitating pain, joint laxity and instability (Deluzio et al. 1999; Deluzio et al. 1997; Lewek et al.). Although our study sample was small (8 patients and 8 controls), the results suggest that treatments and rehabilitation programs improve the gait function and coordination in individuals with knee arthroplasty. These results allow us to apply the model to larger groups of patients with knee osteoarthritis before and after surgery and compare, for example, the differences in outcome of fixed bearing and mobile bearing total knee arthroplasty. In the next chapter (chapter 7), we will show that coordination score is significantly improved in a population of 54 patients after knee replacement.

In the present study we only examined the sagittal movements (flexion-extension) of lower limbs. However, in gait analysis, a 2D sagittal approach seems to be satisfactory, because sagittal plane is the plane where majority of the movement takes place, and gives a lot of information for gait pathologies (Tong and Granat 1999a).

The proposed model is limited to steady state walking, so the transient cycles during gait initiation, termination, turning, or changes in the environment are not supported by the current model. However, the model could be enhanced by including additional control parameters such as stance period, range of flexion-extension of joints, or the control parameters of the previous cycle.

The proposed technique, along with the ambulatory device using body-fixed sensors, provides an analytical tool that is easy to use in the clinical diagnosis of human gait abnormalities. The model can be applied widely in rehabilitation evaluation, prosthesis design, and robotics. The ambulatory device is easily mountable, and it can capture kinematic information over a non-limited distance and outside a laboratory environment without hindrance to natural gait, allowing the patient to walk freely and to reach his/her own steady state speed. In this way, coordination could be estimated during daily walking.

Chapter 7 Clinical Application

Abstract

In this chapter, we applied the gait analysis methods, proposed in previous chapters, in a real clinical application. The goal of this study was to provide gait parameters as a new objective method to assess total knee arthroplasty (TKA) outcome, using the current debate on the advantages of mobile bearing versus fixed bearing tibial plates of these implants as an interesting illustration for surgeons. This randomized controlled double-blind study included 54 patients. Each participant was asked to perform different walking trials at different speeds and conditions, and to complete a general health questionnaire EuroQol questionnaire in 5 dimensions EQ-5D), a disease specific questionnaire for osteoarthritis Western Ontario and McMaster Universities Osteoarthritis Index WOMAC) and a semi-objective specific score filled by the surgeon (Knee Society Score, KSS) was also done. Preoperative results were compared with postoperative (6 weeks, 3 months, 6 months, and 1 year) results. The results indicated that fixed bearing TKA performed better than mobile bearing TKA in the early period (3 months). However, after 6 months the mobile bearing performed as well as the Fixed bearing TKA. In general, the results indicated that gait function in all of the patients can be improved considerably after surgery. We provided objective criteria, using ambulatory gait analysis, for assessing functional recovery following TKA procedure.

7.1 Introduction

Total knee arthroplasty (TKA) is a widely used surgical treatment for severe osteoarthritis (OA) of the knee, which provides consistently good postoperative clinical results. Knee prosthesis designs and their surgical techniques have improved in recent years to provide more satisfactory results of joint reconstruction and improved walking ability (Solak et al. 2005).

Since 1977, mobile bearing knee prostheses have been designed and implanted in order to provide less constrained knee kinematics while minimizing polyethylene wear and reducing bone-cement prosthesis interface stress (Aglietti et al. 2002; Buechel and Pappas 1989; Catani et al. 2003; Lemaire 2002). Clinical and biomechanical studies have claimed that normal joint function and articular surface conformity are incompatible with fixed bearing knees (Goodfellow and O'Connor 1994). Usage can lead to excessive poly-

ethylene wear and full conformity of the bearing surface leads to excessive constraint of joint kinematics. This dilemma can be solved by a prosthesis that has a polyethylene bearing component interposed between a femoral component and a polished tibial plate, in order that the polyethylene insert moves with the femur and slides with the plate (Goodfellow and O'Connor 1994). The mobility of the polyethylene insert permits rotation and gliding; the load can thus be shared by the soft tissues, and there is less loosening stress being transferred to the bone-prosthesis interface.

Almost every manufacturer has introduced a mobile-bearing TKA system, or is developing one to introduce into the market. However, most studies on the outcomes of mobile-bearing TKA are open studies.

Currently, five randomized controlled clinical trials comparing fixed and mobile bearings for TKA have been published (Aglietti et al. 2005; Bhan et al. 2005; Hansson et al. 2005; Kim et al. 2001; Price et al. 2003) as well as two prospective match pair studies (Chiu et al. 2001; Watanabe et al. 2005). No evidence of superiority for one of the two implants with regard to Range of Motion (ROM) or functional performance of the patients could be found as conducted in the systematic Cochrane review and meta-analysis of Jacobs et al. (Jacobs et al. 2004).

Evaluation of the functional capacity of the knee joint has been performed by clinical scoring systems and by static radiographic and clinical examinations. Furthermore, gait analysis has been shown to be of value in distinguishing between functional outcomes of different types of knee surgery (Andriacchi et al. 1997; Chassin et al. 1996; Smith et al. 2006), making preoperative and postoperative gait evaluation, comparing the variables with those of healthy controls (Andriacchi et al. 1982; Berman et al. 1987; Chao et al. 1980; Kroll et al. 1989; Simon et al. 1983), and assessing preoperative and postoperative changes (Andersson et al. 1981; Andriacchi et al. 1977; Chao et al. 1980; Collopy et al. 1977; Kirtley et al. 1985; Kroll et al. 1989; Otsuki et al. 1999; Steiner et al. 1989; Webster et al. 2003). Additionally, ambulatory gait analysis allows long-term monitoring of patient, is applicable for routine evaluation of patient outcomes and has already been validated for hip arthroplasty outcome evaluation (Aminian et al. 2004c).

The purpose of this randomized controlled study was to provide gait parameters as a new objective method to assess total knee arthroplasty outcome between patients with fixed- and mobile-bearing. The measuring system designed for gait analysis during this project, which was described in the previous chapters, was used for this clinical study. Gait analysis and knee scoring system results of 54 patients were evaluated. Preoperative

results were compared with postoperative (6 weeks, 3 months, 6 months, and 1 year) results.

7.2 Methods

7.2.1 Subjects

From February 2003 to April 2006, all patients diagnosed with unilateral (one lower limb, not both) knee osteoarthritis waiting for a TKA were asked to participate in the study. To date, 54 patients signed a consent form and were included and blinded to the type of prosthesis they received. Nexgen (Zimmer, Inc., Warsaw, IN, USA) postero-stabilized cemented implants were used for all patients, the only difference being the Mobile- or Fixed-bearing following the randomized process. Table 7-1 summarizes the demographic data of patients.

Table 7-1 Patient Demographics

Demographics	Total cases	Fixed bearing	Mobile bearing
Number of patients	54	30	24
Age, yr (mean±std)	69.5±8.7	71.2±8.4	67.2±8.6
Gender (Female / Male)	33 / 21	15 / 15	18 / 6
Body weight, kg (mean±std)	77.0±20.1	76.8±15.8	77.3±24.7
Body height, cm (mean±std)	165.3±8.6	164.6±8.7	166.2±8.5
BMI, kg/m ²	28.1±6.4	28.2±4.8	28.0±8.1
Treated side (Left / Right)	23 / 31	9 / 21	14 / 10

BMI=body mass index

7.2.2 Clinical Evaluation

Each patient was asked to complete an auto-administrated quality of life subjective EuroQoL (EQ-5D) in five dimensions questionnaires (Brazier et al. 1993; EuroQoL-Group 1990), an auto-administrated subjective disease-specific WOMAC (Western Ontario McMaster) Osteoarthritis Index (Bellamy et al. 1988), a VAS-pain and stiffness auto-administrated subjective scores (Visual Analog Scale), and a semi-objective disease-specific Knee Society Score (KSS) (Insall et al. 1989) by an independent blinded observer. The Knee Society score rated the patient's overall functional performance of the knee (maximum score 100 points). The KSS was evaluated for both healthy and operated knees. The questionnaires were completed preoperatively and postoperatively at 6 weeks, 3 months, 6 months and 1 year. For the details concerning these clinical evaluations please see chapter 2.

7.2.3 Gait Analysis

Each subject was asked to perform 15 trials at different conditions. The trials included 6 walking trails of 30m long at 3 different self-selected speeds: normal (trials 1 and 2), slow (trials 3 and 4), and fast (trials 5 and 6). Then the patient was asked to perform 2 trials of stair descending (trials 7 and 8), 4 walking trials of 20m long on ramp (inclination = 7.5 deg): going up (trials 10 and 12), and going down (trials 9 and 11). Afterwards, the patient performed 2 trials of stair climbing (trials 13 and 14). Finally the patient performed 5 times of sit-stand-sit movements on a chair (trial 15).

The gait analyses were performed preoperatively and postoperatively at 6 weeks, 3 months, 6 months and 1 year. Lower limb rotations were measured using the kinematic sensors as explained in Chapter 3 and 4. Multi-joint coordination was evaluated using the method described in chapter 6.

In this chapter, we present the spatio-temporal gait results and coordination scores at normal speed (trial 1). Only steady-state parts of walking trials were used for analysis, and the transient (initial and terminal) cycles were eliminated.

7.2.4 Statistical Analysis

Preoperative and postoperative results (including clinical scores and gait analysis results) were compared with paired *t* test, and the results of the Mobile bearing and fixed Bearing groups were compared with independent-samples *t* test. A value of $P < 0.05$ was considered as significant difference. All statistical computations were performed using the MATLAB 7.0 software.

7.3 Results

7.3.1 Clinical Evaluation

From the total of 54 patients who were included in the study and were tested at baseline, we could follow up 52 patients at 6 weeks, 50 patients at 3 months, 40 patients at 6 months and 32 patients at 1 year.

The pain scores, knee scores, and functional scores of all patients are summarized in Table 7-2. The improvement (difference between each follow up test and preoperative test) is shown in Table 7-3. The significant differences ($p < 0.05$) are shaded in gray. Many of the scores have significantly improved after 6 weeks (all WOMAC scores, VAS scores, and KSS-op). The improvements indicated by FCTN-op and EQ5d-Visual scores were significant after 3 months. However, the FCTN-healthy and KSS-healthy scores of the healthy knees did not significantly change after operation.

Table 7-2 Clinical scores of all patients at baseline and different follow up tests at 6-week, 3-month, 6-month, and 1-year

Parameters Mean \pm std	Baseline N=54	6 weeks N=52	3 months N=50	6 months N=40	1 year N=32
VAS-stiffness	6.56 \pm 2.00	3.69 \pm 2.18	2.87 \pm 2.3	2.24 \pm 1.97	2.40 \pm 2.46
VAS-pain	5.84 \pm 2.60	3.89 \pm 2.18	3.06 \pm 2.28	2.27 \pm 2.23	2.38 \pm 2.64
Womac-pain	11.85 \pm 3.07	6.36 \pm 3.39	5.17 \pm 3.66	4.40 \pm 3.78	4.72 \pm 4.56
Womac-stiffness	4.84 \pm 1.49	3.3 \pm 1.39	2.58 \pm 1.61	2.58 \pm 1.68	2.52 \pm 1.99
Womac-function	36.84 \pm 11.72	22.38 \pm 9.99	17.17 \pm 11.20	14.6 \pm 10.27	16.68 \pm 14.27
Womac-total	53.51 \pm 15.24	32.02 \pm 13.84	24.91 \pm 15.68	21.58 \pm 14.81	23.92 \pm 20.29
Womac%-pain	59.24 \pm 15.31	31.76 \pm 16.92	25.84 \pm 18.30	22.00 \pm 18.90	23.60 \pm 22.76
Womac%-stiffness	60.39 \pm 18.6	41.21 \pm 17.28	32.18 \pm 20.12	32.25 \pm 21.00	31.50 \pm 24.77
Womac%-function	54.17 \pm 17.24	32.9 \pm 14.68	25.25 \pm 16.47	21.47 \pm 15.10	24.53 \pm 20.98
Womac%-total	55.74 \pm 15.87	33.36 \pm 14.41	25.95 \pm 16.34	22.49 \pm 15.43	24.92 \pm 21.14
KSS-op	49.78 \pm 16.7	66.35 \pm 14.10	70.1 \pm 14.02	76.90 \pm 11.60	73.48 \pm 15.23
KSS-healthy	79.04 \pm 16.82	83.8 \pm 16.78	81.88 \pm 18.56	77.94 \pm 19.02	77.88 \pm 17.79
FCTN-op	60.6 \pm 16.82	58.8 \pm 19.45	73.71 \pm 14.87	83.60 \pm 16.76	84.20 \pm 17.66
FCTN-healthy	79.41 \pm 20.45	82.6 \pm 18.83	82.60 \pm 15.17	84.6 \pm 16.90	83.00 \pm 18.26
EQ5d-Visual	69.88 \pm 22.44	73.34 \pm 17.75	76.56 \pm 16.65	80.1 \pm 17.46	74.80 \pm 19.78

VAS=visual analog scale, KSS=knee society score, EQ5d=EuroQol measure, s=healthy knee, raid=stiffness, op=operated knee, visual=VAS. A lower WOMAC and VAS scores and higher KSS, FCTN and EQ5d scores indicate improvement. For the definition of different scores please see the text and chapter 2.

Chapter 7: Clinical Application

Table 7-3 Differences in clinical scores between Follow up tests and Pre-op test. The statistically significant differences ($p < 0.05$) between the groups are shaded in gray. The p-value is provided only for non-significant changes

Clinical Score	Pre-op vs. 6 weeks, N=52	Pre-op vs. 3 months, N=50	Pre-op vs. 6 months, N=40	Pre-op vs. 1 year, N=32
VAS-stiffness	-2.92±2.44	-3.74±2.28	-4.21±2.87	-3.45±3.2
VAS-pain	-2.09±3.02	-2.7±2.99	-3.47±3.45	-2.98±3.4
Womac-pain	-5.33±4.19	-6.49±3.63	-7.21±3.99	-7.05±5.48
Womac-stiffness	-1.46±1.8	-2.02±1.82	-2.18±2.01	-2.2±2.63
Womac-function	-13.8±13.25	-19.7±12.62	-20.82±13.55	-21.4±16.91
Womac-total	-20.59±17.6	-28.21±17.05	-30.21±18.35	-30.65±24.28
Womac%-pain	-26.63±20.95	-32.44±18.14	-36.03±19.95	-35.25±27.41
Womac%-stiffness	-18.21±22.47	-25.29±22.74	-27.21±25.09	-27.5±32.85
Womac%-function	-20.3±19.49	-28.97±18.56	-30.62±19.92	-31.47±24.86
Womac%-total	-21.44±18.33	-29.38±17.76	-31.46±19.12	-31.93±25.29
KSS-op	15.33±18.65	20±22.08	28.85±22.98	21.2±21.05
KSS-healthy	7.52±14.71	2.86±17.21 p=0.28	-0.82±17.13 p=0.78	0±15.49 p=1.0
FCTN-op	-2.17±24.55 p=0.65	12.79±20.07	22.79±20.38	25.5±18.77
FCTN-healthy	1.63±19.12 p=0.51	1.28±21.27 p=0.69	2.06±18.91 p=0.53	1±15.36 p=0.77
EQ5d-Visual	7.18±24.7 p=0.062	11.2±21.08	11.4±24.01	16.75±21.48

VAS=visual analog scale, KSS=knee society score, EQ5d=EuroQol measure, s=healthy knee, raid=stiffness, op=operated knee, visual=VAS. A lower WOMAC and VAS scores and higher KSS, FCTN and EQ5d scores indicate improvement.

The difference between clinical scores of Fixed bearing and Mobile bearing groups at 3-month, 6-month, and 1-year follow ups are reported in Tables 7-4, 7-5, and 7-6 respectively. The first two columns (cols. 1 and 2) of each table report the scores of each group at the corresponding follow up test. The second two columns (cols. 3 and 4) of each table report the improvement (difference between the follow up result and baseline value) for each group. Significant differences ($p < 0.05$) of each comparison are shaded in gray.

At 3-month follow up, the VAS-pain score was 2.63 for Fixed bearing and 4.18 for mobile bearing groups; the difference between the groups was significant ($p = 0.029$). The other

scores did not show statistical differences between the two groups. KSS-healthy which expresses the KSS score for the healthy knee has improved for fixed bearing group and degraded for mobile bearing group (9.25 vs. -5.21; $p=0.0048$). This explains also why score was not significant when mixing both groups (Table 7-3).

At 6-month follow up, the FCTN-s score was 79.71 for Fixed bearing and 90.59 for mobile bearing groups; the difference between the groups was significant ($p=0.038$). Also, the improvement indicated by KSS-healthy score was 6.71 in Fixed bearing group while a degradation of -8.35 was observed for Mobile bearing group; the difference between the groups was significant ($p=0.0081$). The other scores did not show statistical differences between the two groups.

At 1-year follow up, the FCTN-s and EQ5d_Visual scores were significantly different between the fixed- and mobile-bearing groups ($p=0.042$ and $p=0.024$ respectively). However, the improvement was higher for fixed bearing group.

Chapter 7: Clinical Application

Table 7-4 Group comparisons (Fixed- and Mobile-bearing) using the clinical scores. The comparison is made between the clinical scores at 3 months (cols. 1 and 2), and between the patient improvements (difference between 3 months and baseline, cols. 3 and 4). The statistically significant differences ($p < 0.05$) between the groups are shaded in gray

Clinical Score	3 Months		Difference 3M - PreOp	
	Fixed Bearing N=27	Mobile Bearing N=23	Fixed Bearing N=27	Mobile Bearing N=23
VAS-stiffness	2.35±2.24	3.5±2.37	-4.08±2.34	-3.32±2.19
VAS-pain	2.63±2.16	4.18±2.38	-3.15±2.39	-2.13±3.6
Womac-pain	4.79±4.04	5.95±3.39	-6.92±3.65	-5.95±3.63
Womac-stiffness	2.63±1.69	2.89±1.52	-2.21±1.86	-1.79±1.78
Womac-function	14.96±12.57	19.79±9.77	-20.63±12.83	-18.53±12.61
Womac-total	22.38±17.49	28.63±14	-29.75±17.4	-26.26±16.86
Womac%-pain	23.96±20.22	29.74±16.95	-34.58±18.23	-29.74±18.14
Womac%-stiffness	32.81±21.11	36.18±19.05	-27.6±23.31	-22.37±22.27
Womac%-function	22±18.48	29.1±14.37	-30.33±18.86	-27.24±18.54
Womac%-total	23.31±18.22	29.83±14.59	-30.99±18.13	-27.36±17.57
KSS-op	69.33±13.75	68.26±14.58	23.38±23.61	15.74±19.76
KSS-healthy	82.46±20.08	76.79±19.13	9.25±16.12	-5.21±15.36
FCTN-op	75.21±18.27	72.11±10.18	14.17±23.53	11.05±15.05
FCTN-healthy	81.25±14.54	81.05±16.63	4.58±22.11	-2.89±19.95
EQ5d-Visual	79.85±17.14	77.89±11.7	13.81±19.71	7.89±22.81

VAS=visual analog scale, KSS=knee society score, EQ5d=EuroQol measure, s=healthy knee, raid=stiffness, op=operated knee, visual=VAS. A lower WOMAC and VAS scores and higher KSS, FCTN and EQ5d scores indicate improvement.

Table 7-5 Group comparisons (Fixed- and Mobile-bearing) using the clinical scores. The comparison is made between the clinical scores at 6 months (cols. 1 and 2), and between the patient improvements (difference between 6 months and baseline, cols. 3 and 4). The statistically significant differences ($p < 0.05$) between the groups are shaded in gray

Clinical Score	6 Months		Difference 6M - PreOp	
	Fixed Bearing N=21	Mobile Bearing N=19	Fixed Bearing N=21	Mobile Bearing N=19
VAS-stiffness	1.97±2.08	2.85±2.04	-4.74±2.92	-3.68±2.81
VAS-pain	2.29±2.15	2.79±2.39	-3.59±3.24	-3.35±3.74
Womac-pain	3.94±3.83	5.35±2.91	-7.76±4.55	-6.65±3.39
Womac-stiffness	2.35±1.37	3±1.37	-2.65±2	-1.71±1.96
Womac-function	12.47±10.28	16.29±8.57	-20.53±14.53	-21.12±12.92
Womac-total	18.76±14.68	24.65±12.32	-30.94±19.64	-29.47±17.55
Womac%-pain	19.71±19.16	26.76±14.57	-38.82±22.74	-33.24±16.95
Womac%-stiffness	29.41±17.08	37.5±17.12	-33.09±24.98	-21.32±24.51
Womac%-function	18.34±15.12	23.96±12.61	-30.19±21.38	-31.06±19
Womac%-total	19.55±15.29	25.67±12.83	-32.23±20.46	-30.7±18.28
KSS-op	79.41±10.98	74.24±11.84	33.76±26.21	23.94±18.74
KSS-healthy	78.41±21.59	74.24±21.31	6.71±15.61	-8.35±15.53
FCTN-op	78.53±18.09	87.94±11.6	17.06±22.15	28.53±17.21
FCTN-healthy	79.71±17.72	90.59±10.88	-0.29±21.83	4.41±15.8
EQ5d-Visual	78.09±22.63	81.03±16.03	10.88±24.01	11.91±24.74

VAS=visual analog scale, KSS=knee society score, EQ5d=EuroQol measure, s=healthy knee, raid=stiffness, op=operated knee, visual=VAS. A lower WOMAC and VAS scores and higher KSS, FCTN and EQ5d scores indicate improvement.

Chapter 7: Clinical Application

Table 7-6 Group comparisons (Fixed- and Mobile-bearing) using the clinical scores. The comparison is made between the clinical scores at 1 year (cols. 1 and 2), and between the patient improvements (difference between year and baseline, cols. 3 and 4). The statistically significant differences ($p<0.05$) between the groups are shaded in gray

Clinical Score	1 Year		Difference 1Y – PreOp	
	Fixed Bearing N=17	Mobile Bearing N=15	Fixed Bearing N=17	Mobile Bearing N=15
VAS-stiffness	2.33±2.92	3.14±2.28	-4.72±4.13	-2.41±1.77
VAS-pain	2.56±3.21	2.77±2.62	-4.06±3.57	-2.09±3.14
Womac-pain	5.33±5.92	5.18±3.71	-8.11±6.99	-6.18±4.02
Womac-stiffness	2.67±2.29	2.73±1.79	-2.89±3.22	-1.64±2.01
Womac-function	20.33±18.34	17.09±11.8	-26.11±20.28	-17.55±13.34
Womac-total	28.33±25.86	25±17	-37.11±29.75	-25.36±18.55
Womac%-pain	26.67±29.58	25.91±18.55	-40.56±34.95	-30.91±20.1
Womac%-stiffness	33.33±28.64	34.09±22.42	-36.11±40.24	-20.45±25.17
Womac%-function	29.9±26.97	25.13±17.36	-38.4±29.82	-25.8±19.61
Womac%-total	29.52±26.94	26.04±17.71	-38.66±30.99	-26.42±19.32
KSS-op	76.44±16.42	70.73±15.23	25±26.12	18.09±16.5
KSS-healthy	76.33±19.07	81±20.57	4.44±15.92	-3.64±14.85
FCTN-op	78.33±16.96	90±10	25.56±23.91	25.45±14.57
FCTN-healthy	76.11±17.28	90±10.95	3.89±21.03	-1.36±8.97
EQ5d-Visual	62.5±22.84	82.73±13.67	22.78±21.95	11.82±20.77

VAS=visual analog scale, KSS=knee society score, EQ5d=EuroQol measure, s=healthy knee, raid=stiffness, op=operated knee, visual=VAS. A lower WOMAC and VAS scores and higher KSS, FCTN and EQ5d scores indicate improvement.

7.3.2 Gait Parameters

The spatio-temporal gait parameters and coordination scores measured during gait analysis of all patients at normal walking speed are listed in Table 7-7. Correspondingly, the variability (CV%) of spatio-temporal gait parameters are summarized in Table 7-8.

Table 7-9 shows the difference of gait parameters between each follow up test and pre-operative test for all patients. The significant differences ($p < 0.05$) are shaded in gray. Many of the parameters have significantly changed (improved) after 3 months, but there were no significant difference between preoperative results and postoperative values at 6 weeks. For example, the walking speed has significantly increased at 3-month, 6-month, and 1-year follow ups. This increase is due to both decreasing the Gait Cycle Time ($p < 0.05$) and increasing Stride length ($p < 0.05$). Besides, the range of rotations of treated and contralateral sides of knee, shank, and thigh, along with maximum angular velocities of knee and shank, and coordination score were all significantly increased at 3-month, 6-month, and 1-year follow ups.

In the same way, Table 7-10 shows the difference of variability (CV%) of gait parameters between follow up tests and pre-operative test for all patients. Similarly, the significant differences ($p < 0.05$) are shaded in gray. Many of the variabilities have decreased after 3-month or 6-month follow ups, but there were no significant difference between preoperative variabilities and postoperative values at 6 weeks. For example, the variabilities of stride length, range of rotations of treated and contralateral sides of knee, shank, and thigh, and also maximum angular velocities of knee and shank were all significantly decreased at 3-month, 6-month, and 1-year follow ups. In addition, the variabilities of Gait Cycle Time, and Stance times (normalized to Gait Cycle Time) were significantly decreased at 6-month and 1-year follow ups.

Chapter 7: Clinical Application

Table 7-7 Gait parameters of all patients at baseline and different follow up tests at 6 weeks, 3 months, 6 months and 1 year during walking at normal speed

Gait Parameter	Baseline N=54	6 weeks N=52	3 months N=50	6 months N=40	1 year N=32
Gait Cycle Time (GCT), s	1.26±0.16	1.29±0.16	1.21±0.13	1.18±0.1	1.19±0.13
Treated side Stance, %	60.72±3.64	61±2.49	61.03±2.05	60.81±1.91	61.26±2.37
Contralateral side Stance, %	63.15±2.44	63.05±2.14	61.93±1.78	61.48±2.3	61.8±1.96
Double Support, DS%	24±3.99	24.06±3.46	22.95±3.53	22.27±3.89	23.08±3.79
Limp, %	2.58±1.96	2.31±1.15	1.86±0.8	1.65±0.82	1.71±1.12
Treated side Stride, m	1.12±0.18	1.15±0.18	1.21±0.15	1.25±0.15	1.18±0.17
Contralateral side Stride, m	1.12±0.18	1.15±0.18	1.21±0.15	1.25±0.15	1.18±0.17
Speed, m/s	0.91±0.2	0.92±0.2	1.02±0.18	1.07±0.16	1.01±0.21
Normalized Speed, /s	0.55±0.11	0.55±0.12	0.62±0.1	0.64±0.09	0.61±0.13
Treated side Shank Peak Velocity, PS _ω T, deg/s	271.59±68.61	267.4±56.68	305.68±52.52	323.85±47.65	311.92±66.04
Contralateral side Shank Peak Velocity, PS _ω C, deg/s	311.78±52.93	309.75±49.43	333.81±51	337.72±50.72	326.68±61.63
Treated Knee Peak Velocity, PK _ω T, deg/s	280.53±81.37	277.36±72.59	317.18±70.13	338.63±58.38	327.84±73.66
Contralateral Knee Peak Velocity, PK _ω C, deg/s	300.64±64.43	299.67±62.73	327.75±66.3	343.74±62.21	327.21±78.98
Treated side Thigh Rotation, R _α T, deg	36.83±6.19	39.44±6.16	40.29±5.3	41.88±5.7	39.38±6.58
Contralateral side Thigh Rotation, R _α C, deg	36.66±6.16	36.95±5.86	39.12±6.26	40.16±5.86	37.95±6.21
Treated side Shank Rotation, R _β T, deg	62.8±11.03	64.08±9.73	68.95±8.49	70.99±8.05	68.57±10.18
Contralateral side Shank Rotation, R _β C, deg	66.66±8.86	67.21±8.39	70.76±7.52	71.99±7.46	69.41±9.37
Treated Knee Rotation, R _γ T, deg	47.78±11.79	46.12±10.64	52.25±9.04	54.61±8.78	54.22±10.09
Contralateral Knee Rotation, R _γ C, deg	54.16±8.53	55.49±8.44	58.01±7.93	57.63±7.61	56.73±8.97
Coordination Score	5.22±1.32	6.10±1.02	6.49±0.96	6.6±0.91	6.59±0.84

Table 7-8 Variability (CV%) of Spatio-temporal gait parameters of the patients at baseline and different follow up tests at 6 weeks, 3 months, 6 months and 1 year during walking at normal speed

Gait Parameter (CV%)	Baseline N=54	6 weeks N=52	3 months N=50	6 months N=40	1 year N=32
Gait Cycle Time (GCT)	2.6±0.9	2.6±1.2	2.4±0.9	2.3±0.8	2.5±1
Treated side Stance	2.4±1.3	2.4±2.3	1.9±1.0	1.8±0.7	1.8±0.7
Contralateral side Stance	2.3±1.9	2.1±1.8	1.9±1.0	1.7±0.7	1.8±0.9
Double Support (DS)	7.6±4.6	8±14	6.4±2.3	6.3±3.3	6.2±2.8
Limp	1.50±0.97	1.33±0.56	1.20±0.49	1.09±0.5	1.17±0.64
Treated side Stride	2.5±1.2	2.3±1.4	2.0±0.7	2±0.8	2.1±0.9
Contralateral side Stride	2.6±1.5	2.4±1.7	2.1±0.8	2±0.8	2.1±0.9
Speed	4.1±1.7	4.0±2.5	3.6±1.3	3.3±1	3.8±1.5
Normalized Speed	4.1±1.7	4.0±2.5	3.6±1.3	3.3±1	3.8±1.5
Treated side Shank Peak Velocity, PS _ω T	6.2±3.3	5.6±2.6	4.6±1.8	4.1±1.4	4.4±1.4
Contralateral side Shank Peak Velocity, PS _ω C	5.4±2.3	5.0±3.0	4.4±1.5	4.4±1.6	4.7±2.4
Treated Knee Peak Velocity, PK _ω T	7.3±4.1	6.6±3.7	5.5±2.5	5.1±1.9	5.6±2.6
Contralateral Knee Peak Velocity, PK _ω C	6.7±2.9	6.0±2.6	5.3±2.1	4.8±2.2	5.9±3.1
Treated side Thigh Rotation, R _α T	3.5±1.4	3.0±1.4	2.7±1.0	2.6±0.9	3±1
Contralateral side Thigh Rotation, R _α C	3.6±1.4	3.2±1.5	3.0±1.0	2.9±0.9	3.2±1
Treated side Shank Rotation, R _β T	2.9±1.7	2.7±1.4	2.0±0.7	1.9±0.7	2.1±0.9
Contralateral side Shank Rotation, R _β C	2.4±1.2	2.2±1.2	2.0±0.9	1.9±0.8	2.1±1.1
Treated Knee Rotation, R _γ T	5.2±3.9	4.4±2.7	3.1±1.5	3±1	2.9±1
Contralateral Knee Rotation, R _γ C	3.7±1.8	3.2±1.5	2.7±1.0	2.8±1.3	2.8±1.2

*Variability of Limp is indicated by “Standard Deviation” instead of “CV%” since its mean is near zero.

Chapter 7: Clinical Application

Table 7-9 Difference in gait parameters between Follow up tests and Pre-op test. The statistically significant differences ($p < 0.05$) between the groups are shaded in gray

Gait Parameter	Pre-op vs. 6 weeks, N=52	Pre-op vs. 3 months, N=50	Pre-op vs. 6 months, N=40	Pre-op vs. 1 year, N=32
Gait Cycle Time (GCT), s	0.03±0.13	-0.06±0.1	-0.11±0.13	-0.1±0.14
Treated side Stance, %	0.18±4.16	0.28±3.38	0.44±4.14	0.31±3.82
Contralateral side Stance, %	0.06±2.48	-1.38±2.73	-1.89±3.26	-1.54±3.32
Double Support, DS%	0.12±3.73	-1.26±3.46	-1.65±4.64	-1.45±4.37
Limp, %	-0.15±2.44	-0.71±2.07	-1.03±2.24	-1.03±2.36
Treated side Stride, m	0.02±0.12	0.09±0.11	0.13±0.11	0.1±0.14
Contralateral side Stride, m	0.02±0.12	0.09±0.11	0.13±0.11	0.1±0.14
Speed, m/s	-0.01±0.16	0.11±0.14	0.18±0.14	0.15±0.18
Normalized Speed, /s	0±0.1	0.07±0.08	0.11±0.09	0.09±0.11
Treated side Shank Peak Velocity, $PS\omega T$, deg/s	-13.36±68.28	30.58±56.15	59.09±58.07	51.45±61.85
Contralateral side Shank Peak Velocity, $PS\omega C$, deg/s	-6.14±39.68	19.87±33.18	29.96±31.48	28.16±43.07
Treated Knee Peak Velocity, $PK\omega T$, deg/s	-13.18±78.16	29.94±66.23	63.65±58.35	56.35±77.73
Contralateral Knee Peak Velocity, $PK\omega C$, deg/s	-6.96±47.78	22.19±47.33	40.29±47.02	42.12±61.32
Treated side Thigh Rotation, $R\alpha T$, deg	2.01±5.59	3.32±5.19	5.02±5.97	2.89±6.42
Contralateral side Thigh Rotation, $R\alpha C$, deg	0.06±4.44	2.32±4.54	3.61±3.87	3.58±5.51
Treated side Shank Rotation, $R\beta T$, deg	-0.18±9.08	5.26±8.05	8.72±8.28	8.31±9.61
Contralateral side Shank Rotation, $R\beta C$, deg	-0.08±6.41	3.71±5.2	5.76±5.25	5.15±6.87
Treated Knee Rotation, $R\gamma T$, deg	-3.36±11.93	3.39±10.42	7.23±10.58	8.19±11.9
Contralateral Knee Rotation, $R\gamma C$, deg	0.79±5.99	3.25±4.79	3.32±4.74	4.25±6.53
Coordination Score	0.71±1.18	1.19±0.93	1.52±1.21	1.52±1.28

Table 7-10 Difference in gait variability between Follow up tests and Pre-Op test. The statistically significant differences ($p < 0.05$) between the groups are shaded in gray

Gait Parameter (CV%)	Pre-op vs. 6 weeks, N=52	Pre-op vs. 3 months, N=50	Pre-op vs. 6 months, N=40	Pre-op vs. 1 year, N=32
Gait Cycle Time	0.0±1.4	-0.2±0.9	-0.4±1.0	-0.5±1.7
Treated side Stance	0.1±2.8	-0.4±1.5	-0.7±1.6	-0.7±1.7
Contralateral side Stance	-0.2±0.9	-0.4±2.0	-0.7±2.1	-0.7±2.3
Double Support	0.5±11.0	-1±4.9	-1.4±6.2	-1.7±6.0
Limp	-0.13±1.12	-0.27±0.87	-0.41±1.1	-0.46±1.15
Treated side Stride	-0.2±1.7	-0.4±1.1	-0.8±1.2	-0.6±1.0
Contralateral side Stride	-0.2±1.6	-0.5±1.3	-0.8±1.4	-0.8±1.3
Speed	-0.1±2.7	-0.4±1.7	-1.0±1.5	-0.6±2.1
Normalized Speed	-0.1±2.7	-0.4±1.7	-1.0±1.5	-0.6±2.1
Treated side Shank Peak Velocity, $PS\omega T$	-0.4±4	-1.6±3.1	-2.5±3.2	-2.2±3.6
Contralateral side Shank Peak Velocity, $PS\omega C$	-0.1±3.2	-1.0±1.9	-1.2±2.1	-0.9±2.6
Treated Knee Peak Velocity, $PK\omega T$	-0.2±4.9	-1.7±3.8	-2.6±3.8	-2.1±4.2
Contralateral Knee Peak Velocity, $PK\omega C$	-0.6±3.1	-1.3±2.5	-2.2±2.7	-1.0±2.0
Treated side Thigh Rotation, $R\alpha T$	-0.3±2	-0.5±1.3	-0.9±1.5	-0.5±1.4
Contralateral side Thigh Rotation, $R\alpha C$	-0.4±1.9	-0.5±1.4	-0.8±1.6	-0.5±1.4
Treated side Shank Rotation, $R\beta T$	-0.2±2.2	-0.7±1.4	-1.1±1.6	-0.8±1.4
Contralateral side Shank Rotation, $R\beta C$	-0.2±1.5	-0.4±0.8	-0.7±0.8	-0.4±0.8
Treated Knee Rotation, $R\gamma T$	-0.4±4.4	-1.8±3.4	-2.5±4.1	-2.6±4.1
Contralateral Knee Rotation, $R\gamma C$	-0.3±2.2	-0.9±1.7	-1.1±1.5	-0.8±1.8

The difference between gait parameters of fixed bearing and mobile bearing groups at 3 months, 6 months, and 1 year follow ups are reported in Tables 7-11, 7-12, and 7-13 respectively. The first two columns (cols. 1 and 2) of each table report the gait parameters of each group at the corresponding follow up test. The second two columns (cols. 3 and 4) of each table report the improvement (difference between the follow up result and baseline value) for each group. Significant differences ($p < 0.05$) of each comparison are shaded in gray.

At 3 months follow up, the improvements of Treated Knee Rotation and Treated Knee Peak Velocity in fixed bearing group were significantly higher than the corresponding improvements in the mobile bearing group ($p = 0.022$ and $p = 0.045$ respectively; see Table 7-11, cols. 3 and 4). Additionally, the Treated side Stance in the fixed bearing group was significantly less than the values in the mobile bearing group ($p = 0.033$).

At 6 months follow up, there was no statistically significant difference between the gait parameters of the two groups (Table 7-12). However, at 1-year follow up, some parameters were significantly different between the two groups (Table 7-13, cols. 1 and 2). For example, the Treated side Stance was 62.20% for Fixed bearing and 60.25% for Mobile bearing groups; the difference between the groups was significant ($p = 0.026$). The Limp in fixed bearing group (2.43%) was significantly higher than the mobile bearing group (0.99%) ($p = 0.0003$). The Stride length of the fixed bearing group (1.10m) was significantly less than the mobile bearing group (1.25m), (0.019). Also, the Speed, Contra-lateral side shank peak velocity, Treated side thigh rotation, Contra-lateral knee rotation, and Coordination score were significantly different between the two groups (p -values=0.038, 0.016, 0.027, 0.023, and 0.012 respectively). The results indicate that the group with mobile bearing TKA has gained better scores at 1 year follow up test.

Table 7-11 Comparison between Fixed bearing and Mobile bearing at 3 months follow up. The comparison is made between the gait parameters at 3 months (cols. 1 and 2), and between the patient improvements (difference between 3 months and baseline, cols. 3 and 4). The statistically significant differences ($p < 0.05$) between the two groups are shaded in gray.

Gait Parameter	3 Months		Difference 3M - PreOp	
	Fixed Bearing N=27	Mobile Bearing N=23	Fixed Bearing N=27	Mobile Bearing N=23
Gait Cycle Time (GCT), s	1.22±0.15	1.19±0.13	-0.06±0.10	-0.05±0.10
Treated side Stance, %	60.95±2.27	61.05±1.69	-0.72±1.9	1.41±4.29
Contralateral side Stance, %	62.02±1.94	61.75±1.39	-0.94±2.86	-1.88±2.56
Double Support, DS%	22.97±3.87	22.76±2.72	-1.63±3.61	-0.83±3.31
Limp, %	1.89±0.75	1.91±0.88	-0.68±2.04	-0.74±2.16
Treated side Stride, m	1.21±0.19	1.21±0.12	0.10±0.09	0.08±0.12
Contralateral side Stride, m	1.21±0.19	1.21±0.12	0.1±0.09	0.07±0.12
Speed, m/s	1.01±0.21	1.03±0.14	0.11±0.12	0.1±0.16
Normalized Speed, /s	0.61±0.12	0.62±0.08	0.07±0.07	0.06±0.1
Treated side Shank Peak Velocity, PS ω T, deg/s	301.67±59.55	306.06±49.94	41.91±46.53	17.63±64.16
Contralateral side Shank Peak Velocity, PS ω C, deg/s	322.87±58.05	349.43±44.21	22.03±32.57	17.4±34.50
Treated Knee Peak Velocity, PK ω T, deg/s	314.82±78.07	314.21±68.16	48.28±50.23	8.99±76.71
Contralateral Knee Peak Velocity, PK ω C, deg/s	313.45±75.43	339.22±57.57	24.28±41.79	19.81±53.94
Treated side Thigh Rotation, R α T, deg	40.15±6.45	40.54±4.44	4.10±3.68	2.42±6.49
Contralateral side Thigh Rotation, R α C, deg	39.32±7.66	39.27±5.13	2.86±4.21	1.71±4.91
Treated side Shank Rotation, R β T, deg	68.27±10.26	68.34±6.62	7.06±7.43	3.20±8.40
Contralateral side Shank Rotation, R β C, deg	69.95±9.33	71.08±5.92	4.17±5.08	3.19±5.41
Treated Knee Rotation, R γ T, deg	51.43±9.79	51.62±8.68	6.66±10.07	-0.34±9.75
Contralateral Knee Rotation, R γ C, deg	56.02±9.19	59.32±6.71	3.19±4.78	3.32±4.93
Coordination Score	6.38±1.1	6.62±0.81	1.16±0.83	1.26±1.05

Chapter 7: Clinical Application

Table 7-12 Comparison between Fixed bearing and Mobile bearing at 6 months follow up. The comparison is made between the gait parameters at 6 months (cols. 1 and 2), and between the patient improvements (difference between 6 months and baseline, cols. 3 and 4). The statistically significant differences ($p < 0.05$) between the two groups are shaded in gray.

Gait Parameter	6 Months		Difference 6M - PreOp	
	Fixed Bearing N=21	Mobile Bearing N=19	Fixed Bearing N=21	Mobile Bearing N=19
Gait Cycle Time (GCT), s	1.18±0.10	1.15±0.10	-0.10±0.15	-0.12±0.11
Treated side Stance, %	60.91±2.04	60.41±1.61	-0.44±2.42	1.43±5.38
Contralateral side Stance, %	61.46±2.55	61.20±1.84	-1.38±3.66	-2.46±2.73
Double Support, DS%	22.35±4.23	21.57±3.02	-1.81±4.63	-1.47±4.78
Limp, %	1.86±0.86	1.48±0.82	-0.75±2.19	-1.33±2.32
Treated side Stride, m	1.21±0.19	1.27±0.11	0.12±0.10	0.14±0.13
Contralateral side Stride, m	1.21±0.19	1.27±0.11	0.12±0.10	0.14±0.13
Speed, m/s	1.03±0.18	1.11±0.13	0.15±0.12	0.20±0.15
Normalized Speed, /s	0.63±0.10	0.67±0.08	0.10±0.08	0.12±0.09
Treated side Shank Peak Velocity, $PS\omega T$, deg/s	317.51±56.05	329.15±41.02	60.29±56.32	57.74±61.68
Contralateral side Shank Peak Velocity, $PS\omega C$, deg/s	327.15±53.78	354.44±49.15	29.97±31.2	29.95±32.75
Treated Knee Peak Velocity, $PK\omega T$, deg/s	335.55±61.22	341.41±59.06	68.45±59.7	58.29±58.14
Contralateral Knee Peak Velocity, $PK\omega C$, deg/s	334.17±61.44	354.61±67.42	38.85±47.4	41.9±47.99
Treated side Thigh Rotation, $R\alpha T$, deg	40.88±7.06	42.73±4.49	5.04±4.68	5.00±7.30
Contralateral side Thigh Rotation, $R\alpha C$, deg	39.59±6.76	40.48±5.19	3.56±4.11	3.67±3.71
Treated side Shank Rotation, $R\beta T$, deg	69.70±9.69	71.26±6.51	9.22±7.87	8.17±8.92
Contralateral side Shank Rotation, $R\beta C$, deg	70.85±9.37	72.79±5.76	5.95±5.68	5.56±4.90
Treated Knee Rotation, $R\gamma T$, deg	53.1±9.12	54.91±8.54	9.42±11.92	4.78±8.55
Contralateral Knee Rotation, $R\gamma C$, deg	56.06±9.00	58.42±6.22	3.59±5.02	3.02±4.53
Coordination Score	6.41±0.88	6.81±0.93	1.44±1.24	1.60±1.21

Table 7-13 Comparison between Fixed bearing and Mobile bearing at 1 year follow up. The comparison is made between the gait parameters at 1 year (cols. 1 and 2), and between the patient improvements (difference between 1 year and baseline, cols. 3 and 4). The statistically significant differences ($p < 0.05$) between the two groups are shaded in gray.

Gait Parameter	1 Year		Difference 1Y - PreOp	
	Fixed Bearing N=17	Mobile Bearing N=15	Fixed Bearing N=17	Mobile Bearing N=15
Gait Cycle Time (GCT), s	1.21±0.12	1.17±0.16	-0.10±0.17	-0.09±0.1
Treated side Stance, %	62.2±2.57	60.25±1.79	0.35±2.43	0.26±5.01
Contralateral side Stance, %	61.99±2.18	61.45±1.44	-1.45±4.06	-1.63±2.45
Double Support, DS%	24.23±3.95	21.70±2.93	-1.07±5.21	-1.86±3.39
Limp, %	2.43±1.22	0.99±0.44	-0.63±2.55	-1.45±2.14
Treated side Stride, m	1.10±0.19	1.25±0.11	0.11±0.16	0.10±0.12
Contralateral side Stride, m	1.10±0.19	1.25±0.11	0.11±0.16	0.10±0.12
Speed, m/s	0.92±0.22	1.09±0.18	0.13±0.19	0.16±0.17
Normalized Speed, /s	0.57±0.14	0.65±0.11	0.09±0.12	0.09±0.10
Treated side Shank Peak Velocity, PS ω T, deg/s	296.34±70.47	325.86±66.06	66.36±67.69	35.48±52.66
Contralateral side Shank Peak Velocity, PS ω C, deg/s	299.56±66.79	355.86±49.6	23.98±44.82	32.64±42.31
Treated Knee Peak Velocity, PK ω T, deg/s	309.16±85.8	343.26±59.63	76.53±80.67	34.74±70.94
Contralateral Knee Peak Velocity, PK ω C, deg/s	300.83±89.88	355.68±63.2	43.68±73.33	40.45±47.98
Treated side Thigh Rotation, R α T, deg	36.35±7.43	41.72±4.52	3.69±6.98	2.03±5.89
Contralateral side Thigh Rotation, R α C, deg	36.07±7.43	39.61±4.76	3.98±6.80	3.16±3.91
Treated side Shank Rotation, R β T, deg	65.35±12.81	70.95±6.74	9.99±11.18	6.51±7.58
Contralateral side Shank Rotation, R β C, deg	65.69±12.03	72.76±4.82	5.28±9.1	5.01±3.51
Treated Knee Rotation, R γ T, deg	51.73±11.20	55.96±8.69	12.24±13.94	3.84±7.51
Contralateral Knee Rotation, R γ C, deg	52.78±11.29	60.46±4.01	4.13±8.23	4.37±4.36
Coordination Score	6.18±0.83	6.94±0.69	1.60±1.64	1.44±0.79

7.4 Discussion and Conclusion

In this study, the gait analysis system was used for patients who underwent TKA. The gait parameters were obtained in dynamic use of the knee, when walking freely in a corridor.

The results indicated that gait functions in all of the patients are improved considerably after surgery. The patients had the ability to increase their speed by increasing stride length and cadence. Significant increases in range of rotations of treated and contralateral sides of knee, shank, and thigh, along with maximum angular velocities of knee and shank were seen. Moreover, the patients were able to achieve significant increases in coordination score. On the other hand, many of the variabilities of gait parameters have decreased after surgery. For example, the variabilities of stride length, range of rotations of treated and contralateral sides of knee, shank, and thigh, maximum angular velocities of knee and shank, Gait Cycle Time, and Stance times were all significantly decreased after 3 (or 6) months. As a result, functional improvement was associated with an increase in walking performance (higher speed, higher range of rotations), an increase of walking regularity (lower gait variability) and a better multi-joint coordination. In addition, the Peak Velocities and Rotations of both knees (treated and contralateral) had the same value and variability after 1 year (Tables 7-7 and 7-8). This implies that the patients could walk more symmetrically.

Comparing the results of Fixed- and Mobile-bearing TKA, the improvements of Treated knee rotation, Treated knee Peak Velocity, and Treated side stance were significantly different between the two groups at 3 months follow up. The results indicated that the Fixed bearing TKA performed better than Mobile bearing TKA in the early period (3 months). However, after 6 months, the Mobile bearing performed as well as the Fixed bearing TKA, and the tendency grows in benefit of mobile bearing after 1 year. Nevertheless, the study is still going on and these results should be confirmed when all patients will be at least at one year of follow-up.

The clinical scores (excluding KSS-healthy and FCTN-healthy scores which are related to Contralateral knee) that could detect changes between fixed bearing and mobile bearing groups were VAS-Pain at 3 months, and EQ5d-Visual at 1 year.

In summary, we propose the following pertinent parameters (as well as their variabilities) for outcome evaluation: Gait Cycle Time, Stride length, Speed, Treated and Contralateral Knee Peak Velocities and Rotations, and Coordination Score.

We provided objective criteria, using ambulatory gait analysis, for assessing functional recovery following TKA procedure. These results cannot be obtained through other

clinical evaluations, and complement the clinical scores by a useful objective dynamic evaluation.

Chapter 8 Conclusions and Future Research

8.1 Contributions of Dissertation

The primary objective of this thesis was to design and validate a new gait analysis system that can be used for clinical applications. Through an orthopedic application (TKA) the emphasis was put on kinematic parameters affected by locomotion disorders in order to provide an objective outcome evaluation based on these parameters. The main results and contributions of this thesis can be summarized as follows:

1. Ambulatory recording system: A specific sensor based motion recorder system was designed. The system is a portable ambulatory device with the following design criteria: lightweight, easily mountable, and can be used for long term monitoring without hindrance to natural activities. The human movements are captured with five kinematic sensors using accelerometers and gyroscopes. A minimal sensor configuration was proposed with one sensor module mounted on each segment (thighs, shanks, and sacrum). Each sensor module included 2 orthogonal accelerometers and a gyroscope.
2. A new method to accurate measurement of uniaxial joint angles based on a combination of accelerometers and gyroscopes was proposed. In the proposed technique, joint angles were found without the need for integration, so absolute angles could be obtained which were free from any source of drift. Moreover, the algorithm is able to provide joint angles in real-time. The method was validated by measuring knee flexion-extension angles of eight subjects, walking at three different speeds, and comparing the results with a reference motion measurement system. The results were very close to those of the reference system presenting very small errors (rms=1.3, mean=0.2, SD=1.1 deg) and excellent correlation coefficient (0.997). The results of this study has been published in a journal article (Dejnabadi et al. 2005a) and has been presented in two conferences (Dejnabadi et al. 2002; Dejnabadi et al. 2004).
3. A new method of estimating lower limbs orientations was proposed. The method considered human locomotion and biomechanical constraints, and provided a solution to fusing the data of gyroscopes and accelerometers that yielded stable and

drift-free estimates of segment orientation. The method was validated by measuring lower limb motions (Shank and Thigh orientations in sagittal plane) of eight subjects, walking at three different speeds, and comparing the results with a reference motion measurement system. The results were very close to those of the reference system presenting very small errors (Shank: rms=1.0, Thigh: rms=1.6 deg) and excellent correlation coefficients (Shank: $r=0.999$, Thigh: $r=0.998$). The results of this study is published in a journal article (Dejnabadi et al. 2006) and has been presented in two conferences (Dejnabadi et al. 2005c, d).

4. A gait analysis tool using the ambulatory system was developed. Outputs from the software included spatio-temporal parameters of gait, kinematic diagrams, and visualization of patients' gait at various conditions. The spatio-temporal parameters provide a tool for objective outcome measures to quantify the expected gait improvement of patients. The kinematic diagrams provide additional information for representing a segment or joint movement and its variability in continuous format. The graphs help clinician qualitatively assess time evolution of lower limb movements, variability at different phases of gait, symmetry, and ranges of rotations. Finally, the visualization tool, which were developed in collaboration with Computer Vision Laboratory of EPFL (CVLab), provide additional tool to see the time evolution of lower limb movements. It gives the physician visually appealing and easy to interpret information about how the patient performs several activities such as walking at different speeds or climbing ramps and stairs. In addition, it allows evaluating the progression of a patient at different follow up tests by superposing several skeletons. The results of spatio-temporal gait analysis was published in *Gait & Posture* (Aminian et al. 2004c) and *Clinical Rehabilitation* (Lindemann et al. 2006), where a comparison with questionnaire-based evaluation is also provided. The results related to visualization is published in *IEEE journal* (Dejnabadi et al. 2006) and presented in two conferences (Casanova et al. 2004; Dejnabadi et al. 2005d).
5. A new method for quantitative analysis of inter-joint coordination during gait was proposed. We provided a general model to capture the whole dynamics of the lower limbs movement and showed the kinematic synergies at various walking speeds. We indicated how an integration of different analysis tools such as Harmonic Analysis, Principal Components Analysis, and Artificial Neural Network helped overcome high-dimensionality, temporal dependence, and nonlinear relationships of the gait patterns. The trained model was fed with only 2 control parameters (cadence and stride length) at each gait cycle, and predicted the

corresponding gait waveforms. Considering the differences between predicted and actual gait waveforms, we defined a coordination score at various walking speeds which ranged between 0 and 10. The scores determined the overall coordination as well as contribution of each joint to the total coordination. In the first phase, we applied the model on 8 patients with knee arthroplasty at different follow ups as well as 8 healthy subjects, walking at 3 different speeds. The results showed that treatments and rehabilitation programs improve the gait coordination in individuals with knee arthroplasty. For instance, considering the patients' scores at normal speeds, the mean value of scores at baseline was 4.4, which significantly increased to 5.7 ($p=0.008$) and 6.6 ($p=0.008$) at 6 weeks and 6 months follow up tests respectively. The results of this study has been submitted to an IEEE journal (Dejnabadi et al. Submitted).

6. A clinical protocol was conducted in which gait analysis and knee scoring system results of 54 patients were evaluated. We conducted a randomized controlled study to assess total knee arthroplasty outcome between patients with fixed bearing and mobile bearing tibial plates of implants. Preoperative results were compared with postoperative (6 weeks, 3 months, 6 months, and 1 year) results. Various statistical analyses were done to compare the outcomes of the two groups at different follow up tests. The results indicated that fixed bearing TKA performed better than mobile bearing TKA in the early period (3 months). However, after 6 months the mobile bearing performed as well as the Fixed bearing TKA. In general, the results indicated that gait function in all of the patients can be improved considerably after surgery. In summary, we proposed the following pertinent parameters (as well as their variabilities) for outcome evaluation: Gait Cycle Time, Stride length, Speed, Treated and Contralateral Knee Peak Velocities and Rotations, and Coordination Score. We provided objective criteria, using ambulatory gait analysis, for assessing functional recovery following TKA procedure. These results cannot be obtained through other clinical evaluations, and complement the clinical scores by a useful objective dynamic evaluation. The results of is presented in several conferences (Dejnabadi et al. 2005d; Jolles et al. 2006; Jolles et al. 2004; Jolles et al. 2005a, b), and an article is under submission.

8.2 Perspectives and Future Research

This thesis can be extended to the following directions:

8.2.1 Movement analysis and visualization

The method of finding uniaxial joint angles, presented in chapter 3, is real time and can also be used for other joints. So a whole skeleton visualization is possible which is applicable in virtual reality.

Moreover, a potential improvement of the model would be to extend the principle in 3D by employing 3D accelerometers and 3D gyroscopes on each segment. The technique of finding uniaxial joint angles, presented in chapter 3, was based on estimating the acceleration of the joint Center of Rotation (COR) by placing a pair of virtual sensors on the adjacent segments at the COR. The model and the equations can be modified to shift the 3D sensors to the COR and find 3D angles using orientations of the 3D virtual accelerometers on the COR.

Furthermore, the kinematic sensors can be merged with other techniques such as video data in order to improve the performance of both systems and extend to 3D as well. In our earlier studies, we were working on recovering motion in the frontal plane by combining the information provided by kinematic sensors with image-data from inexpensive and commercially available synchronized cameras (Casanova et al. 2004). This extended approach should let us incorporate full 3-D motion into gait analysis and will be the subject of future work.

8.2.2 Gait analysis

The gait analysis program, explained in chapter 5, can be used for assessment of other gait pathologies. Future extension of the algorithm should focus to automatically detect different types of walking and activities of a patient at various conditions and focus on long-term outcomes.

We conducted a clinical protocol in which the patients were asked to perform 15 trials at different conditions such as walking at different speeds, climbing and descending stairs, walking on ramp, and sit-stand-sit movements. However, in chapter 7 we only analyzed and reported the results of walking at normal speed (trial 1). Future works should examine the outcomes of patients at other conditions. Accordingly, new models should be developed to define quantitative scores for stair climbing and descending, and sit-stand-sit movements.

8.2.3 Orthopedics and rehabilitation

The method of finding knee joint angle, presented in chapter 3, assumed the joint Center of Rotation (COR) as a fixed position point. However, the COR changes slightly depending

on the knee angle. An improvement of the model would be to consider the instant (dynamic) COR of knee joint during flexion-extension.

In chapter 7 we applied classical statistical methods to find significant parameters that discriminate the two groups of patients with fixed bearing and mobile bearing TKA. However, advanced statistical methods could better model the datasets and show patients' improvements. For example, considering age, gender and weight in a multivariate model would be helpful. Additionally, it is necessary to build a normative database by including a large group of healthy people in the clinical protocol. Then compare each patient with its (interpolated) matched age, gender and weight healthy subject. This comparison would give the information that how much a patient could be expected to (or has the potential to) improve, and then normalize his/her scores to this maximally expected improvement.

In the clinical protocol, predefined and controlled activities of patients were assessed. Future works should examine the gait and other activities of patients during freely daily activities in long term. In general, the proposed clinical protocol can be used for other orthopedic and rehabilitation programs related to lower extremity treatments.

8.2.4 Neuroscience

We applied the method of coordination analysis, presented in chapter 6, on patients with knee arthroplasty. However, the method can be used for coordination assessment of other gait disorders, especially neurological disorders such as Parkinson's disease.

References

- Abelew TA, Miller MD, Cope TC, and Nichols TR.** Local Loss of Proprioception Results in Disruption of Interjoint Coordination During Locomotion in the Cat. *J Neurophysiol* 84: 2709-2714, 2000.
- AbuFaraj ZO, Harris GF, Abler JH, and Wertsch JJ.** A Holter-type, microprocessor-based, rehabilitation instrument for acquisition and storage of plantar pressure data. *Journal of Rehabilitation Research and Development* 34: 187-194, 1997.
- Acton FS.** Numerical Methods that Work. *The Mathematical Association of America*: 221-228, 1990.
- Aglietti P, Baldini A, Buzzi R, Lup D, and De Luca L.** Comparison of mobile-bearing and fixed-bearing total knee arthroplasty: a prospective randomized study. *J Arthroplasty* 20: 145-153, 2005.
- Aglietti P, Insall JN, Buzzi R, and Walker P.** Meniscal-bearing knee - Principles, technique and primary results. In Scuderi G.R., Tria A.J., editors. *Surgical techniques in total knee arthroplasty*. New-York: Springer-Verlag. 90-96, 2002.
- Aigner T, Sachse A, Gebhard PM, and Roach HI.** Osteoarthritis: Pathobiology--targets and ways for therapeutic intervention. *Advanced Drug Delivery Reviews* 58: 128-149, 2006.
- Alexandrov A, Aurenty R, Massion J, Mesure S, and Viallet F.** Axial synergies in parkinsonian patients during voluntary trunk bending. *Gait & Posture* 8: 124-135, 1998.
- Amblard B, Assaiante C, Lekhel H, and Marchand AR.** A Statistical Approach to Sensorimotor Strategies - Conjugate Cross-Correlations. *Journal of Motor Behavior* 26: 103-112, 1994.
- Amendola A, Rorabeck CH, Bourne RB, and Apyan PM.** Total knee arthroplasty following high tibial osteotomy for osteoarthritis. *J Arthroplasty* 4 (Suppl): S11-17, 1989.
- Aminian K, De Andres E, Rezakhanlou K, Fritsch C, Schutz Y, Depairon M, Leyvraz PF, and Robert P.** Motion analysis in clinical practice using ambulatory accelerometry. In: *Modelling and Motion Capture Techniques for Virtual Environments*, 1998, p. 1-11.
- Aminian K and Najafi B.** Capturing human motion using body-fixed sensors: outdoor measurement and clinical applications. *Computer animation and virtual worlds* 15: 79-94, 2004.
- Aminian K, Najafi B, Bula C, Leyvraz P-F, and Robert P.** Spatio-temporal parameters of gait measured by an ambulatory system using miniature gyroscopes. *Journal of Biomechanics* 35: 689-699, 2002a.

Aminian K, Najafi B, Bula C, Leyvraz PF, and Robert P. Spatio-temporal parameters of gait measured by an ambulatory system using miniature gyroscopes. *Journal of Biomechanics* 35: 689-699, 2002b.

Aminian K, Robert P, Buchser EE, Rutschmann B, Hayoz D, and Depairon M. Physical activity monitoring based on accelerometry: validation and comparison with video observation. *Medical & Biological Engineering & Computing* 37: 304-308, 1999.

Aminian K, Trevisan C, Najafi B, Dejnabadi H, Frigo C, Pavan E, Telonio A, Cerati F, Marinoni EC, Robert P, and Leyvraz P-F. Evaluation of an ambulatory system for gait analysis in hip osteoarthritis and after total hip replacement. *Gait & Posture* 20: 102-107, 2004a.

Aminian K, Trevisan C, Najafi B, Dejnabadi H, Frigo C, Pavan E, Telonio A, Cerati F, Marinoni EC, Robert P, and Leyvraz PF. Evaluation of an ambulatory system for gait analysis in hip osteoarthritis and after total hip replacement. *Gait & Posture* 20: 102-107, 2004b.

Aminian K, Trevisan C, Najafi B, Dejnabadi H, Frigo C, Pavan E, Telonio A, Cerati F, Marioni EC, Robert P, and Leyvraz PF. Evaluation of an ambulatory system for gait analysis in hip osteoarthritis and after total hip replacement. *Gait & Posture* 20: 102-107, 2004c.

Andersson GBJ, Andriacchi TP, and Galante JO. Correlations between changes in gait and in clinical status after knee arthroplasty. *Acta Orthop Scand* 52: 569, 1981.

Andriacchi TP, Galante JO, and Fermier RW. The influence of total knee replacement design on walking and stair climbing. *J Bone Joint Surg* 64A: 1328, 1982.

Andriacchi TP, Ogle JA, and Galante JO. Walking speed as a basis for normal and abnormal gait measurements. *J Biomech* 10: 261, 1977.

Andriacchi TP, Yoder D, Conley A, Rosenberg A, Sum J, and Galante JO. Patellofemoral design influences function following total knee arthroplasty. *Journal of Arthroplasty* 12: 243-249, 1997.

Armstrong RA and Whiteside LA. Results of cementless total knee arthroplasty in an older rheumatoid arthritis population. *J Arthroplasty* 6: 357-362, 1991.

Ayyappa E. Words about words: the terminology of human walking, bipedal exchange. *Monograph of the American Academy of Orthotists and Prosthetists Gait Society* 1, 1994.

Bachmann ER, Xiaoping Y, McKinney D, McGhee RB, and Zyda MJ. Design and implementation of MARG sensors for 3-DOF orientation measurement of rigid bodies. 2003, p. 1171-1178 vol.1171.

Banks SA and Hodge WA. Accurate measurement of three-dimensional knee replacement kinematics using single-plane fluoroscopy. *Ieee Transactions on Biomedical Engineering* 43: 638-649, 1996.

Banks SA, Markovich GD, and Hodge WA. In vivo kinematics of cruciate-retaining and -substituting knee arthroplasties. *J Arthroplasty* 12: 297-304, 1997a.

- Banks SA, Markovich GD, and Hodge WA.** The mechanics of knee replacements during gait. In vivo Fluoroscopic analysis of two designs. *Am J Knee Surg* 10: 261-267, 1997b.
- Barela JA, Whitall J, Black P, and Clark JE.** An examination of constraints affecting the intralimb coordination of hemiparetic gait. *Human Movement Science* 19: 251-273, 2000.
- Barrack RL, Smith P, Munn B, Engh G, and Rorabeck C.** Comparison of surgical approaches in total knee arthroplasty. *Clinical Orthopaedics and Related Research*: 16-21, 1998.
- Barshan B and Durrant-Whyte HF.** Inertial navigation systems for mobile robots. *Robotics and Automation, IEEE Transactions on* 11: 328-342, 1995.
- Barton JG and Lees A.** An application of neural networks for distinguishing gait patterns on the basis of hip-knee joint angle diagrams. *Gait & Posture* 5: 28-33, 1997.
- Beek PJ, Peper CE, and Daffertshofer A.** Modeling rhythmic interlimb coordination: Beyond the Haken-Kelso-Bunz model. *Brain and Cognition* 48: 149-165, 2002.
- Bellamy N, Buchanan WW, Goldsmith CH, Campbell J, and Stitt LW.** Validation study of WOMAC: a health status instrument for measuring clinically important patient relevant outcomes to antirheumatic drug therapy in patients with osteoarthritis of the hip or knee. *J Rheumatol* 15: 1833-1840, 1988.
- Berman AT, Zarro VJ, and Bosacco SC.** Quantitative gait analysis after unilateral or bilateral total knee replacement. *J Bone Joint Surg* 69A: 1340, 1987.
- Bernstein N.** The Coordination and Regulation of Movement. *Pergamon Press, Oxford*, 1967.
- Berthoz A.** The Brain's Sense of Movement. *Harvard University Press, Cambridge*: 141-144, 2000.
- Bhan S, Malhotra R, Kiran EK, Shukla S, and Bijjawara M.** A comparison of fixed-bearing and mobile-bearing total knee arthroplasty at a minimum follow-up of 4.5 years. *J Bone Joint Surg* 87: 2290-2296, 2005.
- Bianchi L, Angelini D, Orani GP, and Lacquaniti F.** Kinematic Coordination in Human Gait: Relation to Mechanical Energy Cost. *J Neurophysiol* 79: 2155-2170, 1998.
- Bloomberg JJ and Mulavara AP.** Changes in walking strategies after spaceflight. *Engineering in Medicine and Biology Magazine, IEEE* 22: 58-62, 2003.
- Bouten CVC, Koekoek KTM, Verduin M, Kodde R, and Janssen JD.** A triaxial accelerometer and portable data processing unit for the assessment of daily physical activity. *Biomedical Engineering, IEEE Transactions on* 44: 136-147, 1997.
- Braido P and Zhang X.** Quantitative analysis of finger motion coordination in hand manipulative and gestic acts. *Human Movement Science* 22: 661-678, 2004.
- Brazier J, Jones N, and Kind P.** Testing the validity of the EuroQol and comparing it with the SF-36 health survey questionnaire. *Quality of Life Research* 2: 169-180, 1993.

References

- Buckwalter JA and Martin JA.** Osteoarthritis. *Advanced Drug Delivery Reviews* 58: 150-167, 2006.
- Buechel FF and Pappas MJ.** New Jersey Low Contact Stress knee replacement system. Ten-year evaluation of meniscal bearings. *Orthop Clin North America* 20: 147-177, 1989.
- Burgess-Limerick R, Abernethy B, and Neal RJ.** Relative phase quantifies interjoint coordination. *Journal of Biomechanics* 26: 91-94, 1993.
- Callaghan JJ, Insall JN, Greenwald AS, Dennis DA, Komistek RD, Murray DW, Bourne RB, Rorabeck CH, and Dorr LD.** Mobile-bearing knee replacement: concepts and results. *Inst Course Lect* 50: 431-449, 2001.
- Calvitti A and Beer RD.** Analysis of a distributed model of leg coordination - I. Individual coordination mechanisms. *Biological Cybernetics* 82: 197-206, 2000.
- Canny J.** A Computational Approach to Edge-Detection. *IEEE Transactions on Pattern Analysis and Machine Intelligence* 8: 679-698, 1986.
- Cappozzo A, Cappello A, DellaCroce U, and Pensalfini F.** Surface-marker cluster design criteria for 3-D bone movement reconstruction. *Ieee Transactions on Biomedical Engineering* 44: 1165-1174, 1997.
- Cappozzo A, Catani F, Croce UD, and Leardini A.** Position and Orientation in-Space of Bones During Movement - Anatomical Frame Definition and Determination. *Clinical Biomechanics* 10: 171-178, 1995.
- Cappozzo A, Catani F, Leardini A, Benedetti M, and Croce UD.** Position and orientation in space of bones during movement: experimental artefacts. *Clinical Biomechanics* 11: 90-100, 1996a.
- Cappozzo A, Catani F, Leardini A, Benedetti MG, and DellaCroce U.** Position and orientation in space of bones during movement: Experimental artefacts. *Clinical Biomechanics* 11: 90-100, 1996b.
- Carson RG and Swinnen SP.** Coordination and movement pathology: models of structure and function. *Acta Psychologica* 110: 357-364, 2002.
- Casanova E, Dejnabadi H, Jolles BM, Aminian K, and Fua P.** 3D Motion Analysis and Synthesis from Inertial Gyroscopes and Image Data. *ESMAC*, Warsaw. Gait & Posture, 20S, 2004, p. S85.
- Catani F, Benedetti MG, Felice RD, Buzzi R, Giannini S, and Aglietti P.** Mobile and fixed bearing total knee prosthesis functional comparison during stair climbing. *Clinical Biomechanics* 18: 410-418, 2003.
- Chan-Su L and Elgammal A.** Gait style and gait content: bilinear models for gait recognition using gait re-sampling. 2004, p. 147-152.
- Chao EY, Laughman RK, and Stauffer RN.** Biomechanical gait evaluation of pre and postoperative total knee replacement patients. *Arch Orthop Trauma Surg* 97: 309, 1980.

- Chassin EP, Mikosz RP, Andriacchi TP, and Rosenberg AG.** Functional analysis of cemented medial unicompartmental knee arthroplasty. *Journal of Arthroplasty* 11: 553-559, 1996.
- Chau T.** A review of analytical techniques for gait data. Part 1: fuzzy, statistical and fractal methods. *Gait & Posture* 13: 49-66, 2001a.
- Chau T.** A review of analytical techniques for gait data. Part 2: neural network and wavelet methods. *Gait & Posture* 13: 102-120, 2001b.
- Cheron G, Bengoetxea A, Dan B, and Draye J-P.** Multi-joint coordination strategies for straightening up movement in humans. *Neuroscience Letters* 242: 135-138, 1998.
- Chiu KY, Ng TP, Tang WM, and Lam P.** Bilateral total knee arthroplasty: One mobile-bearing and one fixed-bearing. *J Orthop Surg (Hong Kong)* 9: 45-50, 2001.
- Coley B, Najafi B, Paraschiv-Ionescu A, and Aminian K.** Stair climbing detection during daily physical activity using a miniature gyroscope. *Gait & Posture* 22: 287-294, 2005.
- Collopy MC, Murray MP, and Gardner GM.** Kinesiologic measurements of functional performance before and after geometric total knee replacement: one-year follow-up of 20 cases. *Clin Orthop* 126: 196, 1977.
- Cordo P, Carlton L, Bevan L, Carlton M, and Kerr GK.** Proprioceptive coordination of movement sequences: role of velocity and position information. *J Neurophysiol* 71: 1848-1861, 1994.
- Courtine G and Schieppati M.** Tuning of a Basic Coordination Pattern Constructs Straight-Ahead and Curved Walking in Humans. *J Neurophysiol* 91: 1524-1535, 2004.
- Crosbie J and Vachalathiti R.** Synchrony of pelvic and hip joint motion during walking. *Gait & Posture* 6: 237-248, 1997.
- Cunado D, Nixon MS, and Carter JN.** Automatic extraction and description of human gait models for recognition purposes. *Computer Vision and Image Understanding* 90: 1-41, 2003.
- Daffertshofer A, Lamoth CJC, Meijer OG, and Beek PJ.** PCA in studying coordination and variability: a tutorial. *Clinical Biomechanics* 19: 415-428, 2004.
- Dalessandro P.** The New Shorter Oxford-English-Dictionary - Brown,L. *Library Journal* 119: 109-109, 1994.
- Dauids K and Renshaw I.** Movement models from sports reveal fundamental insights into coordination processes. *Exercise and Sport Sciences Reviews* 33: 36-42, 2005.
- Dejnabadi H, Aminian K, Najafi B, Trevisan C, Telonio A, Frigo C, Pavan E, Marinoni EC, Robert P, and Leyvraz P-F.** Joint and Segment Angles of Lower Limbs in Hip Osteoarthritis and Total Hip Replaced Patients Measured Using Physilog System. *EORS, 12th Annual Meeting, Lausanne, 2002*, p. O-96.

References

Dejnabadi H, Jolles BM, and Aminian K. A New Approach for Quantitative Analysis of Inter-Joint Coordination during Gait. *IEEE Transactions on Biomedical Engineering*, Submitted.

Dejnabadi H, Jolles BM, and Aminian K. A new approach to accurate measurement of uniaxial joint angles based on a combination of accelerometers and gyroscopes. *IEEE Transactions on Biomedical Engineering*, 52: 1478-1484, 2005a.

Dejnabadi H, Jolles BM, and Aminian K. A New Approach to Accurate Measurement of Uniaxial Joint Angles Based on a Combination of Accelerometers and Gyroscopes. *Biomedical Engineering, IEEE Transactions on* 52: 1478-1484, 2005b.

Dejnabadi H, Jolles BM, and Aminian K. A New Technique for Accurate Measuring of Knee Flexion-Extension Angle Using Body-Fixed Sensors. *ESMAC*, Warsaw. *Gait & Posture*, 20S, 2004, p. S73.

Dejnabadi H, Jolles BM, Casanova E, Fua P, and Aminian K. Estimation and visualization of lower limbs orientation using body fixed sensors. *Proceedings of the Meeting of the Swiss Society for Biomedical Engineering (SSBE)*, Lausanne, 2005c.

Dejnabadi H, Jolles BM, Casanova E, Fua P, and Aminian K. Estimation and Visualization of Sagittal Kinematics of Lower Limbs Orientation Using Body-Fixed Sensors. *IEEE Transactions on Biomedical Engineering*, 53: 1385-1393, 2006.

Dejnabadi H, Jolles BM, Casanova E, Fua P, and Aminian K. Joint angle monitoring in osteoarthritis patients using body fixed sensors. *ISPGR 2005*, Marseille. *Gait & Posture*, 21, 2005d, p. S76.

Dejnabadi H, Jolles BM, Najafi B, Trevisan C, Marinoni EC, and Aminian K. A Robust Gait parameterization technique for hip arthroplasty outcome evaluation. *ISPGR, Posture and Gait Throughout the lifespan, SR Lord and HB Menz(ed)*: 52, 2003.

Deluzio KJ, Wyss UP, Costigan PA, Sorbie C, and Zee B. Gait assessment in unicompartmental knee arthroplasty patients: Principal component modelling of gait waveforms and clinical status. *Human Movement Science* 18: 701-711, 1999.

Deluzio KJ, Wyss UP, Zee B, Costigan PA, and Serbie C. Principal component models of knee kinematics and kinetics: Normal vs. pathological gait patterns. *Human Movement Science* 16: 201-217, 1997.

Den Otter AR, Geurts ACH, Mulder T, and Duysens J. Gait recovery is not associated with changes in the temporal patterning of muscle activity during treadmill walking in patients with post-stroke hemiparesis. *Clinical Neurophysiology* 117: 4-15, 2006.

Dennis DA, Komistek RD, Colwell CE, Ranawat CS, Scott RD, Thornhill TS, and Lapp MA. In vivo anteroposterior femorotibial translation of total knee arthroplasty: a multicenter analysis. *Clin Orthop* 356: 47-57, 1998.

Dennis DA, Komistek RD, Hoff WA, and Gabriel SM. In vivo knee kinematics derived using an inverse perspective technique. *Clinical Orthopaedics and Related Research*: 107-117, 1996.

Dennis DA, Komistek RD, Walker SA, Cheal EJ, and Stiehl JB. Femoral condylar lift-off in vivo in total knee arthroplasty. *J Bone Joint Surg* 83: 33-39, 2001.

- deQuervain IAK, Stussi E, Muller R, Drobny T, Munzinger U, and Gschwend N.** Quantitative gait analysis after bilateral total knee arthroplasty with two different systems within each subject. *Journal of Arthroplasty* 12: 168-179, 1997.
- Donker SF and Beek PJ.** Interlimb coordination in prosthetic walking: effects of asymmetry and walking velocity. *Acta Psychologica* 110: 265-288, 2002.
- Dujardin FH, Ertaud JY, Aucoeur T, Nguyen J, and Thomine JM.** Smoothing technique using Fourier transforms applied to stereometric data obtained from optoelectronic recordings of human gait. *Human Movement Science* 16: 275-282, 1997.
- Dunbar MJ.** Subjective outcomes after knee arthroplasty. *Acta Orthopaedica Scandinavica* 72: 5-63, 2001.
- Earhart GM and Bastian AJ.** Selection and Coordination of Human Locomotor Forms Following Cerebellar Damage. *J Neurophysiol* 85: 759-769, 2001.
- Ehara Y, Fujimoto H, Miyazaki S, Mochimaru M, Tanaka S, and Yamamoto S.** Comparison of the performance of 3D camera systems .2. *Gait & Posture* 5: 251-255, 1997.
- EuroQoL-Group.** EuroQoL--a new facility for the measurement of health-related quality of life. *Health Policy* 16: 199-208, 1990.
- Fantozzi S, Benedetti MG, Leardini A, Banks SA, Cappello A, Assirelli D, and Catani F.** Fluoroscopic and gait analysis of the functional performance in stair ascent of two total knee replacement designs. *Gait & Posture* 17: 225-234, 2003.
- Fehring TK and Valadie AL.** Knee Instability after Total Knee Arthroplasty. *Clinical Orthopaedics and Related Research*: 157-162, 1994.
- Field-Fote EC and Tepavac D.** Improved intralimb coordination in people with incomplete spinal cord injury following training with body weight support and electrical stimulation. *Physical Therapy* 82: 707-715, 2002.
- Finch E, Brooks D, Stratford PW, and Mayo N.** *Physical rehabilitation outcome measures (2nd ed.)*: BC Decker Inc, Hamilton, 2002.
- Foxlin E.** Inertial head-tracker sensor fusion by a complementary separate-bias Kalman filter. *Virtual Reality Annual International Symposium, 1996., Proceedings of the IEEE 1996*, 1996, p. 185-194, 267.
- Foxlin E and Harrington M.** WearTrack: a self-referenced head and hand tracker for wearable computers and portable VR. *Wearable Computers, 2000. The Fourth International Symposium on*, 2000, p. 155-162.
- Frigo C, Bardare M, Corona F, Casnaghi D, Cimaz R, and Naj Fovino PL.** Gait alterations in patients with juvenile chronic arthritis: a computerised analysis. *J Orthop Rheumatol* 9: 82-90, 1996.
- Frigo C, Ferrarin M, Frasson W, Pavan E, and Thorsen R.** EMG signals detection and processing for on-line control of functional electrical stimulation. *Journal of Electromyography and Kinesiology* 10: 351-360, 2000.

References

- Frigo C and Tesio L.** Speed-Dependent Variations of Lower-Limb Joint Angles During Walking - a Graphic Computerized Method Showing Individual Patterns. *American Journal of Physical Medicine & Rehabilitation* 65: 51-62, 1986.
- Fritsch FN and Carlson RE.** Monotone Piecewise Cubic Interpolation. *Siam Journal on Numerical Analysis* 17: 238-246, 1980.
- Gamage SSHU and Lasenby J.** New least squares solutions for estimating the average centre of rotation and the axis of rotation. *Journal of Biomechanics* 35: 87-93, 2002.
- GmbH ZM.** Measuring System for 3D-Motion Analysis CMS-HS,. *Tech Data and Operating Instructions Text Release 8/99*, 1999.
- Goodfellow J and O'Connor J.** The role of congruent mobile bearings in knee arthroplasty. *The Knee* 2, 1994.
- Grasso R, Bianchi L, and Lacquaniti F.** Motor Patterns for Human Gait: Backward Versus Forward Locomotion. *J Neurophysiol* 80: 1868-1885, 1998.
- Grasso R, Zago M, and Lacquaniti F.** Interactions Between Posture and Locomotion: Motor Patterns in Humans Walking With Bent Posture Versus Erect Posture. *J Neurophysiol* 83: 288-300, 2000.
- Grieve DW.** Gait patterns and the speed of walking. *Biomedical Engineering* 3: 119-122, 1968a.
- Grieve DW.** Gait patterns and the speed of walking. *Biomedical Engineering* 3: 119-122, 1968b.
- Gueguen N, Charbonneau M, Robert G, Coyle T, Prince F, and Mouchnino L.** Intersegmental coordination: Motor pattern in humans stepping over an obstacle with mechanical ankle joint friction. *Journal of Biomechanics* 38: 1491-1500, 2005.
- Hagan MT and Menhaj MB.** Training feedforward networks with the Marquardt algorithm. *IEEE Transactions on Neural Networks*, 5: 989-993, 1994.
- Haid M and Breitenbach J.** Low cost inertial orientation tracking with Kalman filter. *Applied Mathematics and Computation* 153: 567-575, 2004.
- Halvorsen K, Lesser M, and Lundberg A.** A new method for estimating the axis of rotation and the center of rotation. *Journal of Biomechanics* 32: 1221-1227, 1999.
- Hamill J, Haddad JM, and McDermott WJ.** Issues in quantifying variability from a dynamical systems perspective. *Journal of Applied Biomechanics* 16: 407-418, 2000.
- Hansson U, Toksvig-Larsen S, Jorn LP, and Ryd L.** Mobile vs. fixed meniscal bearing in total knee replacement, a randomized radiostereometric study. *The Knee* 12: 414-418, 2005.
- Harris WH.** Traumatic Arthritis of Hip after Dislocation and Acetabular Fractures - Treatment by Mold Arthroplasty - an End-Result Study Using a New Method of Result Evaluation. *Journal of Bone and Joint Surgery-American Volume A* 51: 737-8, 1969.

- Heyn A, Mayagoitia RE, Nene AV, and Veltink PH.** The kinematics of the swing phase obtained from accelerometer and gyroscope measurements. *Engineering in Medicine and Biology Society, 1996. Bridging Disciplines for Biomedicine. Proceedings of the 18th Annual International Conference of the IEEE*, 1996, p. 463-464 vol.462.
- Higgins JR and Higgins S.** Motor Control and Learning - a Behavioral Emphasis, 2nd Edition - Schmidt, Ra. *Quest* 42: 213-216, 1990.
- Hirsch HS, Lotke PA, and Morrison LD.** The Posterior Cruciate Ligament in Total Knee Surgery - Save, Sacrifice, or Substitute. *Clinical Orthopaedics and Related Research*: 64-68, 1994.
- Hoff WA, Komistek RD, Dennis DA, Gabriel SM, and Walker SA.** Three-dimensional determination of femoral-tibial contact positions under in vivo conditions using fluoroscopy. *Clinical Biomechanics* 13: 455-472, 1998.
- Hunt AE, M. Smith R, Torode M, and Keenan A-M.** Inter-segment foot motion and ground reaction forces over the stance phase of walking. *Clinical Biomechanics* 16: 592-600, 2001.
- Insall JN, Dorr LD, Scott RD, and Scott WN.** Rationale of the Knee Society clinical rating system. *Clin Orthop Rehat Res*: 13-14, 1989.
- Insall JN, Ranawat CS, Aglietti P, and Shine J.** A comparison of four models of total knee-replacement prostheses. *J Bone Joint Surg* 58: 754-765, 1976.
- Ivanenko YP, Grasso R, Macellari V, and Lacquaniti F.** Control of Foot Trajectory in Human Locomotion: Role of Ground Contact Forces in Simulated Reduced Gravity. *J Neurophysiol* 87: 3070-3089, 2002.
- Jackson JE.** A User's Guide To Principal Components. *Wiley, New York* 2003.
- Jacobs W, Anderson P, Limbeek J, and Wymenga A.** Mobile bearing vs fixed bearing prostheses for total knee arthroplasty for post-operative functional status in patients with osteoarthritis and rheumatoid arthritis. *Cochrane Database Syst Rev*: CD003130, 2004.
- James CR.** Considerations of Movement Variability in Biomechanics Research. In: *Stergiou N, Editor, Innovative Analysis of Human Movement, Human Kinetics, Champaign, IL* 29-62, 2004.
- Jerde TE, Soechting JF, and Flanders M.** Biological constraints simplify the recognition of hand shapes. *IEEE Transactions on Biomedical Engineering* 50: 265-269, 2003.
- Jerri AJ.** The Gibbs Phenomenon in Fourier Analysis, Splines and Wavelet Approximations. *Kluwer Academic Publishers*: 12-25, 1998.
- Jolles BM, Aminian K, Dejnabadi H, and Leyvraz PF.** Mobile or fixed bearing for knee arthroplasty? Results of a randomized trial using gait analysis. *American Academy of Orthopedic Surgeons (AAOS) Annual Meetings, Chicago*, 2006, p. 550.
- Jolles BM, Aminian K, Dejnabadi H, Voracek C, and Leyvraz PF.** 3D Kinematic Sensors to Help Choosing Between Mobile And Fixed Bearing Total Knee Arthroplasty. *EORS, 14th Annual Meeting, Amstersam*, 2004, p. O-60.

References

- Jolles BM, Aminian K, Dejnabadi H, Voracek C, Pichonnaz C, and Leyvraz PF.** Mobile or fixed bearing for total knee arthroplasty? First results of a double-blind randomized controlled trial using ambulatory gait analysis. *Swiss Med Forum. Suppl.* 25, 2005a, p. S8.
- Jolles BM, Aminian K, Dejnabadi H, Voracek C, Pichonnaz C, and Leyvraz PF.** Using 3D kinematic sensors to choose between mobile or fixed bearing total knee arthroplasty. *Proceedings of the CHUV Research Day*, Lausanne, 2005b, p. 231.
- Joseph J and Kaufman EE.** Preliminary results of Miller-Galante uncemented total knee arthroplasty. *Orthopedics* 13: 511-516, 1990.
- Kaufman KR, Hughes C, Morrey BF, Morrey M, and An KN.** Gait characteristics of patients with knee osteoarthritis. *Journal of Biomechanics* 34: 907-915, 2001.
- Keller RB, Rudicel SA, and Liang MH.** Outcomes Research in Orthopedics. *Journal of Bone and Joint Surgery-American Volume* 75A: 1562-1574, 1993.
- Kelso JAS.** Dynamic patterns: the self-organization of brain and behavior. *MIT Press, Cambridge, MA* 1995.
- Kelso JAS.** Human motor behavior. An introduction. *London: Lawrence Erlbaum Associates*: 4, 1982.
- Kemp B, Janssen AJMW, and van der Kamp B.** Body position can be monitored in 3D using miniature accelerometers and earth-magnetic field sensors. *Electroencephalography and Clinical Neurophysiology/Electromyography and Motor Control* 109: 484-488, 1998.
- Kim YH, Kook HK, and Kim JS.** Comparison of fixed-bearing and mobile-bearing total knee arthroplasties. *Clin Orthop Rehat Res*: 101-115, 2001.
- Kirshner B and Guyatt G.** A Methodological Framework for Assessing Health Indexes. *Journal of Chronic Diseases* 38: 27-36, 1985.
- Kirtley C, Whittle MW, and Jefferson RJ.** Influence of walking speed on gait parameters. *J Biomed Eng* 7: 282, 1985.
- Kiss RM, Kocsis L, and Knoll Z.** Joint kinematics and spatial-temporal parameters of gait measured by an ultrasound-based system. *Medical Engineering & Physics* 26: 611-620, 2004.
- Kleissen RFM, Litjens MCA, Baten CTM, Harlaar J, Hof AL, and Zilvold G.** Consistency of surface EMG patterns obtained during gait from three laboratories using standardised measurement technique. *Gait & Posture* 6: 200-209, 1997.
- Knight JL, Atwater RD, and Grothaus L.** Clinical results of the modular porous-coated anatomic (PCA) total knee arthroplasty with cement: A 5-year prospective study. *Orthopedics* 20: 1025-1033, 1997.
- Ko Y-G, Challis JH, and Newell KM.** Learning to coordinate redundant degrees of freedom in a dynamic balance task. *Human Movement Science* 22: 47-66, 2003.
- Konig A, Scheidler M, Rader C, and Eulert J.** The need for a dual rating system in total knee arthroplasty. *Clinical Orthopaedics and Related Research*: 161-167, 1997.

- Kreibich DN, Vaz M, Bourne RB, Rorabeck CH, Kim P, Hardie R, Kramer J, and Kirkley A.** What is the best way of assessing outcome after total knee replacement? *Clinical Orthopaedics and Related Research*: 221-225, 1996.
- Kroll MA, Otis JC, and Sculco TP.** The relationships of stride characteristics to pain before and after total knee arthroplasty. *Clin Orthop* 239: 191, 1989.
- Kugler PN, Kelso JAS, and Turvey MT.** On the concept of coordinative structures as dissipative structures: theoretical lines of convergence. In: G.E. Stelmach and J. Requin, Editors,. *Tutorials in Motor Behavior I, North-Holland, Amsterdam* 3-47, 1980.
- Kurz M and Stergiou N.** Applied dynamic systems theory for the analysis of movement. In: Innovative Analysis of Human Movement. *Human Kinetics, Champaign, USA* 93-119, 2004.
- Kurz MJ and Stergiou N.** Effect of normalization and phase angle calculations on continuous relative phase. *Journal of Biomechanics* 35: 369-374, 2002.
- Lafuente R, Belda JM, Sanchez-Lacuesta J, Soler C, Poveda R, and Prat J.** Quantitative assessment of gait deviation: contribution to the objective measurement of disability. *Gait & Posture* 11: 191-198, 2000.
- Lamoth CJC, Beek PJ, and Meijer OG.** Pelvis-thorax coordination in the transverse plane during gait. *Gait & Posture* 16: 101-114, 2002.
- Lamoth CJC, Daffertshofer A, Meijer OG, Moseley GL, Wuisman P, and Beek PJ.** Effects of experimentally induced pain and fear of pain on trunk coordination and back muscle activity during walking. *Clinical Biomechanics* 19: 551-563, 2004.
- Lee RYW, Laprade J, and Fung EHK.** A real-time gyroscopic system for three-dimensional measurement of lumbar spine motion. *Medical Engineering & Physics* 25: 817-824, 2003.
- Lemaire R.** Mobile-bearing knee prostheses. In *Lemaire R, Witvoet J, editors Total knee arthroplasty Paris: Elsevier SAS*: 57-70, 2002.
- Lewek MD, Scholz J, Rudolph KS, and Snyder-Mackler L.** Stride-to-stride variability of knee motion in patients with knee osteoarthritis. *Gait & Posture* In Press, Corrected Proof.
- Li L and Caldwell GE.** Muscle coordination in cycling: effect of surface incline and posture. *J Appl Physiol* 85: 927-934, 1998.
- Li L, Haddad JM, and Hamill J.** Stability and variability may respond differently to changes in walking speed. *Human Movement Science* 24: 257-267, 2005.
- Lieberman JR, Dorey F, Shekelle P, Schumacher L, Kilgus DJ, Thomas BJ, and Finerman GA.** Outcome after total hip arthroplasty - Comparison of a traditional disease-specific and a quality-of-life measurement of outcome. *Journal of Arthroplasty* 12: 639-645, 1997.
- Lieberman JR, Dorey F, Shekelle P, Schumacher L, Thomas BJ, Kilgus DJ, and Finerman GA.** Differences between patients' and physicians' evaluations of outcome after

References

total hip arthroplasty. *Journal of Bone and Joint Surgery-American Volume* 78A: 835-838, 1996.

Lindemann U, Becker C, Unnewehr I, Muche R, Aminian K, Dejnabadi H, Nikolaus T, Puhl W, Huch K, and Dreinhofer KE. Gait analysis and WOMAC are complementary in assessing functional outcome in total hip replacement. *Clinical Rehabilitation* 20: 413-420, 2006.

Luinge HJ and Veltink PH. Inclination measurement of human movement using a 3-D accelerometer with autocalibration. *Neural Systems and Rehabilitation Engineering, IEEE Transactions on [see also IEEE Trans on Rehabilitation Engineering]* 12: 112-121, 2004.

Luinge HJ and Veltink PH. Measuring orientation of human body segments using miniature gyroscopes and accelerometers. *Medical & Biological Engineering & Computing* 43: 273-282, 2005.

Macellari V and Giacomozzi C. Multistep pressure platform as a stand-alone system for gait assessment. *Medical & Biological Engineering & Computing* 34: 299-304, 1996.

Magdalena L and Monasterio F. Fuzzy controlled gait synthesis for a biped walking machine. *Second IEEE International Conference on Fuzzy Systems*, 1993, p. 1334-1339 vol.1332.

Marghitu DB and Hobatho MC. Dynamics of children with torsional anomalies of the lower limb joints. *Chaos Solitons & Fractals* 12: 2411-2419, 2001.

Marins JL, Yun X, Bachmann ER, McGhee RB, and Zyda MJ. An extended Kalman filter for quaternion-based orientation estimation using MARG sensors. *Intelligent Robots and Systems, 2001. Proceedings. 2001 IEEE/RSJ International Conference on*, 2001, p. 2003-2011 vol.2004.

Martin TA, Norris SA, Greger BE, and Thach WT. Dynamic Coordination of Body Parts During Prism Adaptation. *J Neurophysiol* 88: 1685-1694, 2002.

Mayagoitia RE, Nene AV, and Veltink PH. Accelerometer and rate gyroscope measurement of kinematics: an inexpensive alternative to optical motion analysis systems. *Journal of Biomechanics* 35: 537-542, 2002.

Medendorp WP, Crawford JD, Henriques DYP, Van Gisbergen JAM, and Gielen CCAM. Kinematic Strategies for Upper Arm-Forearm Coordination in Three Dimensions. *J Neurophysiol* 84: 2302-2316, 2000.

Meyer K, Applewhite HL, and Biocca FA. A Survey of Position Trackers. *Presence: Teleoperators and Virtual Environments* 1: 173-200, 1992.

Minns RJ. The role of gait analysis in the management of the knee. *Knee* 12: 157-162, 2005.

Mitra S, Amazeen PG, and Turvey MT. Intermediate motor learning as decreasing active (dynamical) degrees of freedom. *Human Movement Science* 17: 17-65, 1998.

Molet T, Boulic R, and Thalmann D. Human motion capture driven by orientation measurements. *Presence-Teleoperators and Virtual Environments* 8: 187-203, 1999.

- Moorehead JD, Montgomery SC, and Harvey DM.** Instant center of rotation estimation using Reuleaux technique and a Lateral Extrapolation technique. *Journal of Biomechanics* 36: 1301-1307, 2003.
- Morlock M, Schneider E, Bluhm A, Vollmer M, Bergmann G, Muller V, and Honl M.** Duration and frequency of every day activities in total hip patients. *Journal of Biomechanics* 34: 873-881, 2001.
- Morris JRW.** Accelerometry--A technique for the measurement of human body movements. *Journal of Biomechanics* 6: 729-732, 1973.
- Mouchnino L, Mille ML, Martin N, Baroni G, Cincera M, Bardot A, Delarque A, Massion J, and Pedotti A.** Behavioral outcomes following below-knee amputation in the coordination between balance and leg movement. *Gait & Posture* In Press, Corrected Proof.
- Murphy MC, Zarins B, Jasty M, and Mann RW.** In vivo measurement of the three dimensional skeletal motion at the normal knee. *Trans Orthop Res Soc*: 142, 1985.
- Myles CM, Rowe PJ, Walker CRC, and Nutton RW.** Knee joint functional range of movement prior to and following total knee arthroplasty measured using flexible electrogoniometry. *Gait & Posture* 16: 46-54, 2002a.
- Myles CM, Rowe PJ, Walker CRC, and Nutton RW.** Knee joint functional range of movement prior to and following total knee arthroplasty measured using flexible electrogoniometry. *Gait & Posture* 16: 46-54, 2002b.
- Nafei A, Kristensen O, Kjaersgaardandersen P, Hvid I, and Jensen J.** Total Condylar Arthroplasty for Gonarthrosis - a Prospective 10-Year Study of 138 Primary Cases. *Acta Orthopaedica Scandinavica* 64: 421-427, 1993.
- Najafi B.** *Physical activity monitoring and risk of falling evaluation in elderly people.* Dissertation no. 2672: Swiss Federal Institute of Technology, Lausanne, 2003.
- Ohno-Machado L and Rowland T.** Neural network application in physical medicine and rehabilitation. *American Journal of Physical Medicine & Rehabilitation* 78: 392-398, 1999.
- Orloci L.** Data Centering - a Review and Evaluation with Reference to Component Analysis. *Systematic Zoology* 16: 208-&, 1967.
- Otsuki T, Nawata K, and Okuno M.** Quantitative evaluation of gait pattern in patients with osteoarthritis of the knee before and after total knee arthroplasty. *J Orthop Science* 4: 99, 1999.
- Overhoff HM, Lazovic D, Liebing M, and Macher C.** Total knee arthroplasty: coordinate system definition and planning based on 3-D ultrasound image volumes. *International Congress Series* 1230: 292-299, 2001.
- Patla AE and Clous SD.** Visual assessment of human gait: reliability and validity. *Rehabil Res* 1: 87-96, 1997.
- Perry J.** *Gait analysis: normal and pathological function.* Slack, Thorofare, NJ, 1992.

References

- Peters BT, Haddad JM, Heiderscheit BC, Van Emmerik REA, and Hamill J.** Limitations in the use and interpretation of continuous relative phase. *Journal of Biomechanics* 36: 271-274, 2003.
- Price AJ, Rees JL, Beard D, Juszczak E, Carter S, White S, de Steiger R, Dodd CA, Gibbons M, McLardy-Smith P, Goodfellow JW, and Murray DW.** A mobile-bearing total knee prosthesis compared with a fixed-bearing prosthesis, a multicenter single-blind randomized controlled trial. *J Bone Joint Surg* 85: 62-67, 2003.
- Ramsey DK and Wretenberg PF.** Biomechanics of the knee: methodological considerations in the in vivo kinematic analysis of the tibiofemoral and patellofemoral joint. *Clinical Biomechanics* 14: 595-611, 1999.
- Rehbinder H and Hu X.** Drift-free attitude estimation for accelerated rigid bodies. *Automatica* 40: 653-659, 2004.
- Reinschmidt C, van den Bogert AJ, Lundberg A, Nigg BM, Murphy N, Stacoff A, and Stano A.** Tibiofemoral and tibiocalcaneal motion during walking: external vs. skeletal markers. *Gait & Posture* 6: 98-109, 1997a.
- Reinschmidt C, van den Bogert AJ, Nigg BM, Lundberg A, and Murphy N.** Effect of skin movement on the analysis of skeletal knee joint motion during running. *Journal of Biomechanics* 30: 729-732, 1997b.
- Reisman DS, Block HJ, and Bastian AJ.** Interlimb Coordination During Locomotion: What Can be Adapted and Stored? *J Neurophysiol* 94: 2403-2415, 2005.
- Reisman DS and Scholz JP.** Aspects of joint coordination are preserved during pointing in persons with post-stroke hemiparesis. *Brain* 126: 2510-2527, 2003.
- Richards JG.** The measurement of human motion: A comparison of commercially available systems. *Human Movement Science* 18: 589-602, 1999.
- Ridderikhoff A, Peper CE, and Beek PJ.** Unraveling Interlimb Interactions Underlying Bimanual Coordination. *J Neurophysiol* 94: 3112-3125, 2005.
- Roduit R, Besse PA, and Micallef JP.** Flexible angular sensor. *Ieee Transactions on Instrumentation and Measurement* 47: 1020-1022, 1998.
- Roetenberg D, Luinge HJ, Baten CTM, and Veltink PH.** Compensation of magnetic disturbances improves inertial and magnetic sensing of human body segment orientation. *Ieee Transactions on Neural Systems and Rehabilitation Engineering* 13: 395-405, 2005.
- Romanò CL, Frigo C, Randelli G, and Pedotti A.** Analysis of the gait of adults who had residua of congenital dysplasia of the hip. *J Bone Joint Surg* 78A: 1468-1479, 1996.
- Ronse C and Heijmans HJAM.** The algebraic basis of mathematical morphology : II. Openings and closings. *CVGIP: Image Understanding* 54: 74-97, 1991.
- Rosenbaum DA.** Human Motor Control. *Academic Press*: 5-54, 121-143, 1991.
- Rushworth MFS, Johansen-Berg H, and Young SA.** Parietal Cortex and Spatial-Postural Transformation During Arm Movements. *J Neurophysiol* 79: 478-482, 1998.

- Ryd L, Karrholm J, and Ahlvin P.** Knee scoring systems in gonarthrosis - Evaluation of interobserver variability and the envelope of bias. *Acta Orthopaedica Scandinavica* 68: 41-45, 1997.
- Sadeghi H, Mathieu PA, Sadeghi S, and Labelle H.** Continuous curve registration as an intertrial gait variability reduction technique. *IEEE Transactions on Neural Systems and Rehabilitation Engineering*, 11: 24-30, 2003.
- Sainburg RL, Ghilardi MF, Poizner H, and Ghez C.** Control of limb dynamics in normal subjects and patients without proprioception. *J Neurophysiol* 73: 820-835, 1995.
- Sainburg RL, Poizner H, and Ghez C.** Loss of proprioception produces deficits in inter-joint coordination. *J Neurophysiol* 70: 2136-2147, 1993.
- Salarian A, Russmann H, Vingerhoets FJG, Dehollain C, Blanc Y, Burkhard PR, and Aminian K.** Gait assessment in Parkinson's disease: toward an ambulatory system for long-term monitoring. *Biomedical Engineering, IEEE Transactions on* 51: 1434-1443, 2004.
- Saleh M and Murdoch G.** In Defense of Gait Analysis - Observation and Measurement in Gait Assessment. *Journal of Bone and Joint Surgery-British Volume* 67: 237-241, 1985.
- Sanger TD.** Human arm movements described by a low-dimensional superposition of principal components. *Journal of Neuroscience* 20: 1066-1072, 2000.
- Sati M, de Guise JA, Larouche S, and Drouin G.** Quantitative assessment of skin-bone movement at the knee. *Knee* 3, 1996.
- Saunders JB, Inman VT, and Eberhart HD.** The major determinants in normal and pathological gait. *The Journal Of Bone And Joint Surgery American Volume* 35-A: 543-558, 1953.
- Savitzky A and Golay MJE.** Smoothing + Differentiation of Data by Simplified Least Squares Procedures. *Analytical Chemistry* 36: 1627-8, 1964.
- Schmidt RA.** Motor control and learning: A behavior emphasis. *Illinois: Human Kinetics Publishers*, 1988.
- Schollhorn WI.** Applications of artificial neural nets in clinical biomechanics. *Clinical Biomechanics* 19: 876-898, 2004.
- Scholz JP.** Dynamic pattern theory - Some implications for therapeutics. *Physical Therapy* 70: 827-843, 1990.
- Schwartz MH and Rozumalski A.** A new method for estimating joint parameters from motion data. *Journal of Biomechanics* 38: 107-116, 2005.
- Scott Kelso JA and Clark JE.** The Development of Movement Control and Co-ordination. *Wiley Series in Developmental Psychology* 5-78, 1982.
- Secco EL and Magenes G.** A feedforward neural network controlling the movement of a 3-DOF finger. *IEEE Transactions on Systems, Man and Cybernetics, Part A*, 32: 437-445, 2002.

References

- Shiratsu A and Coury H.** Reliability and accuracy of different sensors of a flexible electrogoniometer. *Clinical Biomechanics* 18: 682-684, 2003a.
- Shiratsu A and Coury HJCG.** Reliability and accuracy of different sensors of a flexible electrogoniometer. *Clinical Biomechanics* 18: 682-684, 2003b.
- Shoemake K.** Animating Rotations with Quaternion Curves. *Computer Graphics (SIGGRAPH '85 Proceedings)* 19: 245-254, 1985.
- Sidaway B, Heise G, and Schoenfelder-Zhodi B.** Quantifying the variability of angle-angle plots. *Journal of Human Movement Studies* 29: 181-197, 1995.
- Simon SR, Trieshmann HW, and Burdett RG.** Quantitative gait analysis after total knee arthroplasty for monoarticular degenerative arthritis. *J Bone Joint Surg* 65A: 605, 1983.
- Skinner FK and Mulloney B.** Intersegmental coordination in invertebrates and vertebrates. *Current Opinion in Neurobiology* 8: 725-732, 1998.
- Smith AJ, Lloyd DG, and Wood DJ.** A kinematic and kinetic analysis of walking after total knee arthroplasty with and without patellar resurfacing. *Clinical Biomechanics* 21: 379-386, 2006.
- Solak SA, Kentel B, and Ates Y.** Does bilateral total knee arthroplasty affect gait in women? *The Journal of Arthroplasty* 20: 745-750, 2005.
- Steiner ME, Simon SR, and Pisciotta JC.** Early changes in gait and maximum knee torque following knee arthroplasty. *Clin Orthop* 238: 175, 1989.
- Stergiou N, Moraiti C, Giakas G, Ristanis S, and Georgoulis AD.** The effect of the walking speed on the stability of the anterior cruciate ligament deficient knee. *Clinical Biomechanics* 19: 957-963, 2004.
- Stergiou N, Scholten SD, Jensen JL, and Blanke D.** Intralimb coordination following obstacle clearance during running: the effect of obstacle height. *Gait & Posture* 13: 210-220, 2001.
- Stiehl JB, Dennis DA, Komistek RD, and Crane HS.** In vivo determination of condylar lift-off and screw-home in a mobile-bearing total knee arthroplasty. *J Arthroplasty* 14: 293-299, 1999.
- Stockham TG, Jr.** Image processing in the context of a visual model. *Proceedings of the IEEE* 60: 828-842, 1972.
- Sutherland DH.** The evolution of clinical gait analysis part III - kinetics and energy assessment. *Gait & Posture* 21: 447-461, 2005.
- Sutherland DH.** The evolution of clinical gait analysis: Part II Kinematics. *Gait & Posture* 16: 159-179, 2002.
- Sutherland DH, Kaufman KR, and Moitoza JR.** Kinematics of normal human walking. In: Rose J, and Gamble JG, Editors, *Human walking, Williams & Wilkins, Baltimore, MD* 23-45, 1994.

- Swinnen SP and Carson RG.** The control and learning of patterns of interlimb coordination: past and present issues in normal and disordered control. *Acta Psychologica* 110: 129-137, 2002.
- Titterton DH and Weston JL.** Strapdown inertial navigation technology. *Stevenage, UK: Peregrinus*: 178-179, 1997.
- To CS, Kirsch RF, Kobetic R, and Triolo RJ.** Simulation of a functional neuromuscular stimulation powered mechanical gait orthosis with coordinated joint locking. *IEEE Transactions on Neural Systems and Rehabilitation Engineering*, 13: 227-235, 2005.
- Tong K and Granat MH.** A practical gait analysis system using gyroscopes. *Medical Engineering & Physics* 21: 87-94, 1999a.
- Tong KY and Granat MH.** A practical gait analysis system using gyroscopes. *Medical Engineering & Physics* 21: 87-94, 1999b.
- Turvey MT.** Coordination. *American Psychologist* 45: 938-953, 1990.
- Unuma M, Anjyo K, and Takeuchi R.** Fourier principles for emotion-based human figure animation. *Proceedings of the 22nd Annual Conference on Computer Graphics and Interactive Techniques*: 91-96, 1995.
- Vaganay J, Aldon MJ, and Fournier A.** Mobile robot attitude estimation by fusion of inertial data. 1993, p. 277-282 vol.271.
- Valmassy RL.** Clinical biomechanics of the lower extremities. *St Louis: Mosby Publishing Yearbook*: 32-38, 1996.
- Vaughan CL, Davis BL, and O'Coonor JC.** Dynamics of human gait. *Champaign, IL: Human Kinetics Publishers*, 1992.
- Verschueren SMP, Swinnen SP, Cordo PJ, and Dounskaia NV.** Proprioceptive control of multijoint movement: unimanual circle drawing. *Experimental Brain Research* 127: 171-181, 1999.
- Verschueren SMP, Swinnen SP, Desloovere K, and Duysens J.** Effects of tendon vibration on the spatiotemporal characteristics of human locomotion. *Experimental Brain Research* 143: 231-239, 2002.
- Wallace SA.** Perspectives on the Coordination of Movement. *Advances in Psychology* 61: 1-45, 329-363, 1989.
- Watanabe T, Tomita T, Fujii M, Hashimoto J, Sugamoto K, and Yoshikawa H.** Comparison between mobile-bearing and fixed-bearing knees in bilateral total knee replacements. *Int Orthop* 29: 179-181, 2005.
- Webster KE, Wittwer JE, and Feller JA.** Quantitative gait analysis after medial unicompartamental knee arthroplasty for osteoarthritis. *The Journal of Arthroplasty* 18: 751-759, 2003.
- Weidenhielm L, Olsson E, Brostrom LA, Borjessonhederstrom M, and Mattsson E.** Improvement in Gait One Year after Surgery for Knee Osteoarthrosis - a Comparison

References

between High Tibial Osteotomy and Prosthetic Replacement in a Prospective Randomized Study. *Scandinavian Journal of Rehabilitation Medicine* 25: 25-31, 1993.

White R, Agouris I, and Fletcher E. Harmonic analysis of force platform data in normal and cerebral palsy gait. *Clinical Biomechanics* 20: 508-516, 2005.

Willemsen ATM, van Alste JA, and Boom HBK. Real-time gait assessment utilizing a new way of accelerometry. *Journal of Biomechanics* 23: 859-863, 1990.

Winter DA. Biomechanics and Motor Control of Human Movement (third ed.). *Wiley, Toronto* 13-57, 2005.

Wu WH and Meijer OG. Gait in patients with pregnancy-related pain in the pelvis: an emphasis on the coordination of transverse pelvic and thoracic rotations. *Clinical Biomechanics* 17: 678-686, 2002.

Xiaoping Y, Aparicio C, Bachmann ER, and McGhee RB. Implementation and Experimental Results of a Quaternion-Based Kalman Filter for Human Body Motion Tracking. 2005, p. 317-322.

Xiaoping Y, Bachmann ER, Kavousanos-Kavousanakis A, Yildiz F, and McGhee RB. Design and implementation of the MARG human body motion tracking system. 2004, p. 625-630 vol.621.

Xiaoping Y, Lizarraga M, Bachmann ER, and McGhee RB. An improved quaternion-based Kalman filter for real-time tracking of rigid body orientation. 2003, p. 1074-1079 vol.1072.

Yang NF, Zhang M, Huang CH, and Jin DW. Synergic analysis of upper limb target-reaching movements. *Journal of Biomechanics* 35: 739-746, 2002.

Zhu HS, Wertsch JJ, Harris GF, Loftsgaarden JD, and Price MB. Foot Pressure Distribution During Walking and Shuffling. *Archives of Physical Medicine and Rehabilitation* 72: 390-397, 1991.

Zhu R and Zhou Z. A real-time articulated human motion tracking using tri-axis inertial/magnetic sensors package. *Neural Systems and Rehabilitation Engineering, IEEE Transactions on [see also IEEE Trans on Rehabilitation Engineering]* 12: 295-302, 2004.

Zihlmann MS, Gerber H, Stacoff A, Burckhardt K, Szekely G, and Stussi E. Three-dimensional kinematics and kinetics of total knee arthroplasty during level walking using single plane video-fluoroscopy and force plates: A pilot study. *Gait & Posture* In Press, Corrected Proof.

Zijlstra W. Assessment of spatio-temporal parameters during unconstrained walking. *European Journal of Applied Physiology* 92: 39-44, 2004.

Zijlstra W and Bisseling R. Estimation of hip abduction moment based on body fixed sensors. *Clinical Biomechanics* 19: 819-827, 2004.

Zijlstra W and Hof AL. Assessment of spatio-temporal gait parameters from trunk accelerations during human walking. *Gait & Posture* 18: 1-10, 2003.

Zuffi S, Leardini A, Catani F, Fantozzi S, and Cappello A. A model-based method for the reconstruction of total knee replacement kinematics. *Ieee Transactions on Medical Imaging* 18: 981-991, 1999.

Curriculum Vitae

Personal Information

Name: Hooman DEJNABADI

Date of birth: 17 May 1971

Marital Status: Married

Residential Address: Av. de Florissant 12, 1020 Renens, Switzerland

Email: hooman.dejnabadi@epfl.ch

Education

2001-2006: Ecole Polytechnique Fédérale de Lausanne (EPFL), Lausanne, Switzerland,
Research Assistant and PhD student at the Laboratory of Movement Analysis and
Measurement.

1993-1996: Sharif University of Technology, Tehran, Iran

Masters of Science (M.Sc.) in Biomedical Engineering.

Thesis: Intelligent system for analyzing movement disabilities in Parkinson dis-
ease using accelerometer sensors.

1989-1993: Sharif University of Technology, Tehran, Iran

Bachelor of Science (B.Sc.) in Electronics and Electrical Engineering.

Thesis: Design and implementation of MCS-51 family microcontrollers In-Circuit
Emulator.

Honors

Honor Diploma in International Physics Olympiad, Warsaw, Poland, 1989

Professional Experience

- Ecole Polytechnique Fédérale de Lausanne (EPFL), Laboratory of Movement Analy-
sis and Measurement <http://lmam.epfl.ch/> , Research Assistant, 2001 – 2006.

- FaraSanat Shomal Co. and RadRavesh Co., Tehran, Technical Manager and Designer of NDT systems, 1993 – 2001.
- Bamdad Electronic Co., Tehran, Managing Director, 1996 – 1999.

Publications

Journal Papers

Dejnabadi H, Jolles BM, and Aminian K. A New Approach for Quantitative Analysis of Inter-Joint Coordination during Gait. *IEEE Transactions on Biomedical Engineering*, Submitted.

Dejnabadi H, Jolles BM, and Aminian K. Estimation and Visualization of Sagittal Kinematics of Lower Limbs Orientation Using Body-Fixed Sensors. *IEEE Transactions on Biomedical Engineering*, 53: 1385-1393, 2006.

Lindemann U, Becker C, Unnewehr I, Muche R, Aminian K, Dejnabadi H, Nikolaus T, Puhl W, Huch K, and Dreinhofer KE. Gait analysis and WOMAC are complementary in assessing functional outcome in total hip replacement. *Clinical Rehabilitation* 20: 413-420, 2006.

Dejnabadi H, Jolles BM, and Aminian K. A new approach to accurate measurement of uniaxial joint angles based on a combination of accelerometers and gyroscopes. *IEEE Transactions on Biomedical Engineering*, 52: 1478-1484, 2005.

Aminian K, Trevisan C, Najafi B, Dejnabadi H, Frigo C, Pavan E, Telonio A, Cerati F, Marioni EC, Robert P, and Leyvraz PF. Evaluation of an ambulatory system for gait analysis in hip osteoarthritis and after total hip replacement. *Gait & Posture* 20: 102-107, 2004.

Paper Proceedings (with peer reviewing)

Jolles BM, Aminian K, Dejnabadi H, and Leyvraz PF. Mobile or fixed bearing for knee arthroplasty? Results of a randomized trial using gait analysis. *American Academy of Orthopedic Surgeons (AAOS) Annual Meetings*, Chicago, 2006, p. 550.

Dejnabadi H, Jolles BM, Casanova E, Fua P, and Aminian K. Joint angle monitoring in osteoarthritis patients using body fixed sensors. *ISPGR 2005*, Marseille. *Gait & Posture*, 21, 2005, p. S76.

Jolles BM, Aminian K, Dejnabadi H, Voracek C, and Leyvraz PF. Ambulatory gait analysis results after total knee arthroplasty: arguments for mobile or fixed bearing? *Proceedings of the 7th Meeting of the European Federation of National Associations of Orthopaedics and Traumatology, EFORT*, 2005a, p. F740.

Dejnabadi H, Jolles BM, and Aminian K. A New Technique for Accurate Measuring of Knee Flexion-Extension Angle Using Body-Fixed Sensors. *ESMAC*, Warsaw. *Gait & Posture*, 20S, 2004, p. S73.

Casanova E, Dejnabadi H, Jolles BM, Aminian K, and Fua P. 3D Motion Analysis and Synthesis from Inertial Gyroscopes and Image Data. *ESMAC*, Warsaw. Gait & Posture, 20S, 2004, p. S85.

Jolles BM, Aminian K, Dejnabadi H, Voracek C, and Leyvraz PF. 3D Kinematic Sensors to Help Choosing Between Mobile And Fixed Bearing Total Knee Arthroplasty. *EORS, 14th Annual Meeting*, Amstersam, 2004, p. O-60.

Jolles BM, Aminian K, Dejnabadi H, Najafi B, Trevisan C, Marinoni E, Dutoit M, and Leyvraz PF. Analyse ambulatoire de la marche après prothèse totale de hanche : évaluation des résultats avec un nouveau paramètre. *Rev Chir Orthop*, 2004, p. 2S104.

Jolles BM, Aminian K, Dejnabadi H, Voracek C, and Leyvraz PF. Mobile or fixed bearing for total knee arthroplasty ? ambulatory gait analysis results. *JBJS Br Proceedings of the 17th Annual Symposium of the International Society for Technology in Arthroplasty, ISTA, Roma (I)*. J Bone Joint Surg B Suppl (in press), 2004.

Dejnabadi H, Jolles BM, Najafi B, Trevisan C, Marinoni EC, and Aminian K. A Robust Gait parameterization technique for hip arthroplasty outcome evaluation. *ISPGR, Sydney. Posture and Gait Throughout the lifespan*, SR. Lord and HB. Menz(ed.), 2003, p. 52.

Jolles BM, Dejnabadi H, Najafi B, Trevisan C, Marinoni EC, Leyvraz PF, and Aminian K. Ambulatory gait analysis for hip arthroplasty outcome evaluation: A new parameter. *Proceedings of the 16th Annual Symposium of the International Society for Technology in Arthroplasty, ISTA*, 2003, p. 35-36.

Dejnabadi H, Aminian K, Najafi B, Trevisan C, Telonio A, Frigo C, Pavan E, Marinoni EC, Robert P, and Leyvraz P-F. Joint and Segmnt Angles of Lower Limbs in Hip Osteoarthritis and Total Hip Replaced Patients Measured Using Physilog System. *EORS, 12th Annual Meeting*, Lausanne, 2002, p. O-96.

Other publications

Dejnabadi H, Aminian K, Najafi B, Jolles BM, Trevisan C, Telonio A, Frigo C, Pavan E, Marinoni EC, Robert P, and Leyvraz PF. Joint and segment angles of lower limbs in hip osteoarthritis and total hip replaced patients measured using physilog system. *J. Bone Joint Surg Suppl*, In Press.

Dejnabadi H, Jolles BM, Casanova E, Fua P, and Aminian K. Estimation and visualization of lower limbs orientation using body fixed sensors. *Proceedings of the Meeting of the Swiss Society for Biomedical Engineering (SSBE)*, Lausanne, 2005.

Voracek C, Pichonnaz C, Dejnabadi H, Aminian K, Broulis B, and Jolles BM. Le physilog, un nouveau système portable pour l'analyse du mouvement. *Proceedings of the Swiss Physiotherapy Association Annual Meeting*, Lausanne, 2005.

Jolles BM, Aminian K, Dejnabadi H, Voracek C, Pichonnaz C, and Leyvraz PF. Mobile or fixed bearing for total knee arthroplasty? First results of a double-blind randomized

controlled trial using ambulatory gait analysis. *Swiss Med Forum*. Suppl. 25, 2005b, p. S8.

Jolles BM, Aminian K, Dejnabadi H, Voracek C, Pichonnaz C, and Leyvraz PF. Using 3D kinematic sensors to choose between mobile or fixed bearing total knee arthroplasty. *Proceedings of the CHUV Research Day*, Lausanne, 2005, p. 231.

Jolles BM, Aminian K, Dejnabadi H, Najafi B, Trevisan C, Marinoni EC, and Leyvraz PF. Ambulatory gait analysis in hip arthroplasty outcome evaluation: a new parameter. *Proceedings of the CHUV Research Day*, 2004, p. 213.

Dejnabadi H. Intelligent system for analyzing movement disabilities in Parkinson disease using accelerometer sensors. *M.Sc. Thesis*. Sharif University of Technology, Tehran, 1996.

Dejnabadi H. Design and implementation of MCS-51 family microcontrollers In-Circuit Emulator. *B.Sc. Thesis*. Sharif University of Technology, Tehran, 1993.

Dejnabadi H and Golshan MA. *MCS-51 Family Microcontrollers and their Applications*. Tehran: Science & Industry University Press, 1993.

Jolles BM, Dejnabadi H, Najafi B, Trevisan C, Marinoni EC, Leyvraz PF, and Aminian K. Ambulatory gait analysis for hip arthroplasty outcome evaluation: a new parameter. *Schweiz Med Wochenschr*, 2003, p. 33S.

Najafi B, Aminian K, Dejnabadi H, Frigo C, Pavan E, Telonio A, Trevisan C, Cerati F, Marinoni EC, Leyvraz PF, and Robert P. Gait Features Assessment in Hip Osteoarthritis and Total Hip Replaced Patients Based on an Ambulatory System (Physilog). *Fourth World Congress of Biomechanics (WCB2002)*, Calgary, Canada. Proceeding CD, 2002.